Università degli Studi di Ferrara

ISTITUTO ITALIANO DI TECNOLOGIA

DOCTORAL COURSE IN
"TRASLATIONAL NEUROSCIENCES AND NEUROTECHNOLOGIES"

CYCLE 32

COORDINATOR Prof. Luciano Fadiga

THERAPEUTIC POTENTIAL OF RGS4 BLOCKADE IN MOVEMENT DISORDERS

Scientific/Disciplinary Sector (SDS) BIO/14

Candidate
Dott. Pisanò Clarissa Anna

_____
(signature)

Supervisor
Prof. Morari Michele

_____
(signature)

Year 2016/2019

ABSTRACT

About one third of marketed drugs target a G-protein coupled receptor (GPCR). Most of these drugs show unwanted side effects, partly due the lack of selectivity and off-target actions. A promising way to improve the clinical efficacy and the safety of these drugs is modulating the G-protein signal transduction, targeting the signaling molecules rather than the GPCR itself. Regulators of G-protein signaling (RGS) are a class of protein which negatively modulate the intracellular pathways evoked by G-proteins. Intracellular signal transduction starts when a ligand binds a GPCR, leading to the dissociation of the heterotrimeric G-protein into Gα and Gβγ subunits. RGS proteins bind the Gα subunit and accelerate the hydrolysis of GTP, turning the GPCR signal off. It has been shown that RGS proteins can theoretically modulate all GPCRs coupled to $G_{i/o}$ or G_q, although some of them are more selective than others. An interesting property of this class of regulators is their tissue- and neuron-specific expression, which makes the signaling regulation very fine, and specific for some but not all the receptor-driven responses. Therefore, targeting an RGS protein could potentiate the activity of an endogenous or exogenous agonist, improving its selectivity or tissue-specificity.

RGS4 is the most studied among RGS proteins. It is mostly expressed in brain areas, such as cortex and basal ganglia, but there is evidence of its expression in lungs and heart. The involvement of RGS4 in various pathological conditions, such as schizophrenia, Parkinson's disease (PD) and L-Dopa induced dyskinesia (LID) has been proven. This thesis adds to these findings, providing evidence of an involvement of RGS4 in neuroleptic-induced parkinsonism (Study I) and disclosing for the first time an RGS4-NOP receptor interaction which can be targeted in LID therapy (Study II).

Drug-induced parkinsonism (DIP) is the most common disorder caused by chronic use of dopaminergic drugs, in particular neuroleptics. In Study I, the ability of two RGS4 inhibitors (CCG-203769 and CCG-203920) in reversing raclopride-induced akinesia was investigated. Dual probe microdialysis was used to monitor in vivo glutamate release in the substantia nigra reticulata to assess whether these inhibitors impact the activity of the indirect pathway and to identify their site of action. Biochemical signatures of D_2 signalling pathway activation following RGS4 inhibition were studied. A preliminary attempt to identify the GPCR targeted by RGS4 was made by challenging RGS4 inhibitors with an mGlu5 receptor antagonist. The main findings were that both RGS inhibitors attenuate neuroleptic-induced parkinsonism, acting at the striatal and nigral levels to attenuate the neuroleptic-induced disinhibition of the indirect pathway. At the striatal level, RGS4 inhibition potentiated the neuroleptic-induced activation of MAPK pathway and did not involve mGlu5 receptors.

LID is a cluster of abnormal involuntary movements (AIMs), caused by chronic administration of L-Dopa, which represent the most disabling complication of dopamine replacement therapy of PD. In Study II, an attempt was made to widen the therapeutic window of a NOP receptor agonist by leveraging the RGS4-NOP receptor interaction. The interaction of RGS4 with the NOP receptor was first demonstrated in a cell model, then in striatal slices. Biochemical readouts of NOP activity were the D_1 receptor-stimulated cAMP accumulation in cell lines, and the D_1 receptor-stimulated number of pERK-positive neurons in slices. The impact of the RGS4 inhibitor CCG-203920 on the antidyskinetic effect of the Nociceptin/orphanin FQ (N/OFQ) opioid peptide (NOP) receptor agonist AT-403 was then evaluated in a rat model of LID. The ability of CCG-203920 to potentiate the antidyskinetic effect relative to the sedative effect of AT-403 was assessed, and the interference of CCG-2003920 with the molecular pathways underlying LID was evaluated using Western analysis of pERK and pGluR1 levels. Finally, Western analysis was also used to monitor levels of RGS4 in the striatum following dopamine-depletion and chronic L-Dopa treatment. The main findings of Study II were the demonstration that RGS4 negatively modulates NOP receptor function, and that RGS4 inhibition potentiates the antidyskinetic effect of the NOP receptor agonist without amplifying its sedative effects. RGS4 inhibition might also be useful to correct the upregulation of RGS4 levels in striatum occurring during dyskinesia expression.

In conclusion, these studies confirmed the involvement of RGS4 in basal ganglia dysfunction and the therapeutic potential of RGS4 inhibitors for treating neuroleptic-induced parkinsonism and LID. Targeting signaling molecules downstream of GPCRs, i.e. RGS proteins, can prove a novel tool to improve drug safety and clinical profile.

RIASSUNTO

Circa un terzo dei farmaci presenti sul mercato sfrutta un meccanismo d'azione che ha come bersaglio i recettori accoppiati a proteine G (GPCR - G-protein coupled receptor). La maggior parte di questi composti provoca effetti collaterali indesiderati, dovuti, in parte, alla mancanza di selettività o a effetti off-target. Una strategia interessante, che mira a migliorare l'efficacia clinica e la sicurezza di questi farmaci, è modulare il signaling della proteina G, utilizzando come target le biomolecole che sono coinvolte nel signaling, piuttosto che direttamente il GPCR. Le proteine regolatrici del signaling delle proteine G (RGS - Regulators of G-protein signaling) sono una classe di regolatori che modula negativamente i pathway intracellulari innescati dalle proteine G. La cascata di trasduzione del segnale inizia quando un ligando lega un GPCR, portando alla dissociazione dell'eterotrimero proteina G nella subunità Gα e nel dimero Gβγ. Le RGS legano la subunità Gα e accelerano la velocità di idrolisi del GTP, spegnendo il segnale del GPCR. Studi precedenti hanno dimostrato che le RGS possono modulare tutti i GPCR accoppiati a proteine Gi/o o Gq, sebbene alcune risultino più selettive di altre. Un'interessante proprietà di questi regolatori è la loro espressione tessuto- e neurone- specifica, che conferisce alle RGS la capacità di modulare finemente il signaling dei GPCR. Per queste ragioni, usare le RGS come target terapeutico può significare potenz iare l'attività di agonisti endogeni o esogeni, incrementandone selettività o tessutospecificità. RGS4 è la proteina RGS più studiata. È principalmente espressa in aree cerebrali come corteccia e gangli della base, ma ci sono evidenze della sua presenza anche nel cuore e nei polmoni. È stato dimostrato il coinvolgimento di RGS4 in diverse patologie come schizofrenia, malattia di Parkinson (MP) e discinesie indotte da L-Dopa (LID - L-Dopa induced dyskinesia). La presente tesi amplia queste conoscenze, mostrando evidenze sperimentali sul ruolo di RGS4 nel parkinsonismo indotto da neurolettici (Studio I) e sull'interazione di RGS4 e il recettore NOP fornendo un nuovo approccio terapeutico per le LID (Studio II). Il parkinsonismo indotto da farmaci (DIP - Drug-induced parkinsonism) è l'effetto collaterale più comune indotto dall'uso cronico di farmaci dopaminergici, in particolar modo dai neurolettici (NIP - neuroleptic-induced parkinsonism). Nello Studio I, è stata investigata l'abilità di due inibitori di RGS4 (CCG-203769 e CCG-203920) di invertire l'acinesia indotta da raclopride. La tecnica di microdialisi è stata usata per monitorare il rilascio di glutammato in vivo nella sostanza nera parte reticolata, al fine di verificare l'impatto dei composti sull'attività della via indiretta e di individuare il loro sito d'azione. Successivamente, è stato analizzato l'effetto dell'inibizione di RGS4 sul signaling D2, attraverso l'analisi di specifici marker molecolari. Infine, è stato condotto uno studio preliminare allo scopo di identificare il GPCR,

modulato da RGS4, che media l'effetto anti-acinetico degli inibitori di RGS4. Inizialmente, abbiamo proposto il recettore glutamatergico mGlu5 come possibile target. Questo studio ha messo in luce che gli inibitori di RGS4 attenuano il NIP, agendo a livello striatale per ridurre la disinibizione della via indiretta mediata dall'azione del neurolettico. A livello striatale, l'inibizione di RGS4 comporta un aumento dell'attivazione della cascata delle MAPK indotta dal neurolettico e non coinvolge il recettore mGlu5. Le LID sono un insieme di movimenti anomali involontari (AIMs - abnormal involuntary movements), causate dall'uso cronico di L-Dopa, che rappresentano la complicazione motoria più disabilitante della terapia dopaminergica sostitutiva della MP. Nello Studio II, si è cercato di allargare la finestra terapeutica di un agonista NOP lavorando sull'interazione RGS4-recettore NOP. In prima battuta, l'interazione di RGS4 con il recettore NOP è stata dimostrata in un modello cellulare, successivamente in fettine di striato. Come readout biochimico dell'attività NOP è stata usata l'inibizione dell'accumulo di cAMP nelle cellule e l'aumento di neuroni pERK- positivi nelle fettine, stimolati da agonista D1. L'impatto dell'inibitore RGS4, CCG-203920, sull'effetto antidiscinetico dell'agonista del recettore della Nocicettina/orfanina FQ (N/OFQ), AT-403, è stato quindi valutato in un modello di ratto di LID. È stata valutata la capacità di CCG-203920 di potenziare l'effetto antidiscinetico rispetto all'effetto sedativo/ipolocomotorio di AT-403. Successivamente, al fine di indagare l'impatto di CCG2003920 sulle vie molecolari alla base delle LID, grazie alla tecnica del Western blot, è stato possibile analizzare i livelli di pERK e pGluR1. Infine, abbiamo usato la stessa tecnica per monitorare i livelli di RGS4 nello striato a seguito della deplezione di dopamina e del trattamento cronico con L-Dopa. I principali risultati dello Studio II sono stati la dimostrazione che RGS4 modula negativamente la funzione del recettore NOP e che l'inibizione dell'RGS4 potenzia l'effetto antidiscinetico dell'agonista del recettore NOP, senza amplificarne gli effetti sedativi. L'inibizione di RGS4 potrebbe anche essere utile per annullare la sovraespressione di RGS4 nello striato che si verifica durante l'espressione delle LID. In conclusione, questi studi hanno confermato il coinvolgimento di RGS4 nelle disfunzioni dei gangli della base e il potenziale terapeutico degli inibitori di RGS4 nel trattamento del NIP e della LID. Il targeting di molecole coinvolte nel signaling a valle dei GPCR, ovvero le proteine RGS, può rivelarsi un nuovo strumento per migliorare la sicurezza e l'efficacia clinica dei farmaci.

Index

CHAPTER I

G-protein coupled receptors: the primary target for drug-based therapy

Modifying the signaling cascade is the underlying mechanism of most therapeutics used in clinic. The most common approach to regulate an intracellular pathway is targeting the receptor, which starts the intracellular signaling. Nowadays, approximately 35% of all marketed drugs are ligands of G-protein coupled receptors (GPCRs)[1].

GPCRs are the largest family of proteins, responding to various types of stimuli, like hormones, neurotransmitters or sensory stimuli. These proteins are composed by seven transmembrane α-helices, an extracellular N-terminus, an intracellular C-terminus and three interhelical loops on each side of the membrane [2, 3]. Despite their number and heterogeneity, GPCRs can interact with a relatively small number of G-proteins to evoke an intracellular signal. Human G-proteins are heterotrimeric proteins, formed by 21 different Gα subunits, 5 Gβ subunits and 12 Gγ subunits, and, traditionally, are classified based on the main function of the Gα subunit ($G\alpha_s$, $G\alpha_{i/o}$, $G\alpha_q$ and $G\alpha_{12}$) [2, 3].

The signaling cascade starts when a ligand binds the extracellular surface of the GPCR, leading to conformational modifications in the intracellular portion of the receptor. These adjustments cause the activation of the G-protein, resulting in GDP-GTP exchange on the Gα subunit and dissociation from the Gβγ dimer [2, 3]. Consequently, Gα and Gβγ can interact with specific effectors and recruit different intracellular pathways. Gα subunits differ in structural and functional properties; nonetheless, all Gα subunits share a highly conserved domain, the GTPase domain, which hydrolyses GTP and sets up the binding surface for the Gβγ dimer. The result of this activity is the switch off the signal transduction and the reassembly of the G-protein heterotrimer [2, 3].

This is the classical simplified view of the G-protein cycle but extinguishing the signal is more than just a Gα-GTPase activity-dependent event.

RGS proteins: a new class of regulators

The first clue about a more complex regulation of G-protein signal was provided by the finding that the Gα subunit-mediated GTPase activity proceeded at very low speed in a purified protein system, which mismatches the dynamics of the intracellular signaling in cells [4-8]. Clearly, there was something else. So, in the early 90s a large class of proteins has been discovered, i.e. the so-called Regulators of G-protein signaling (RGS), which are GTPase-activating proteins (GAP) [9]. The existence and the characterization of RGS proteins was simultaneously demonstrated in *Saccharomyces cerevisiae* (*S. cerevisiae*), *Caenorhabditis elegans* (*C. elegans*) and mammalian cells [4-8].

Today, we know that the family of RGS proteins includes many proteins which share a common 120 amino acid domain, called the RGS domain, responsible for the GAP activity on the GTP-bound Gα subunit of heterotrimeric G-protein.

We can divide the classical human 20 RGS proteins in four subfamilies (R4, R7, R12 and RZ; Table 1) based on the sequence and domain homology [9].

Table 1 *Classification of the 20 classical human RGS proteins.*

Family	**Members**
R4	RGS1,RGS2,RGS3,RGS4,RGS5,RGS8, RGS13,RGS16,RGS18,RGS21
R7	RGS6,RGS7,RGS9,RGS11
R12	RGS10,RGS12,RGS14
RZ	RGS17,RGS19,RGS20

However, an same RGS-like domain has been identified, besides the canonical RGS proteins, in several protein families, such as GRK1-7, ankyrin, AKAPs and Rho-GEFs [10].

As anticipated, most GPCR-based drugs are associated with unwanted side effects, partly due to the low selectivity for the primary target or off-targets activities [9]. The activation of a GPCR does not lead just to the stimulation of Gα subunit-mediated signaling but also to stimulation of the Gβγ dimer-mediated pathways. In addition, the receptor itself can interact with other proteins in a G-protein independent manner [1]. So, targeting the GPCR alone often brings about therapeutic and unwanted effects.

RGS proteins offer a great opportunity to improve the selectivity of GPCRs ligands. Most RGS proteins can interact with different types of G proteins. At the moment, no solid evidence that they can interact with $G\alpha_s$ subunit has been provided yet, although it has been shown that RGS2 can bind this subunit *in vitro* [9, 11]. Some RGS proteins, such as RGS4, can preferentially regulate $G\alpha_{i/o}$ signaling and others do not discriminate between $G\alpha_{i/o}$ or $G\alpha_q$ pathways.

Another important feature of RGS proteins is their tissue specific expression which is independent from the expression of the G-proteins they regulate. This represents a second crucial point to improve drug selectivity. For instance, RGS4 is widely expressed in the striatum [12, 13] where several GPCRs coupled to $G\alpha_{i/o}$ and $G\alpha_q$ are expressed, such as D_2 dopamine (DA) or mGlu5 glutamate (Glu) receptors. In this respect, it has been shown that

RGS4 can modulates mGlu5 signaling [14] but not D_2 signaling, although RGS4 does bind $G\alpha_{i/o}$ [15].

RGS proteins: more than GAP proteins

Although all members of this class of proteins share the same RGS domain, most of them have additional domains which confer some non-canonical functions, besides the GAP activity [9]. Most of these functions are driven by protein-protein interactions, through additional domains. For instance, the R7 family members interact with their effectors $G\beta_5$ and R7BP/R9AP (R7 binding protein/RGS9 associated protein) via the G-protein γ-like (GGL), Disheveled, Egl-10, pleckstrin (DEP) and DEP helical extension domains of these proteins [16]. Specifically, the function of R7 proteins is enhanced by the interaction with R7BP/R9AP, because, being bound to the plasma membrane, they can reinforce the R7 proximity to the G-protein. On the other hand, R7 proteins can interact with $G\beta_5$ through the R7 GGL domain, which regulates the stability of the protein [9]. Another interesting example comes from the study of the function of R12 family members. RGS12 and RGS14 have a $G\alpha_{i/o}$-Loco (GoLoco) domain, which has a similar activity to the RGS one. This domain prevents the G protein activation by inhibiting the GTP exchange. Since this interaction also prevents the association between Gα and Gβγ, this function gives to RGS12 and RGS14 the ability to prolong the Gβγ signaling [17]. However, the presence of additional domains is not always mandatory for the expression of additional functions. Indeed, RGS2, a small protein belonging to the R4 family, has the ability to directly interact with adenylyl cyclase negatively regulating the $G\alpha_s$ mediated signaling, despite the lack of additional domains [11, 18]. Likewise another member of this family, RGS13,lacks any additional domains but suppresses the transcription binding of the transcription factor CREB [19]. Taken together, it is clear why RGS proteins are such interesting targets.

RGS4: a little, interesting friend

Among all RGS proteins, the most studied is RGS4, a very simple protein with no additional domains beside the RGS domain. It does, however, have an unstraightened N-termined amphipathic helix which contributes to RGS4 association with cell membrane. In the human brain, RGS4, a 24 kDa protein, is mainly expressed in the inferior and superior frontal cortex, the cingulate cortex, the insular and the inferior temporal cortex and to a lower extent the caudate, putamen and nucleus accumbens [13]. The expression in the rat brain in quite similar, with some differences such a significant expression also in the

thalamus, hippocampus and amygdala [12]. RGS4 was primarily investigated in schizophrenia, due to its specific expression in brain areas involved in this pathology, such as prefrontal cortex. Nowadays, we have several studies which support the view that RGS4 is a risk factor for schizophrenia, but this hypothesis is weakened by inconsistencies among the cohorts of patients examined [20].

The research around this protein is very intense and dynamic, spanning across different fields. Indeed, there is evidence of the involvement of RGS4 in acute and chronic pain [21-24], PD [25-27] and side-effects of dopamine replacement therapy of PD, such as dyskinesia [28, 29]. In addition, RGS4 is involved in non-neuropsychiatric diseases like different types of cancer [30, 31], obesity [32] and asthma [33].

RGS4 as drug target

Clearly, targeting RGS4 could be useful in several pathologies. Here, we focused on the potential therapeutic effect of the blockade of RGS4 in PD and L-Dopa-induced dyskinesia (LID).

An RGS inhibitor is supposed to potentiate the signal initiated by an endogenous ligand. For instance, this strategy can be used in PD to amplify the dopaminergic stimulus driven by dopamine. Moreover, if associated with an exogenous agonist, an RGS inhibitor can increase the potency and the selectivity of the drug, thus potentiating the signal transduction through the receptor. Specifically, an RGS inhibitor can potentially modulate the therapeutic effect without affecting the unwanted side effects, in the case they are driven by different intracellular pathways which might be regulated by different proteins. Moreover, and perhaps most fascinating, an RGS inhibitor can increase the tissue- or cell-type specificity of the drug. RGS4 is almost absent in the peripheral regions and, as mentioned before, is widespread in CNS [12, 13]. Therefore, targeting RGS4 would potentiate the central activity of a drug and improve its selectivity, directing its action towards the intracellular pathways underlying the therapeutic effects relative to the intracellular pathways mediating the unwanted effects.

CHAPTER II

Introduction

Parkinson's disease

Parkinson's disease (PD) is the most common neurodegenerative motor disorder, affecting 1% of the population ≥60 years of age [34]. Since the first characterization by James Parkinson in 1817 [35],advancements in the PD field never stopped growing, but we are still far from a full understanding of the mechanisms underlying this disease. Degeneration of dopaminergic neurons in the substantia nigra (SN) pars compacta (SNpc) [36, 37] and intracellular inclusions containing aggregates of α-synuclein (α-syn) known as Lewy bodies (LBs) are the neuropathological hallmarks of PD [38].

However, the abnormal deposition of α-syn is not pathognomonic for PD as it also characterizes other pathologies such as dementia with Lewy Bodies (LBs) and multiple system atrophy (MSA), which are collectively known as synucleinopathies [39], and may also occur in tauopathies, like Alzheimer's disease. The accumulation of α-syn results in the formation of LBs which, according to seminal work of Braak and colleagues [40], appears with an ascending pattern in different regions of the brain during the course of the disease [41]. LBs appear in cholinergic and monoaminergic brainstem neurons and in neurons of the olfactory system in the early phases, later spread to the midbrain, where SNpc is located, and then invade the limbic and neocortical regions in the later phases [42]. This indicates that the neurodegeneration in PD is a very early event that begins long before the appearance of motor symptoms, which are correlated to the loss of midbrain dopamine neurons.

Idiopathic PD has, by definition, an unknown etiology. Nonetheless, the contribution of genetics has clearly emerged, originally with the discovery of SNCA as a causative gene then with the identification of an ever-growing number (at least 20 up to now) of PD-associated genes and risk factors. Despite just 5-10% of PD cases having a familial (i.e. monogenic) nature [34], these cases represent an opportunity to highlight the molecular pathways involved in PD development. α-syn proteostasis, mitochondrial dysfunction, oxidative stress, calcium homeostasis, axonal transport and neuroinflammation are some of the molecular pathways targeted by familial PD related genes, making the genetic PD very similar to idiopathic PD [38].

Basal ganglia and pathophysiology of PD

The basal ganglia (BG) network is a cluster of different nuclei in the forebrain, which have important functions in the control of actions and goal-directed behavior. This network receives inputs from the thalamus, the cortex and brainstem nuclei, and projects to the thalamus and back to the cortex [43, 44].

The BG circuit is formed by the striatum, SN, globus pallidus (GP) and subthalamic nucleus (STN).

- The *striatum* is the largest input nucleus of the BG and is anatomically divided into dorsal striatum (*caudate nucleus* and *putamen*) and ventral striatum (*nucleus accumbens*). The dorsal striatum is primarily involved in the control of voluntary movements and executive functions, while the ventral striatum regulates limbic functions of reward and aversion [44]. The dorsal striatum receives several glutamatergic inputs from associative and sensorimotor cortical areas. The striatum receives dopaminergic inputs from SNpc, which play a crucial role in the modulation of the glutamatergic incoming stimuli from cortex. The striatum is mainly (95%) formed by medium-sized spiny neurons (MSNs), which are GABAergic [44, 45]. Traditionally, we can divide these neurons in two large groups, essentially based on projection territories and DA receptors expressed. MSNs forming the so-called "direct pathway" (dMSNs) project to GP internal segment (GPi) and SN pars reticulata (SNpr), whereas MSNs forming the "indirect pathway" (iMSNs) project to GABAergic neurons of GP external segment (GPe). GPe neurons, in turn, project to glutamatergic neurons of STN, that send an excitatory a projection to GPi/SNr [43, 45]. These two populations of striatal MSNs express different membrane receptors and signaling molecules, suggesting differences in their functions during physiological or pathological conditions [45]. First, MSNs express distinct subtypes of DA receptors so they can respond differently to dopaminergic inputs. Thus, dMSNs express G_{olf}-coupled D_1 receptors, which increase the excitability of these neurons and promote long-term potentiation (LTP) at the glutamatergic synapses. Conversely, iMSNs express the G_i-coupled D_2 receptor, which decreases intrinsic excitability, and promotes long-term depression (LTD) at glutamatergic synapses [46, 47]. In the past, these populations of neurons were thought to be completely segregated but now we know that a low percentage (5-10%) of MSNs express both D_1 and D_2 receptors [48, 49].

Although the actual circuit organization involving the direct and the indirect pathways is far more complex, considering these pathways as completely segregated has offered a simple model to interpret motor effects of drugs acting in the BG, and understand the BG regulation of motor function.

The overall result of stimulation of dMSNs is the facilitation of motor activity through inhibition of GPi/SNpr, disinhibition of the thalamus and the potentiation of the transmission between thalamus and cortex. By contrast, iMSNs inhibit GPe and consequently dishinibit subthalamic transmission towards the GPi/SNpr. The result is a decrease in thalamo-cortical firing and inhibition of the planning and execution of voluntary movements. Stimulation of dopaminergic receptors leads to positive modulation of voluntary movement, increasing the activity of dMSNs via D_1 receptor activation and decreasing the activity of iMSNs via D_2 receptor activation. It should be also mentioned that the striatum contains a network of GABAergic and cholinergic interneurons, which play key modulatory roles in all aspects of striatal physiology and striatum-mediated behaviors [50, 51].

Beside MSNs (~90-95% of striatal neurons) the striatum also contains different types of GABAergic and cholinergic (ChIs) interneurons (~2-5% of striatal neurons) that play a crucial role in regulating striatal functions [52]. Among GABAergic interneuron populations there are some differences such as specific expression of binding proteins like parvalbumin in fast spiking interneurons and expression of neuropeptides and enzymes including somatostatin, neuropeptide Y, nitric oxide synthase, and tyrosine hydroxylase (TH) [51].

- The *SN* is divided in two distinct nuclei, the dopaminergic SNpc and the GABAergic SNpr. The SNpc is predominantly composed by DA neurons that receive inputs from the striatum and the ascending reticular activating system and, as mentioned, project to the putamen and the caudate [45]. The SNpr, instead, is mainly composed of tonically-active GABAergic neurons which receives GABAergic afferents from the striatum and GPe, glutamatergic afferents from the STN and peduncolo-pontine nucleus (PPN), and serotonergic innervation from the raphe nucleus. It sends inhibitory stimuli to the ventral anterior and ventrolateral nuclei of the thalamus [53].
- The *GP*, in primates, is divided into the GPe and GPi segments. In rodents, the functions of GPi are exerted by the entopeduncolar nucleus (EPN). Both GP segments receive GABAergic projections from the striatum and glutamatergic projections from the STN. Other structures, such as SNpc and thalamus, project to

the GP. The GPe mainly innervates the STN and, to a lesser extent, the striatum and SN. Most GPi projections, instead, terminate into the thalamus and PPN [53].

- The *STN* is the only glutamatergic nucleus of the BG and receives inputs from the cortex (the so called "hyperdirect" pathway), GPe, SN, and pontine reticular formation and projects to the SNpr and GP. The STN contains a large number (>90%) of medium-sized neurons that use glutamate as a neurotransmitter, and a small number of interneurons [53].

Parkinsonism results from the loss of dopamine modulation of striatal function in the dorsal region, leading to opposing effects on the direct and indirect pathways, which result in overinhibition of the thalamocortical projections (Fig. 1). To reinforce this classical view of PD functioning, lesion of the GPi or the STN proved effective in alleviating parkinsonian bradykinesia in animals and humans.

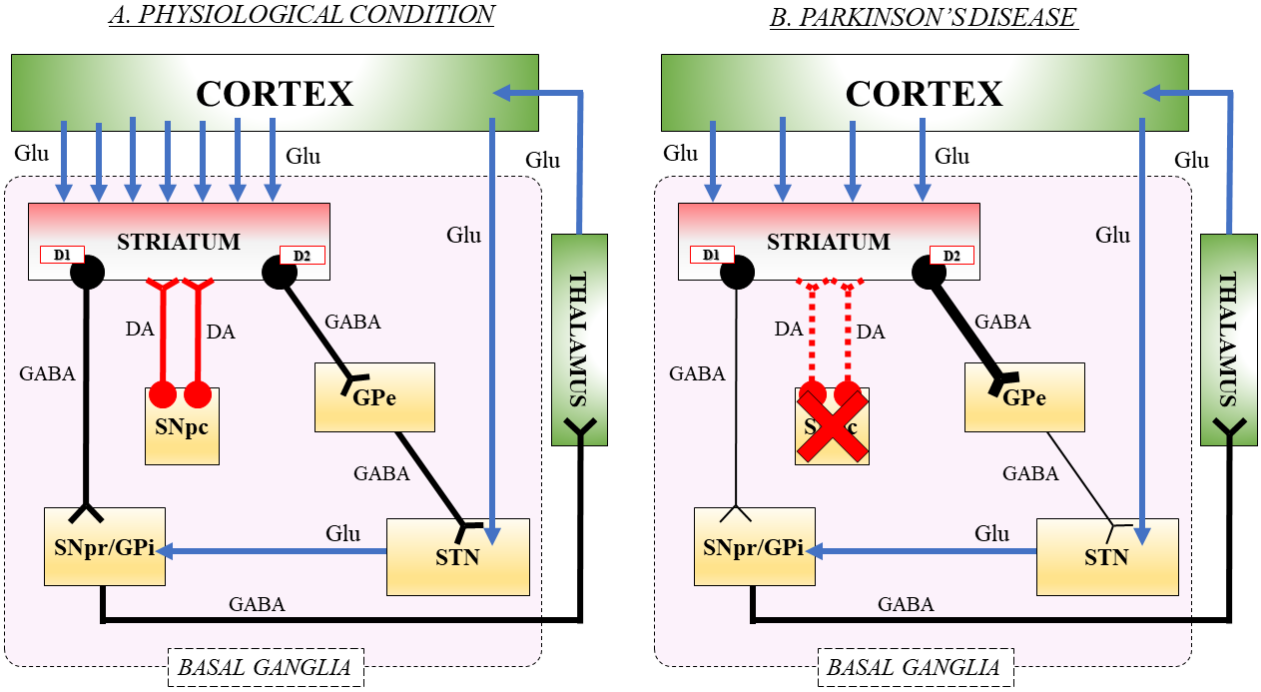

Fig. 1 Schematic representation of basal ganglia circuit in physiological condition (A) and in Parkinson's disease (B). SNpc: Substantia nigra pars compacta; SNpr: Substantia nigra pars reticulata; GPe: Globus pallidus external segment; GPi: Globus pallidus internal segment; STN: subthalamic nucleus; DA: dopamine; Glu: glutamate; GABA: γ-aminobutyric acid.

Neuroleptic-induced parkinsonism

Drug-induced movement disorders include drug-induced parkinsonism (DIP), tardive dyskinesia (TD), tardive dystonia, akathisia, myoclonus and tremor. Among these, DIP is the most common movement disorder induced by dopaminergic drugs [54]. Since the clinical manifestations are very close to the clinical features of PD, most of DIP cases are misdiagnosed as PD, and wrongly treated as parkinsonian syndromes, while most of them

are resolved by interrupting the offending drugs. For this reason, the exact prevalence and incidence are very hard to be reported [55].

DIP was first recognized in 1950s as neuroleptic-induced parkinsonism (NIP), which is expression of the extra-pyramidal effects of typical antipsychotic drugs known as neuroleptics. Indeed, it was first described three years after the introduction of chlorpromazine in the therapy of schizophrenia [56]. After this report, it was ascertained that, due to their antidopaminergic properties, all antipsychotics bear the potential to induce extra-pyramidal side effects, such as parkinsonism, acute dystonia, akathisia and TD [55]. To date, we refer to this type of parkinsonism as DIP because it can be induced by different classes of medications beside neuroleptics, such as gastrointestinal motility drugs [57], calcium channel blockers and antiepileptics [54].

In PD, hypokinesia is due to degeneration of dopaminergic neurons of SNpc (nigrostriatal pathway). Conversely, in DIP, the dopaminergic system is intact and healthy, therefore motor impairment is caused by disruption of dopaminergic signal transmission, in particular postsynaptic D_2 receptor blockade.

Three pathophysiologic mechanisms have been reported in DIP [54]:

- Dysfunction of dopaminergic system, which can be caused by presynaptic dopamine depletion (reserpine, tetrabenazine), false transmitter (methyldopa), D_2 receptor blockage (dopamine receptor antagonists, antiemetic agents, calcium channel blockers), or serotonergic inhibition (selective serotonin reuptake inhibitors)
- Alteration in intracellular machinery, such as mitochondrial respiratory chain dysfunction (calcium channel blockers, valproic acid)
- Dysfunction in the motor circuitry, such as overactivity in the GABAergic system (valproic acid) or cholinomimetic action (tacrine, bethanechol).

Dopamine receptors are widely expressed in the brain. Specifically, the central dopaminergic system involves mesolimbic, mesocortical, tubero-infundibular and nigrostriatal pathways. Neuroleptics act therapeutically on limbic D_2 postsynaptic receptors, but cause extra-pyramidal syndrome by interacting with striatal D_2 receptors on iMSNs [54, 55]. The blockage of D_2 receptors by antipsychotic drugs in the striatum disinhibits iMSNs without affecting dMSNs, leading to the disinhibition of the STN. This results in GABAergic inhibition of the thalamocortical loop through the potentiation of the GPi/SNpr activity. This circuitry change is similar to the BG dysfunction found in PD (Fig. 2).

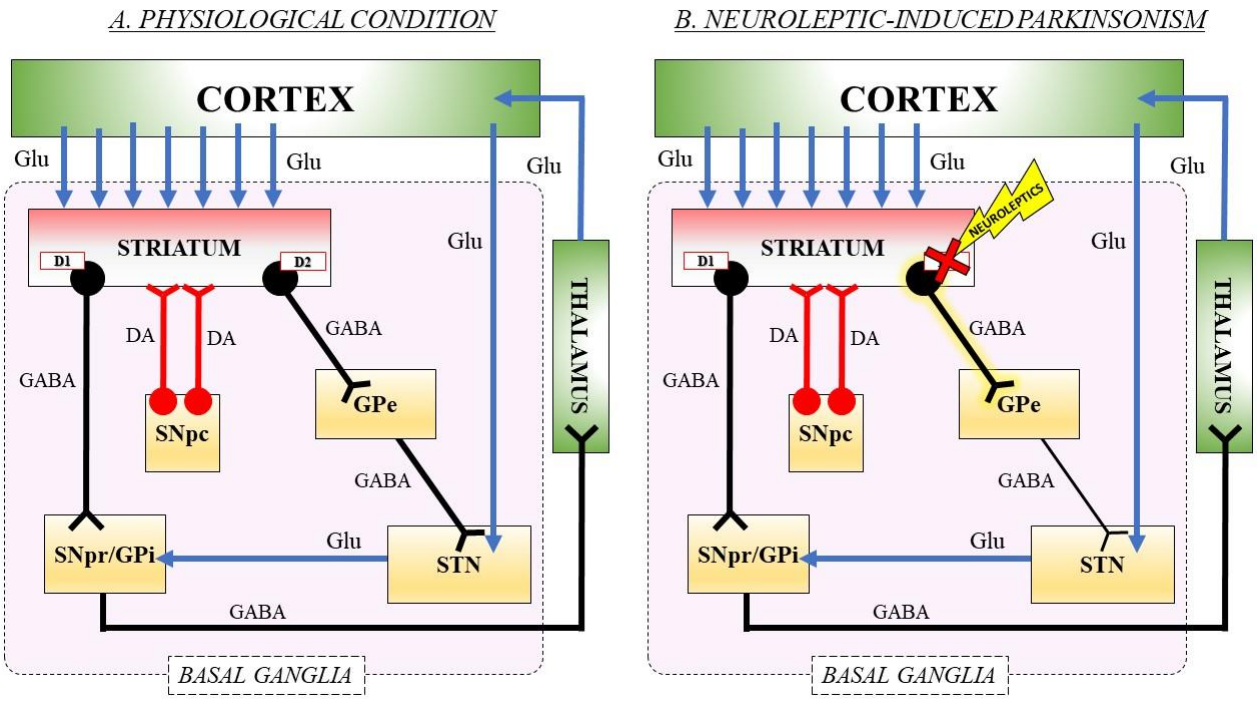

Fig. 2 Schematic representation of basal ganglia circuit in physiological condition (A) and in neuroleptic-induced parkinsonism (B). SNpc: Substantia nigra pars compacta; SNpr: Substantia nigra pars reticulata; GPe: Globus pallidus external segment; GPi: Globus pallidus internal segment; STN: subthalamic nucleus; DA: dopamine; Glu: glutamate.

Typical antipsychotics produce their therapeutic effects acting on 60-80% of D_2 occupancy, while 75-80% of D_2 receptor occupancy causes DIP [58]. Atypical antipsychotics, because of their lower affinity for D_2 receptors and preferential activity on serotonin $5HT_{2A}$ receptors, are considered less liable to extra-pyramidal effects than typical antipychotics. Indeed, some drugs like clozapine and quietiapine bear a very low risk of inducing parkinsonism and are used also to treat psychosis in PD patients since they do not worsen parkinsonian symptoms [55]. On the other hand, olanzapine, although its clozapine-like structure, bears a high risk of extra-pyramidal effects. Indeed, although, like clozapine, this compound shows antiserotonergic and anticholinergic actions, contrary to clozapine, olanzapine has a relatively higher affinity for D_2 receptor in vivo, which has been related to the higher risk to cause DIP [59].

Like for PD, there are several risk factors of DIP. In particular, we should mention, age, clearly because aging means decreased striatal dopamine concentrations and loss of dopaminergic neurons in SN. Contrary to PD, DIP is more common in females than males. However, not all patients who use antipsychotics develop DIP, suggesting a genetic component is involved [55].

RGS4 and PD

RGS4 is a regulator of several GPCRs coupled to $G\alpha_{i/o}$ or $G\alpha_q$ specifically expressed in neurons [12]. Evidence of RGS4 involvement in some CNS disorders such as schizophrenia [20] has been provided. Conversely, the role of RGS4 in PD remains to be proven.

In 2003, downregulation of RGS4 in the DA-depleted striatum of 6-OHDA hemilesioned rat was reported [26]. In the same model, the upregulation of RGS4 specifically in striatal cholinergic interneurons was observed a few years later [25], overall suggesting a fine regulation of RGS4 expression by DA transmission *in vivo* [25, 26].

Lerner and collaborators [60] showed that RGS4 is crucial to determine the susceptibility to parkinsonian motor deficit following nigrostriatal denervation. Genetic deletion of RGS4 attenuated the development of motor impairment following lesion of the nigrostriatal pathway [60]. Recently, we added to these findings and proposed a role of RGS4 in NIP. Indeed, the novel compound, CCG-203769, which belongs to a chemical class of nanomolar-potency small molecule inhibitors of RGS4 [61], was able to attenuate raclopride-induced akinesia in mice [27], suggesting that RGS4 blockade could improve neuroleptic-induced akinesia and, possibly, parkinsonian-like motor symptoms.

Aim of the study

In the present study, we aimed to confirm the therapeutic potential of the whole class of RGS4 inhibitors, investigating the effect of another thiadiazolidinone compound, CCG-203920 [62, 63], in a mouse model of neuroleptic-induced akinesia. In addition, we tried to shed light on the neurochemical mechanisms underlying the antiakinetic effect of these inhibitors. To this aim, we monitored the variations of neurotransmitter Glu and GABA levels, following pharmacological treatment with raclopride in the presence of RGS4 inhibitors, in two key nuclei of BG, i.e. striatum and SNpr. To better understand the molecular pathways underlying these neurochemical alterations, we used Western analysis in haloperidol-treated mice to simultaneously investigate the changes in D_2 signaling. Then, in order to understand which GPCR subtype mediates the antiakinetic effect of RGS4 inhibitors, we made a preliminary attempt to modulate CCG-203920 antiakinetic action with the mGlu5 receptor antagonist, MTEP. Indeed, mGlu receptors regulate cell excitability and synaptic transmission at glutamatergic synapses throughout the brain [64]. The mGlu receptor family counts at least eight distinct receptors which are classified into three major subgroups, group I mGluRs (mGlu1 and mGlu5 subtypes) coupled to Gq,

group II (mGlu 2 and mGlu3 subtypes) and group III (mGlu4, mGlu6, mGlu7, and mGlu8 subtypes) coupled to Gi/o. It has been demonstrated that RGS4 can negatively modulate group I mGlu receptors *in vitro* [65], but more recently McGinty and collaborators specified that RGS4 attenuates amphetamine-induced ERK signaling through mGlu5 *in vivo* [14]. In addition, we reasoned that RGS4 can modulate not just mGlu5 but the A_{2A}-D_2-mGlu5 heteroreceptor complex [66] expressed extrasynaptically on the dendritic spines of iMSNs [67]. In PD, the loss of D_2 receptor transmission also affects the activity of this receptor mosaic, resulting in an augmented co-activation of A_{2A} and mGlu5 receptors. Indeed, Lerner and coll [60] showed a novel mechanism linking dopamine D_2 and adenosine A_{2A} receptor signaling to mobilization of endocannabinoids (eCBs). They found that D_2 and A_{2A} receptors were functionally engaged to modulate eCBs-induced LTD using RGS4 as a scaffold protein (eCD-LTD). This modulation was shown to be driven by the cAMP/PKA pathway, specifically the rise of cAMP inhibits eCB-LTD. Plus, they demonstrated that this synaptic plasticity was strictly connected with the motor behavior and RGS4. Indeed, RGS4 knockout mice were less susceptible to motor impairment induced by DA depletion compared to wild-type controls. Since it was possible to record a correct eCB-LTD in iMSNs of RGS4 knockout mice, they correlated the better motor performance to this type of synaptic plasticity. Based on the fact that eCB-LTD is dependent on mGlu5 stimulation [68] and RGS4 inhibits mGlu5 receptor signaling [65], they concluded that RGS4 is the link between DA signaling, synaptic plasticity and motor behavior, acting on mGlu5 receptor.

Materials and methods

Animals

Male C57BL/6J mice (12-15 weeks), Charles River Laboratories (Calco, Italy), were housed in the animal facility of University of Ferrara, LARP, with free access to food and water, and kept under regular lighting conditions (12 hr dark/light cycle). Animals were housed in groups of 5 for a cage with environmental enrichments. Experimental procedures involving the use of animals were approved by the Ethical Committee of the University of Ferrara and the Italian Ministry of Health (license n. 368/2018). Adequate measures were taken to minimize animal pain and discomfort.

Raclopride-induced akinesia

Prior to pharmacological testing, mice were handled for 1 week by the same operator to reduce stress and trained daily for a week on the behavioral tests until their motor performance became reproducible. On the day of the experiment, raclopride was administered at 1 mg/Kg (i.p.), whereas CCG-203920 at 1 and 10 mg/Kg (i.p.). CCG-203920 was administered 30 min after raclopride. Motor activity was evaluated by different behavioral tests, i.e. the bar, drag and rotarod tests, as previously described [69-72]. These tests were repeated before (control session) and after (30 min) raclopride injection, then 20 and 90 min after CCG-202920 administration. The different tests are useful to evaluate motor functions under static or dynamic conditions.

Bar test

This test measures the ability of the animal to respond to an externally imposed static posture [70]. Mice were gently placed on a table and forepaws were placed alternatively on blocks of increasing heights (1.5, 3 and 6 cm). The time (in seconds) that each paw spent on the block (i.e. the immobility time) was recorded (cut-off time of 20 sec). Performance was expressed as total time spent on the different blocks.

Drag test

This test measures the ability of the animal to balance its body posture with the forelimbs in response to an externally imposed dynamic stimulus (backward dragging) [70]. It gives information regarding the time to initiate and execute a movement. Animals were gently lifted from the tail leaving the forepaws on the table, and then dragged backwards at a constant speed (about 20 cm/sec) for a fixed distance (100 cm). The number of steps made by each paw was counted by two separate observers. Five trials were collected for each animal.

Rotarod test

Finally, the fixed-speed rotarod test integrates different motor parameters such as motor coordination, gait ability, balance, muscle tone and motivation to run. Mice were tested over a wide range of increasing speeds (0-55 rpm; 5 rpm steps, increased every 180 s) on a rotating rod (diameter of the cylinder 8 cm) and the total time spent on the rod was recorded [73, 74].

Microdialysis in raclopride-treated mice

Dual probe microdialysis was used to simultaneously monitor striatal and nigral GABA and Glu release in freely-moving mice [72, 75]. Briefly, two microdialysis probes of concentric design were stereotactically implanted under isoflurane anesthesia (1.5% in air) into dorsolateral striatum and ipsilateral SNpr (2 and 1 mm dialyzing membrane, respectively), according to the following coordinates from bregma and the dural surface (mm)[76]: dorsolateral striatum, anteroposterior +0.6, mediolateral ±2.0, dorsoventral −3.3; SNpr, anteroposterior −3.3, mediolateral ±1.25, dorsoventral −4.6. Probes were secured to the skull by acrylic dental cement and metallic screws. After surgery, mice were allowed to recover, and experiments were run 24 h and 48 h after probe implantation. Microdialysis probes were perfused at a flow rate of 2 µl/min with a modified Ringer solution (in mM: 1.2 $CaCl_2$, 2.7 KCl, 148 NaCl, and 0.85 $MgCl_2$), and samples were collected every 15 min, starting 6 h after the onset of probe perfusion. Raclopride was administered at 1 mg/Kg (i.p.) whereas CCG-203920 or CCG-203769 at 10 mg/Kg (i.p.), 30 min after raclopride injection. In a separate set of experiments CCG-203920 was perfused in the striatum or SNpr through the microdialysis probe (*reverse dialysis*) starting 30 min before raclopride injection and lasting until the end of experiment. MTEP was also perfused in the striatum through the microdialysis probe, starting 30 min before raclopride injection and lasting until the end of experiment. The nominal concentration chosen for both compounds was 10 µM. This was made on the basis of the affinity for their specific targets (CCG-203920 IC_{50} for RGS4 = 54 nM; 665-fold more selective for RGS4 than RGS8 [63]; MTEP IC_{50} for mGlu5 5 nM [77, 78]) and the recovery of the dialysis membrane, which has been estimated to be close to 10% *in vitro* [79]. Therefore, for CCG-203920 and MTEP the actual concentration in brain is estimated to be around 1 µM, which is enough to cover all targets without inducing off-target effects. At the end of experiment, animals were sacrificed, and the correct placement of the probes was verified histologically.

Motor behavior during microdialysis was monitored with the bar test for 1 min every 15 min, in order to correlate the changes in immobility time (a readout of akinesia) with neurochemical changes.

Endogenous Glu and GABA analysis

Glu and GABA levels in the dialysate were measured by HPLC coupled with fluorometric detection as previously described [72, 80, 81]. Thirty microliters of o-

phthalaldehyde/mercaptoethanol reagent were added to 28 µl aliquots of samples and 50 µl of the mixture was automatically injected (Triathlon autosampler; Spark Holland, Emmen, the Netherlands) onto a 5-C18 Hypersil ODS analytical column (3 mm inner diameter, 10 cm length; Thermo-Fisher, USA) perfused at a flow rate of 0.48 ml/min (Jasco quaternary gradient pump PU-2089 PLUS; Jasco, Tokyo, Japan) with a mobile phase containing 0.1 M sodium acetate, 10% methanol and 2.2% tetrahydrofuran (pH 6.5). Glu and GABA were detected by means of a fluorescence spectrophotometer FP-2020 Plus (Jasco, Tokyo, Japan) with the excitation and the emission wavelengths set at 370 and 450 nm respectively. The limits of detection for Glu and GABA were ~1 and ~0.5 nM, respectively, and their retention times were ~3.5 and ~18.0 min, respectively.

Statistical analysis

Motor performance was expressed as time on bar or rod (in seconds; bar and rotarod tests), and number of steps (drag test). In microdialysis studies, GABA and Glu release was expressed as percentage ± SEM of basal values (calculated as mean of the two samples before treatment). Statistical analysis was performed by two-way repeated measures ANOVA or one-way ANOVA, as appropriate. P values <0.05 were considered statistically significant.

Materials

Raclopride and MTEP were purchased from Tocris (Bristol, UK), whereas CCG-203920 and CCG-203769 were provided by Dr RR Neubig (Michigan State University, East Lansing, MI, USA). Raclopride was dissolved in 5% DMSO saline solution, and CCG-203920 and CCG-203769 in saline. MTEP was dissolved in water, up to 10 mM stock solution, then diluted with Ringer to the final concentration of 10 µM.

Results

CCG-203920 reversed the raclopride-induced akinesia

Basal motor activity of naïve mice was similar at the right and left paw; therefore, data were pooled together. The immobility time (bar test, Fig.3A) was 6.00±0.25 sec (n=9), the number of steps (drag test, Fig.3B) was 20.87±0.33 (n=9) and the time on rotating rod (rotarod test, Fig.1C; 0-55 rpm range) was 1090.77±41.5 sec (n=9). According to previous data [27], raclopride administration induced a marked akinesia in mice, increasing four-fold the time on bar (33.2±1.65 sec) and reducing both the number of steps (10.7±0.61, -49%) and the time spent on rod (282±37.3, -73%). The RGS4 inhibitor, CCG-203920 (1 and 10 mg/Kg i.p.), reversed in a dose-dependent manner neuroleptic-induced motor impairment in the bar and drag test (Fig.3A-B). In particular, Fig. 3A also shows that the higher dose of CCG-203920 (10 mg/Kg) almost normalized motor function 90 min after CCG-203920 administration in the bar and drag tests, and also improved motor performance in the rotarod test

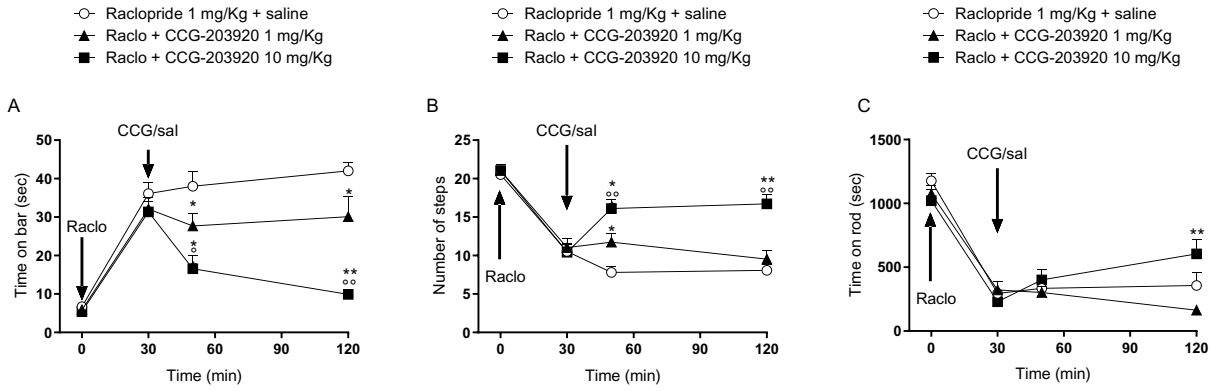

*Fig. 3 Effect of systemic (i.p.) CCG-203920 administration on motor activity in raclopride-treated mice. Motor activity was evaluated in the bar test (A), drag test (B) and rotarod test (C), and data expressed as immobility time (sec, A), number of steps (B) and time on rod (C, sec). Values are mean ± SEM of 9 mice per group. *p<0.05, **p<0.01 different from Raclopride 1 mg/Kg + saline; °p<0.05, °°p<0.01 different from Raclo + CCG-203920 1 mg/Kg. Two-way repeated measure ANOVA followed by the Bonferroni post hoc test.*

CCG-203920 normalized the raclopride-induced increase in nigral Glu levels

In previous studies, we showed acorrelation between haloperidol-induced akinesia and the increase of Glu levels in SNpr [70, 75], suggesting that nigral Glu changes could be a readout of the activation of indirect pathway. We therefore used dual probe microdialysis in awake mice to simultaneously monitor amino acid (Glu and GABA) dialysate concentrations in SNpr and striatum. Sample collection was coupled with measurement of

immobility time (akinesia) in the bar test. To investigate whether RGS4 contributes to neuroleptic-induce akinesia by modulating the indirect pathway, we investigated the effect of CCG-203920 on the rise of nigral Glu release induced by the neuroleptic raclopride.

Nigral basal levels of Glu and GABA were 53.2±6.31 nM (n=23) and 15.1±4.20 nM (n=23), respectively. Raclopride administration increased Glu levels in the SNpr in both groups (~50% in control group and ~89% in the CCG-203920-treated group; calculated 30 min after administration) (Fig.4A). Systemic administration of CCG-203920 (10 mg/Kg, i.p.) reversed the effect of raclopride and normalized nigral Glu levels. Different from nigral Glu, no significant changes in nigral GABA were detected following raclopride alone or in combination with CCG-203920 (Fig.4B). Basal amino-acid levels in striatum were 62.1±7.43 nM (Glu, n=16) and 15.1±4.20 nM (GABA, n=16). Neither raclopride nor CCG-203920 injections significantly modified striatal amino acid levels (Fig.4C-D).

The bar test performed in mice undergoing microdialysis (Fig.5) confirmed both the link between the rise of nigral Glu and akinesia, and the anti-akinetic effect of CCG-203920 observed in studies in freely moving, untethered animals.

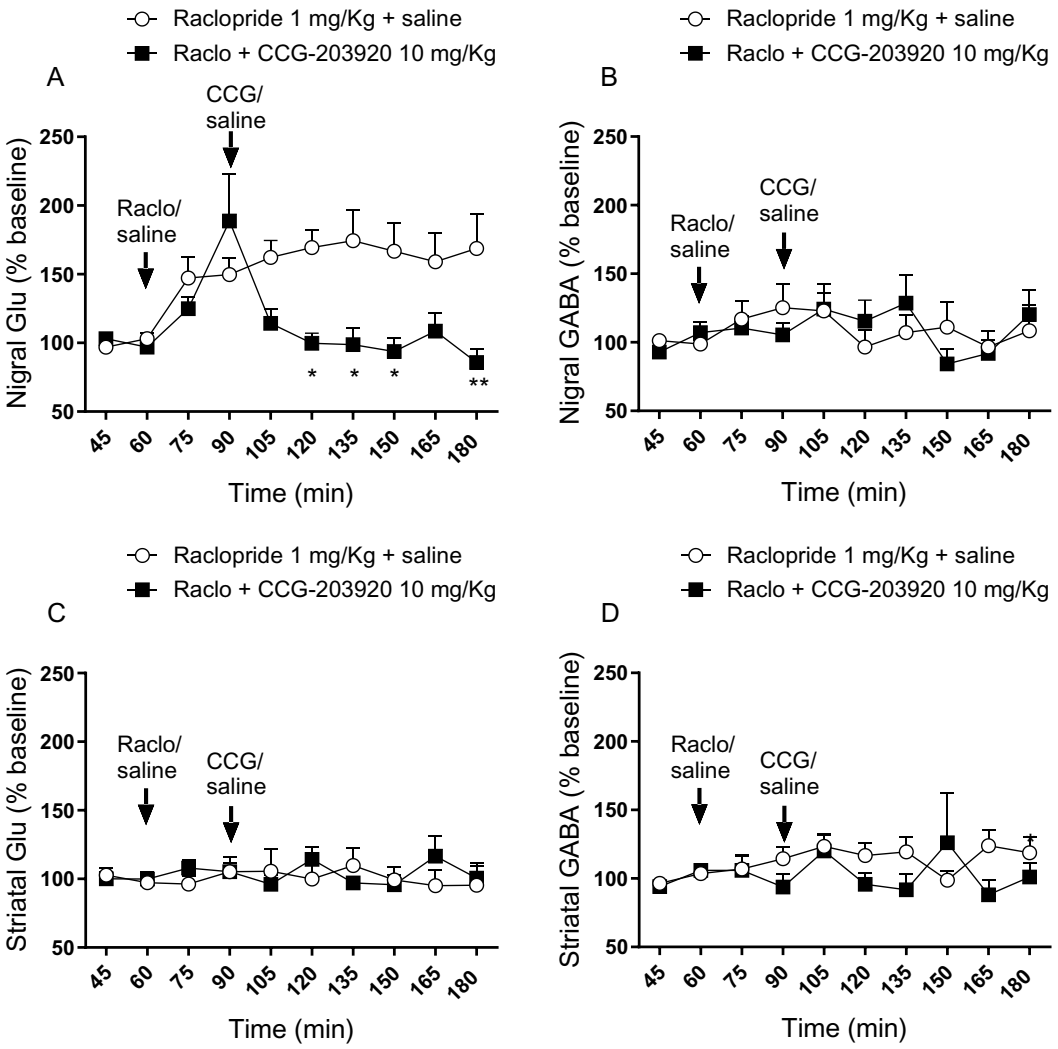

Fig. 4 *Effect of systemic (i.p.) CCG-203920 administration on nigral and striatal GABA and glutamate (Glu) levels measured by microdialysis in raclopride-treated mice. CCG-203920 was administered 30 min after raclopride. Values are mean ± SEM of 10 (SNr) and 8 (striatum) mice per group. *p<0.05 different from Raclopride+saline. Two-way repeated measure ANOVA followed by the Bonferroni post hoc test.*

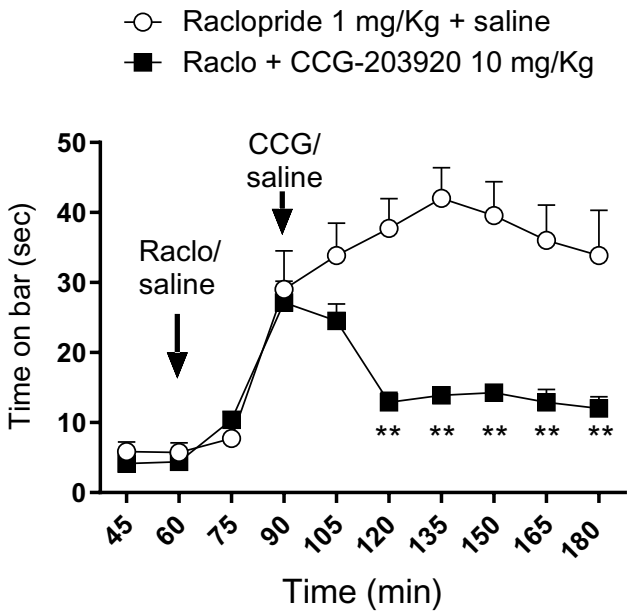

Fig. 5 *Effect of systemic (i.p.) CCG-203920 administration on the immobility time in the bar test performed during microdialysis in raclopride-treated mice. CCG-203920 was administered 30 min after raclopride. Values are mean ± SEM of 7-8 mice per group. **p<0.01 different from Raclopride+saline. Two-way repeated measure ANOVA followed by the Bonferroni post hoc test.*

CCG-203769 reverted the raclopride-induced rise of nigral Glu in mice

In order to demonstrate that the neurochemical effect induced by CCG-203920 is a class-effect and not just the property of a single small-molecule RGS4 inhibitor, we tested in a microdialysis setting CCG-203769, an RGS4 inhibitor with established antiakinetic property [27]. Nigral basal levels of Glu and GABA were 52.2±6.45 nM (n=24) and 29.2±4.27 nM (n=23), respectively. As expected, raclopride administration elevated Glu levels in SNpr (~42% in control group and ~37% in the CCG-203769-treated group; calculated 30 min after administration) (Fig.6A), and CCG-203769, as previously shown for CCG-203920, normalized this increase (Fig.6A). Again, no significant changes in nigral GABA were detected, although a trend for an increase was observed in the CCG-203769 group (Fig.6B).

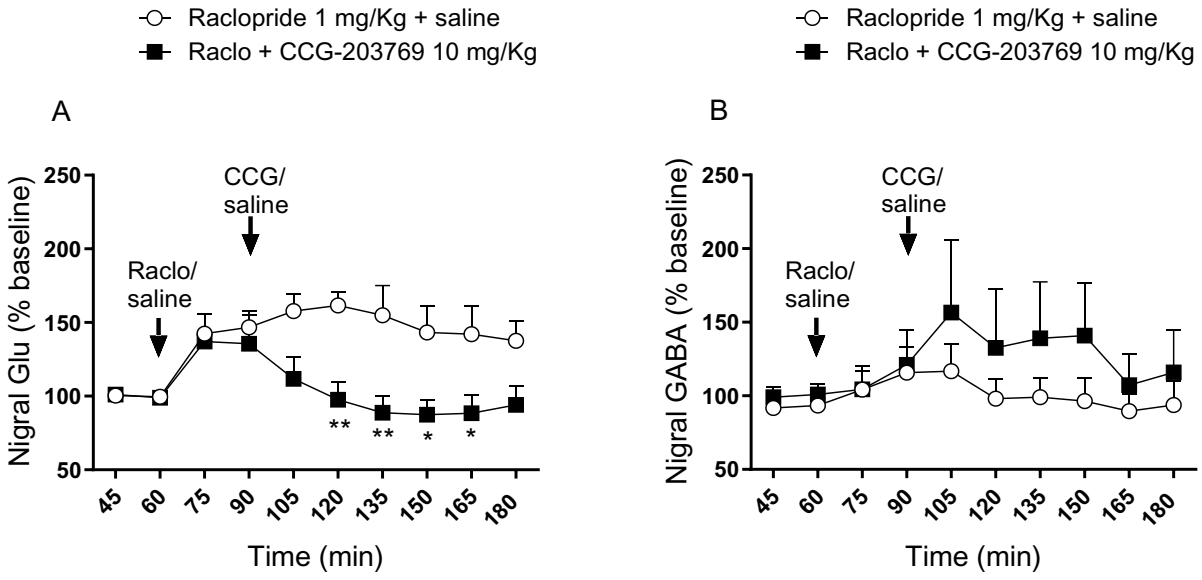

Fig. 6 *Effect of systemic (i.p.) CCG-203769 administration on nigral GABA and glutamate (Glu) levels measured by microdialysis in raclopride-treated mice. CCG-203769 was administered 30 min after raclopride. Values are mean ± SEM of 12 mice per group. *p<0.05, **p<0.01 different from Raclopride+saline. Two-way repeated measure ANOVA followed by the Bonferroni post hoc test.*

CCG-203920 striatal/nigral perfusion prevented the raclopride-induced increase in nigral Glu levels

In previous experiments, CCG compounds were administered systemically, leaving to speculation at what level of the indirect pathway they could act. In order to address this issue, reverse dialysis of CCG-203920 was performed in striatum or SNpr. In this case, reverse dialysis commenced 30 min before systemic raclopride injection. Nigral basal levels of Glu and GABA were 83.2±10.3 nM (n=18) and 4.08±0.56 nM (n=18), respectively. Striatal or nigral perfusions of CCG-203920 did not alter basal levels of neurotransmitters in SNr (Fig.7A-D). As expected, due to the high expression of RGS4 in striatum, intrastriatal perfusion of CCG203920 was able to prevent the raclopride-induced increase of nigral Glu (Fig.7A). Surprisingly because there is no evidence of RGS4 expression in SNr, also nigral perfusion of CCG-203920 evoked the same effect (Fig.7A). No significant changes of nigral GABA were detected during local perfusion of CCG-203920 (Fig.7B). Basal levels of Glu and GABA in striatum were 103±14.9 nM (n=17) and 5.37±1.19 nM (n=17), respectively. No changes of amino acid levels were detected in response to any pharmacological treatments (Fig.7C-D). The bar test performed during microdialysis experiment confirmed that raclopride failed to induce akinesia in animals subjected to intrastriatal or intranigral perfusion with CCG-203920 (Fig.8).

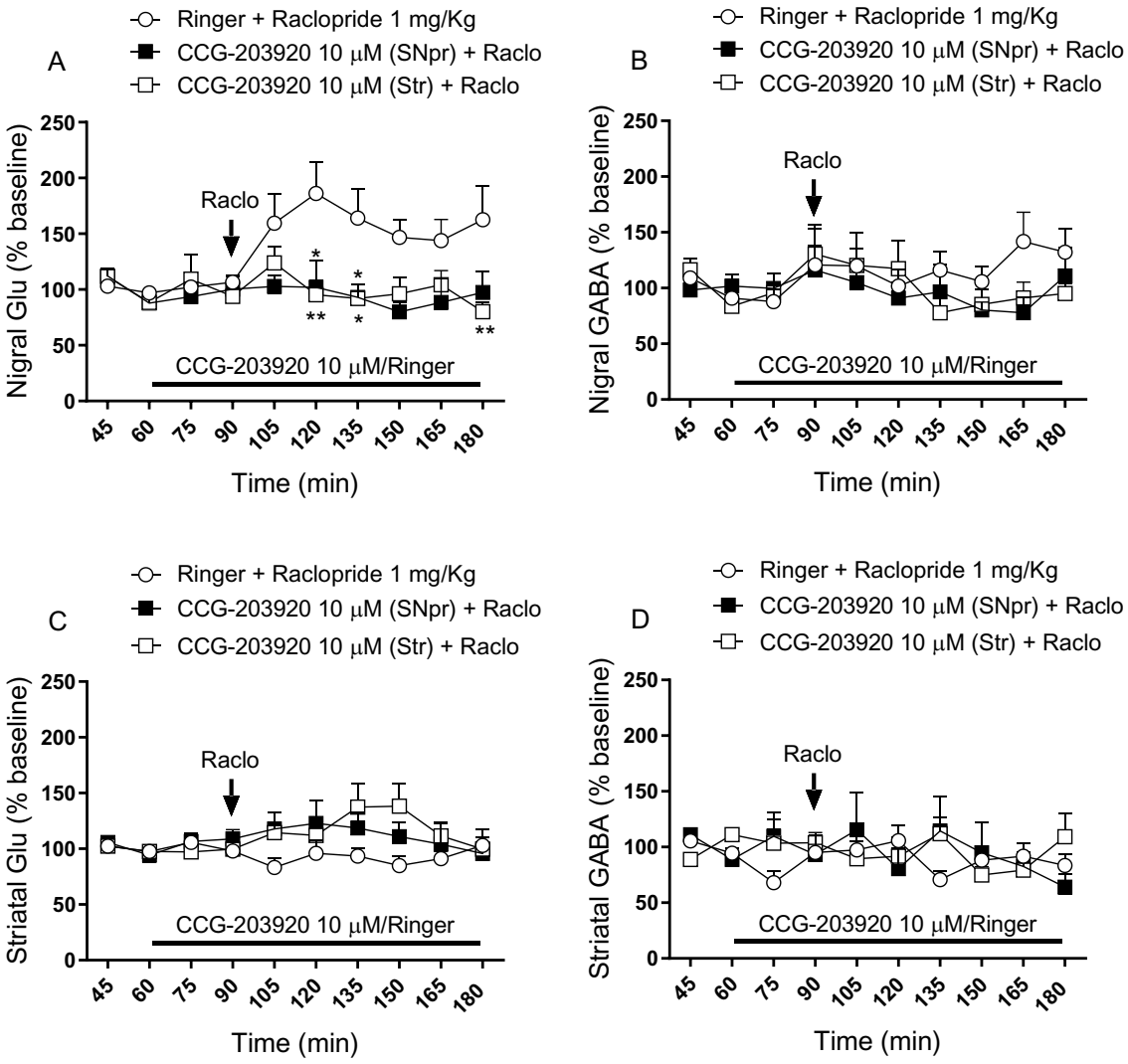

Fig. 7 *Effect of intrastriatal or intranigral reverse dialysis of CCG-203920 on nigral and striatal GABA and glutamate (Glu) levels monitored by microdialysis in raclopride-treated mice. CCG-203920 was perfused in striatum or SNpr (black bar) through the microdialysis probe, starting 30 min before raclopride administration, and maintained until the end of experiment. Values are mean ± SEM of 6 (SNpr) or 5 (striatum) mice per group. *p<0.05, **p<0.01, different from Ringer + Raclopride 1 mg/Kg. Two-way repeated measure ANOVA followed by the Bonferroni post hoc test.*

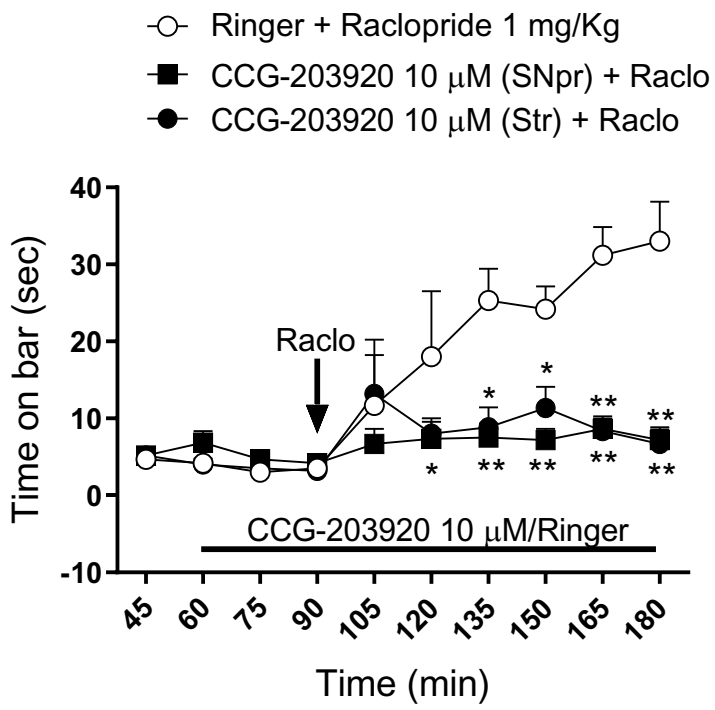

Fig. 8 *Effect of intrastriatal and intranigral reverse dialysis of CCG-203920 on the immobility time in the bar test performed during microdialysis in raclopride-treated mice. CCG-203920 was perfused in striatum or SNpr through the microdialysis probe starting 30 min before raclopride and maintained until the end of experiment. Values are mean ± SEM of 6 mice per group. *p<0.05, **p<0.01 different from Ringer + Raclopride 1 mg/Kg. Two-way repeated measure ANOVA followed by the Bonferroni post hoc test.*

Blockade of striatal mGlu5 receptors did not prevent the attenuation of raclopride effects induced by CCG-203920

In order to disclose which RGS4-regulated GPCR mediates the anti-akinetic effect of RGS4 inhibitors, we focused our attention on those receptors involved in the regulation of basal ganglia functions. In these sets of experiment, we investigated the role of mGlu5 post-synaptic receptors. We reasoned that if mGlu5 receptors were implicated in the anti-akinetic effect induced by RGS4 inhibitors, a selective mGlu5 antagonist (i.e. MTEP) would prevent the antiakinetic effect of CCG-203920 and the associated rise in nigral Glu. Nigral basal levels of Glu and GABA were 58.98±11.85 (n=16) and 9.06±2.06 (n=15), respectively. As expected raclopride induced a rise of nigral Glu levels of the same magnitude in all groups (Fig.9A). Striatal perfusion of MTEP did not alter basal Glu levels or prevent the normalization of nigral Glu induced by CCG-203920 injection (Fig.9A). Basal amino acid levels in striatum were 101.24±21.58 (Glu, n=15) and 5.79±1.20 (GABA, n=15). No significant changes in striatal neurotransmitters were detected following treatments (Fig.9C-D). In line with the neurochemical data, the bar test performed during the microdialysis experiment showed that striatal perfusion of MTEP did not prevent the anti-akinetic effect of CCG-203920 (Fig.10).

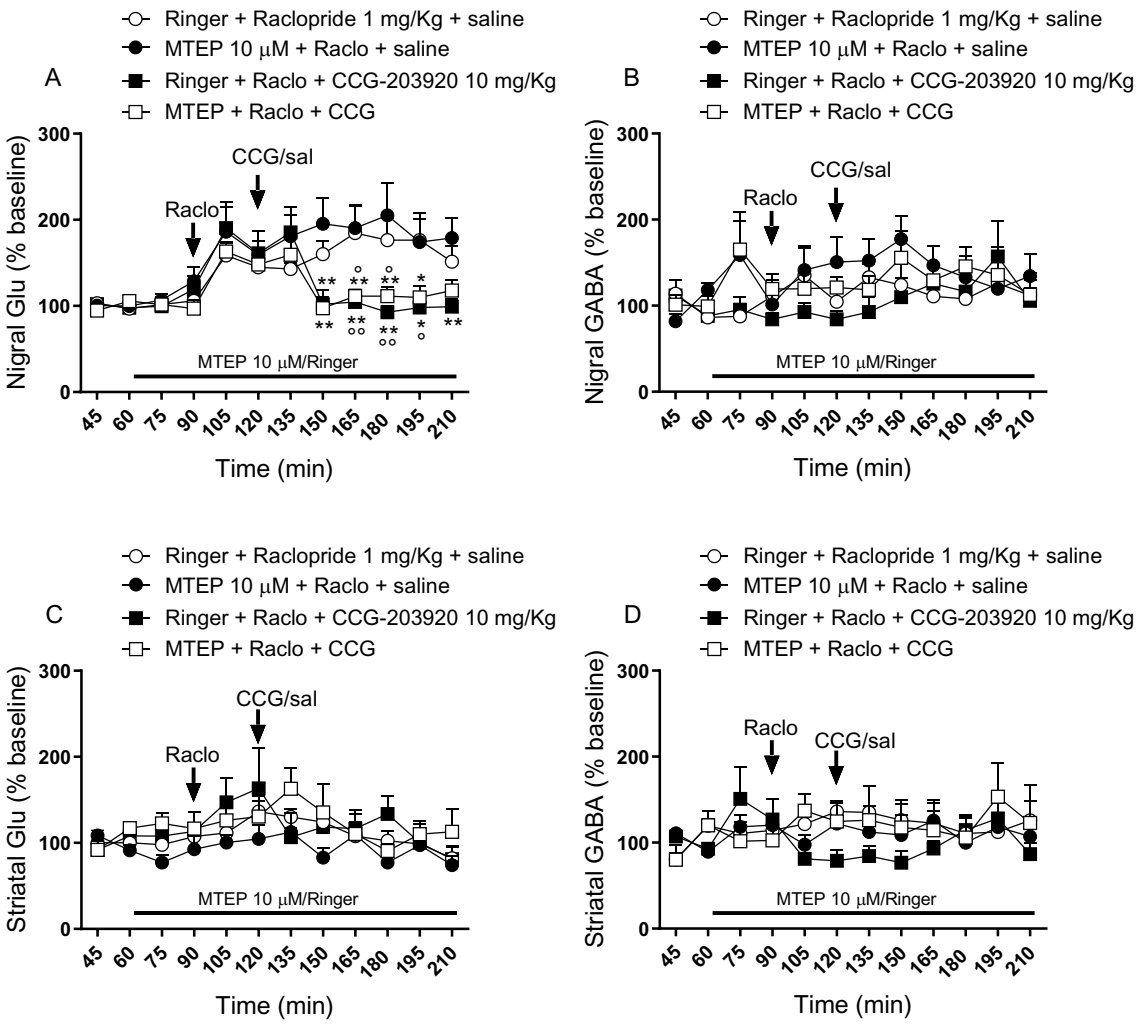

Fig. 9 *Effect of intrastriatal MTEP perfusion (reverse dialysis) on nigral and striatal GABA and glutamate (Glu) levels monitored by microdialysis in raclopride-treated mice. MTEP was perfused in striatum through the microdialysis probe (black bar) starting 30 min before raclopride and maintained until the end of experiment. CCG-203920 (10 mg/Kg i.p.) was administered 30 min after raclopride. Values are mean ± SEM of 8 mice per group. *p<0.05, **p<0.01different from Raclo+CCG-203920 10 mg/Kg. °p<0.05, °°p<0.01, different from Raclo+MTEP+CCG-203920. Two-way repeated measure ANOVA followed by the Bonferroni post hoc test.*

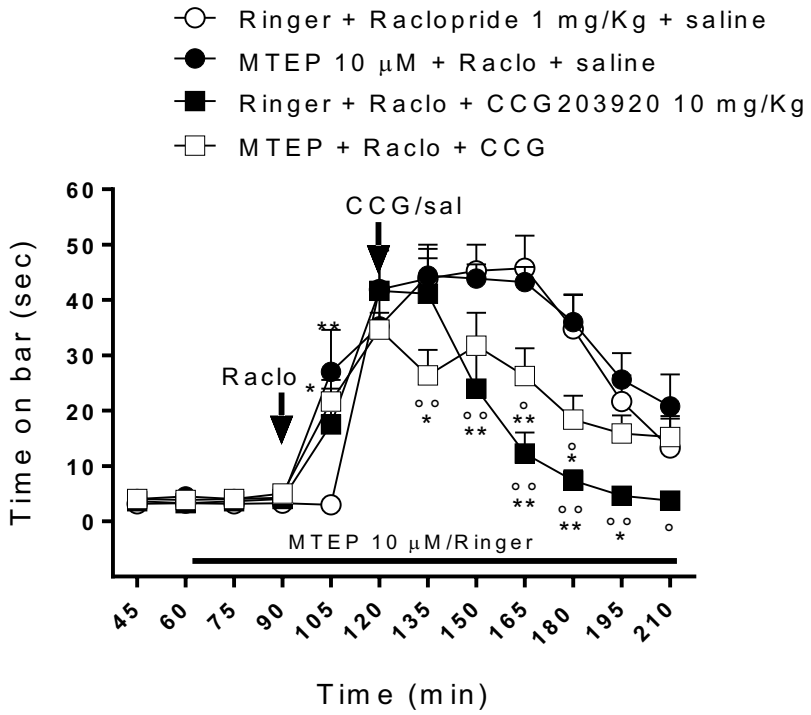

Fig. 10 *Effect of intrastriatal MTEP on the immobility time in the bar test performed during microdialysis in raclopride-treated mice. MTEP was perfused in striatum through the microdialysis probe starting 30 min after raclopride and maintained until the end of experiment. CCG-203920 (10 mg/Kg i.p.) was administered 30 min after raclopride. Values are mean ± SEM of 8 mice per group. *p<0.05, **p<0.01 different from Raclo+ saline. °p<0.05, °°p<0.01 different from MTEP+Raclo+saline. Two-way repeated measure ANOVA followed by the Bonferroni post hoc test.*

CCG-203920 improved haloperidol-induced akinesia in mice

In parallel to the neurochemical assessment, we tried to investigate the impact of RGS4 on the D_2 intracellular pathway, monitoring biochemical markers of the D_2 signaling cascade. In order to achieve our purpose, we decided to use haloperidol (0.3 mg/Kg) since its biochemical effects are well-characterized [82]. Therefore, before performing the molecular analysis, we aimed to demonstrate that, in addition to raclopride-induced akinesia, CCG-203920 was able to reverse haloperidol induced-akinesia. The use of a different neuroleptic would also strengthen the concept that RGS4 inhibition is beneficial for neuroleptic-induced parkinsonism.

Basal motor activity of naïve mice was similar at the right and left paw; therefore, data were pooled together. The immobility time (bar test, Fig.11A) was 4.70±0.70 sec (n=20), the number of steps (drag test, Fig.11B) was 16.9±0.5 (n=20) and the time on rotating rod (rotarod test, Fig.8C; 0-55 rpm range) was 941±31.6 (n=20). In line with that shown for raclopride, haloperidol (0.3 mg/Kg) administration induced a marked akinesia in mice, increasing by six folds the time on bar (34.40±3.5 sec,) and reducing both the number of steps (8.30±0.50, -51%) and the time spent on rod (261±28.8 sec, -72%). CCG-203920 (10 mg/Kg i.p.), improved the motor performance of haloperidol-treated mice, at 90 min after

injection. The effect was significant only in the drag test (Fig.11B) although a clear trend for a reduction of the immobility time was observed (Fig.11A). Conversely, CCG-203920 did not affect the haloperidol-induced inhibition of time on rod (Fig. 11C).

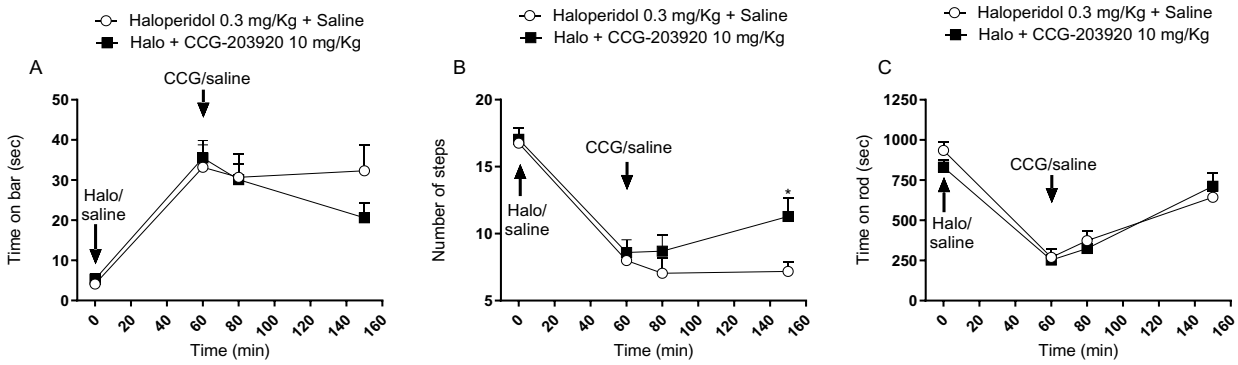

Fig. 11 *Effect of systemic (i.p.) CCG-203920 administration on motor activity in haloperidol-treated mice. Motor activity was evaluated in the bar test (A), drag test (B) and rotarod test (C), and data are expressed as immobility time (sec, A), number of steps (B) and time on rod (C, sec). Values are mean ± SEM of 9 mice per group. *p<0.05 different from Haloperidol 0.3 mg/Kg + saline; (two-way repeated measure ANOVA followed by the Bonferroni post hoc test).*

CCG-203920 enhanced the haloperidol-induced pERK levels in striatum

In order to investigate the impact of our treatment on D_2 signaling, we measured the effect of CCG-203920 on haloperidol-induced pERK levels in striatum.

It is well known that the blockade of striatal D_2 receptors by haloperidol induces an increase in DARPP-32 activity [83] and consequent a rise in the phosphorylation of AMPA receptor subunit, GluR1 [84], and a stimulation of the MAPK pathway with the phosphorylation of ERK [82].

Haloperidol alone was able to increase pERK levels by 99% (Fig.12A), in agreement with previous data [82]. CCG-203920, ineffective alone, induced a further increase in pERK levels when associated with haloperidol (+173%, Fig.12A). Quantification of total protein levels (ERK tot, Fig.12B) showed no effect of CCG-203920, indicating that the changes observed should be related to the activation of the pathway.

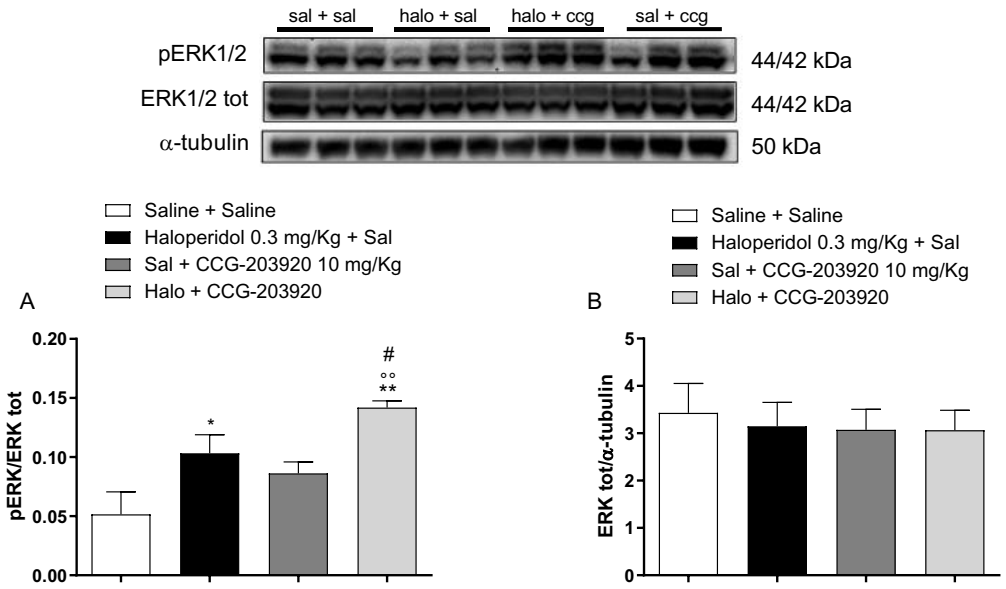

Fig. 12 *CCG-203920 in combination with haloperidol potentiated the MAPK intracellular pathway in striatum. Western blot representative images (upper panel) and quantification (lower panel) of pERK (A) and total ERK (B) in the striatum of naïve mice. Mice were treated with haloperidol (0.3 mg/Kg, i.p.) and/or CCG-203920 (10 mg/Kg, i.p.) and sacrificed 15 min after treatment. Values are mean ± SEM of 4-5 mice per group. *p<0.05, **p<0.01, different from Saline+Saline. °°p<0.01 different from Sal+CCG-203920 10 mg/Kg. #p<0.05, different from Haloperidol 0.3 mg/Kg+Sal. One-way ANOVA followed by Bonferroni post hoc test.*

We also measured pGluR1 levels in striatum (Fig. 13A), but no differences between groups were observed, perhaps due to experimental variability.

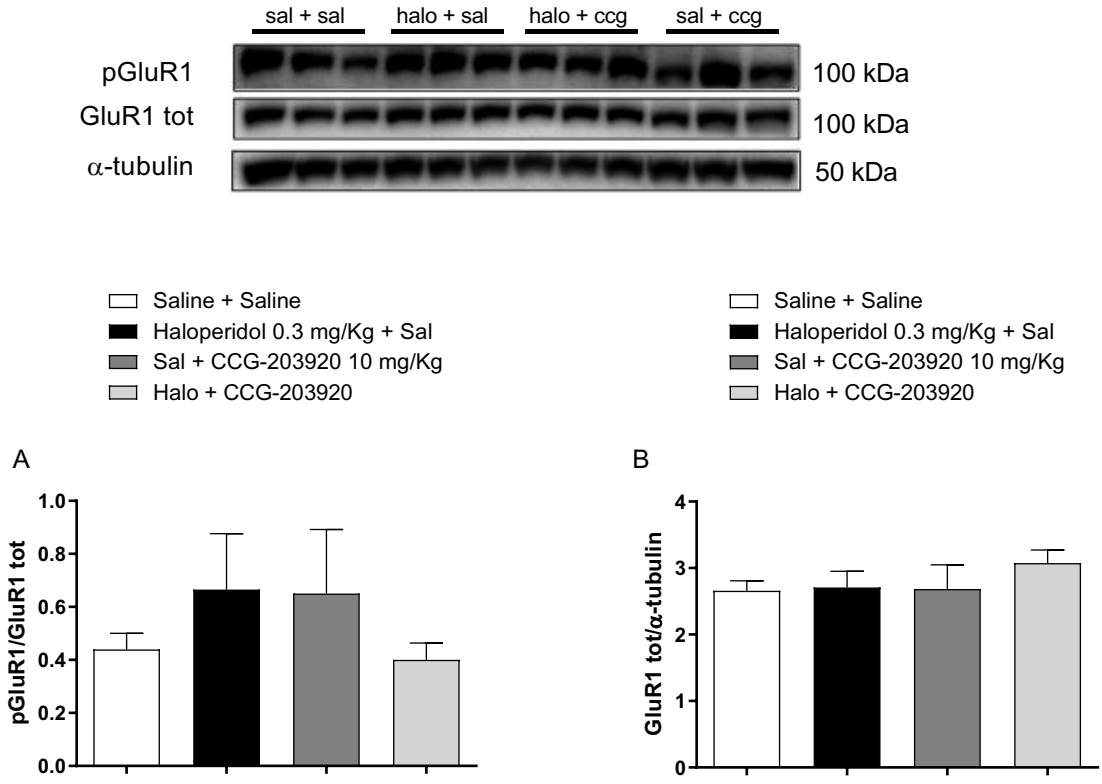

Fig. 13 *Haloperidol and CCG-203920, alone or in combination, did not alter pGluR1 levels in striatum. Western blot representative images (upper panel) and quantification (lower panel) of pGluR1 (A) and total GluR1 (GluR1 tot; B) in the striatum of naïve mice. Mice were treated with haloperidol (0.3 mg/Kg, i.p.) and CCG-203920 (10 mg/Kg, i.p.) and sacrificed 15 min after treatment. In combination experiments, haloperidol and CCG-203920 were administered at the same time. Values are mean ± SEM of 5 mice per group.*

Discussion

We previously reported the antiakinetic effect of a highly selective RGS4 inhibitor, CCG-203769, in raclopride-treated mice, showing for the first time its efficacy in a model of neuroleptic-induced parkinsonism *in vivo* [27]. To confirm the therapeutic potential of the whole class of small molecule RGS4 inhibitors, in the present study we successfully tested another compound of the same chemical class, CCG-203920 [63]. The behavioral assessment showed that CCG-203920 was able to improve raclopride-induced motor impairment in a dose-dependent manner. CCG-203920 replicated the effect of CCG-203769 [27] both in the bar test, which measures akinesia, and in the drag test, which measures akinesia and bradykinesia. However, different from CCG-203769, a mild and delayed positive effect was observed in the rotarod test at the highest dose tested.

One important issue this research should address is which neurochemical mechanism is involved in the antiakinetic effect of RGS4 inhibitors. Using in vivo microdialysis, we previously demonstrated a correlation between haloperidol-induced akinesia and the increase of Glu release in SNpr, a readout of the activation of indirect pathway [70, 75]. The akinesia induced by neuroleptics is due to the blockade of D_2 receptors on iMSNs, which causes inhibition of the thalamus through hyperactivation of the STN [54]. The correlation between the rise of nigral Glu and akinesia is a property of the typical (i.e. first generation) neuroleptics. In fact, in this study raclopride replicated the elevation of nigral Glu previously reported for haloperidol [70, 75]. Therefore, a compound inhibiting raclopride-induced akinesia should also normalize raclopride-induced nigral Glu. Microdialysis showed that both CCG-203920 and CCG-203769 were able to reverse the rise of nigral Glu and the accompanying akinesia in mice. This suggests that RGS4 inhibitors might prevent the overactivity of the indirect pathway associated with blockade of the D_2 receptor in DIP [55], and by extension, with DA neuron loss in PD [85]. Perhaps not too surprising, striatal perfusion of CCG-203920 prevented the raclopride-induced akinesia along with the associated increase of nigral Glu, replicating the effects of its systemic administration. This clearly indicates that CCG-203920 acts in striatum, likely at striato-pallidal MSNs, where both RGS4 [12] and D2 receptors [86] targeted by raclopride [54], are expressed. Nonetheless, RGS4 inhibitors may act at different levels along the indirect pathway to modulate raclopride-induced akinesia. In fact, intranigral perfusion of CCG-203920 was also able to counteract it. This is quite surprising due to the lack of evidence of RGS4 expression in SNpr. However, RGS4 is expressed by nigral DA neurons [12] which plunge their dendrites into SNpr.

Another possible explanation is that at the concentration used CCG-203920 has off-target effects. Although the specificity of CCG compounds should be eventually proven in RGS4 KO mice, we should remind that, as reasoned in the Material and Methods section, the concentration of CCG-203920 used in the perfusion fluid is expected to generate in vivo levels selective for RGS4 blockade relative to RGS8 blockade. These data suggest that RGS4 inhibitors act also outside the striatum, specifically in SNr, to modulate BG functions.

To understand these data, it is necessary to identify which RGS4-modulated GPCR is responsible for the anti-akinetic and anti-glutamatergic effects of RGS4 inhibitors. Unfortunately, our first hypothesis of the involvement of the post-synaptic D_2-A_{2A}-mGlu5 heterotrimer was not proven correct. This specific functional heterotrimer is dramatically implicated in the modulation of iMSNs function [66, 87], possibly with the involvement of RGS4 [60]. Antagonizing D_2 receptors with raclopride, disrupts the function of D_2-A_{2A}-mGlu5 complex, consequently mGlu5 alone is not sufficient to regulate correctly the function of iMSNs. For this reason, our first hypothesis was that RGS4 blockade would cause a reversal of D_2 antagonism effects because of a restoring of the correct regulation of the eCB-LTD, disinhibiting mGlu5 receptor. However, the striatal perfusion of the potent and selective antagonist of mGlu5 receptor, at mGlu5 selective concentrations, did not prevent the CCG-203920 inhibition of raclopride-induced akinesia and nigral Glu release in mice. This ruled out the role of ligagand-mediated activation of mGlu5 in CCG-203920 effects.

As a next target, we hypothesize the involvement of serotonergic system, which is involved in the regulation of BG function. Theoretically, 5HT1 receptors, which are coupled to $G_{i/o}$, and 5HT2 receptors, which are coupled to $G_{q/11}$, could be modulated by RGS4. Previous studies provided evidence of RGS4 modulation of 5HT1 subtypes [15].

In a parallel study, we tried to investigate the impact of the combination of D_2 antagonist and RGS4 inhibitor from a molecular point of view. In fact, it has been shown that typical and atypical neuroleptics differentially regulate gene expression in striatum [82-84], and this effect correlated with their different abilities to elevate pERK levels. In fact, haloperidol-induced a marked and prolonged elevation of pERK whereas clozapine causes a less pronounced and short-lived increase. In addition, clozapine prevented the ability of haloperidol to induce akinesia and *c-fos* expression [88] as well as elevate pERK levels [82]. We then reasoned that a drug with antiakinetic property should attenuate haloperidol-induced pERK levels.

First, we demonstrated that a high dose (10 mg/Kg) of CCG-203920 was able to reduce the akinesia in haloperidol-treated mice. Also, haloperidol injection induced a rise of pERK levels in striatum, as previously reported [82]. Surprisingly, however, CCG-203920 induced a further increase of pERK levels rather that a reduction. Since no effect of CCG-203920 on the expression levels of ERK was observed, we can reasonably relate this effect to the modulation of the activity of D_2 pathway. Therefore, we can conclude that pERK levels do not follow closely the akinesia response. At the moment the mechanism underlying the enhancement of pERK levels induced by RGS4-blockade remains a matter of speculation. It has been shown that haloperidol induces the activation of ERK by antagonizing D_2 receptors [82] and because of this anti-D_2 property, this compound causes parkinsonism. RGS4, as mentioned, cannot regulate directly the G-protein coupled to D_2 receptor, so it is likely to act on another receptor, possibly the 5HT1 receptor. Indeed, $5HT_{1A}$ receptors potentiate D_1 receptor stimulated pERK levels in striatum [89], and RGS4 is involved in $5HT_{1B}$ mediated regulation of the ERK pathway [90]. Moreover, atypical antipsychotics can regulate MAPK cascade through non-dopaminergic mechanisms. For instance, clozapine and quetiapine, which have a low risk to induce DIP, can increase pERK levels in striatum in a D_2-independent manner. Indeed, they can recruit EGFR (epidermal growth factor receptor) [91, 92] to increase striatal pERK. We should also keep in mind that the timing of treatment application performed for the molecular analysis (simultaneous administration of haloperidol and CCG-203920) is different from that of behavioral experiments (CCG-203920 given 60 min after haloperidol). Consequently, the unexpected increase of ERK activation induced by the combination of haloperidol and CCG-203920 might be not related to its antiakinetic effect. This discrepancy is because the phosphorylations are early and transient events [82]. At this point, we should replicate the biochemical experiment under the same conditions of the behavioral study. Moreover, we should more deeply investigate intracellular pathways, extending the molecular analysis to different molecules downstream the D_2 receptor [82-84], such as DARPP-32.

Taken together, our findings confirm that RGS4 inhibitors reverse neuroleptic-induced akinesia, further indicating that they could act both in the striatum and SNpr to counteract cataleptogenic properties of typical neuroleptics. The identification of the GPCR(s) involved in the antiakinetic effect of RGS4 inhibitors would significantly impact the development of the project.

CHAPTER III

Introduction

RGS4 and opioid receptors

RGS4 negatively modulates various GPCRs involved in brain function, such as muscarinic M4, opioid mu (MOP) and delta (DOP), and glutamatergic mGlu5 receptors. It has been shown that RGS4 regulates both MOP and DOP receptors, but the most surprising thing is the highly specific modulation driven by RGS4 on intracellular pathways evoked by these receptors. It has been shown that RGS4 does not affect morphine-induced antinociception but is involved in the reward effect mediated by this drug [93]. Moreover, RGS4 regulates the analgesic properties of MOP receptor agonists, like phentanyl and methadone [93].

Recently, Jutkiewicz and coll [94] published a very interesting work where a highly selective DOP agonist, SNC80, was tested in RGS4 knockout mice. The aim of that study was to investigate whether the different DOP receptor mediated behaviors are regulated by distinct signaling molecules and pathways, in order to improve the safety of DOP receptor agonists. Indeed, DOP receptor agonists are good analgesic drugs and, contrary to the MOP receptor agonists, they do not have side effects like constipation, respiratory depression or abuse liability [95]. Unfortunately, DOP receptor stimulation has a strong pro-convulsant component. Clearly, the knowledge of the underlying mechanisms which drive these effects is crucial to improve the therapeutic efficacy and overall pharmacological profile of a DOP drug. Jutkiewicz and collaborators reported that the genetic deletion of RGS4 or the acute pharmacological blockade of RGS4 by CCG-203769 increased the potency of SNC80 in terms of antinociceptive, antihyperalgesic and antidepressant-like effects, but did not alter the pro-convulsant effect of SNC80 [94].

These findings suggest that RGS4 can selectively modulate DOP-mediated behaviors acting as a negative modulator of some, specific behavioral outcomes. This is very important for drug development in terms of safety improvement and clinical utility.

In this respect, determining the intracellular signaling molecules that regulate specific behaviors might be very useful also to improve the therapeutic potential of Nociceptin/Orphanin FQ (N/OFQ) opioid (NOP) receptor agonists. The NOP receptor is a peculiar ("non-opioid") member of the opioid receptor family [96] and is involved in motor disorders, such as PD [97] and LID [98]. NOP receptor agonists proved to be anti-dyskinetic in animal models of LID [98, 99]. Nonetheless, they also exert strong hypolocomotive/sedative effects [99]. Although previous studies about RGS4 modulation of NOP receptor signaling are controversial [100, 101], in this study we hypothesized that

the blockade of RGS4 can selectively improve the anti-dyskinetic effect of NOP receptor agonism.

L-Dopa induced dyskinesia

After over 50 years of use, L-Dopa is still the most effective drug to treat motor symptoms of PD. Unfortunately, chronic treatment with L-Dopa leads to severe motor complications, among which LID is the most disabling.

LID is a complex disorder with variable clinical phenomenology [102], that can be classified in three forms based on the temporal pattern of the involuntary movement appearance relative to medication intake, that is, peak-dose dyskinesia, diphasic dyskinesia and off-period dystonia [103].

- Peak-dose dyskinesia is related to the peak of plasmatic concentration of L-Dopa and consequently overlaps with the maximal effect of the therapy.
- Diphasic dyskinesia appears right before the ON period and again just before the end of the L-Dopa effect.
- OFF-period dystonia affects the lower limbs with foot inversion, toe flexion, and hallux extension. It tends to be most severe on the side first affected by the disease. It usually appears early in the morning before the first dose of L-Dopa.

LID is a cluster of abnormal involuntary movements, among which are chorea (purposeless, non-rhythmic dance-like movements, which are very common for peak-dose dyskinesia), dystonia (sustained contractions of agonist and antagonist muscles, characterizing all three types of LID), ballism (very large amplitude unilateral or bilateral choreic movements of the proximal parts of the limbs) [102].

Epidemiology and pathophysiology

The prevalence of LID increases along with L-DOPA dosage and therapy duration, and usually emerges 3-5 years after the beginning of chronic administration of L-Dopa. Patients who develop PD at a young age are at highest risk to develop LID. Indeed, a study reported that 70% of PD patients with an age of disease onset between 40 and 49 years developed dyskinesia within 5 years after the start of L-Dopa therapy, whereas, in the same time frame, only 42% of those with an age of onset of 50-59 years developed it [104]. Furthermore, patients with age at onset under 40 years (young-onset PD) had a higher incidence of motor complications than those with late-onset PD [105]. Another risk factor

is the cumulative dose of L-Dopa, indeed there is a direct correlation between the risk of developing LID and the amount of daily dose of L-Dopa. As a matter of fact, one of the strategies to manage LID is to reduce the dose of L-Dopa and increase the frequency of administration, in order to reduce the pulsatile stimulation of dopaminergic receptors.

Another important determinant of LID is the degree of nigrostriatal degeneration. Several preclinical studies showed that the extent of DA neuron loss [106-109] is strictly correlated to the onset and the severity of LID. Indeed, healthy humans or primates do not develop dyskinesia after chronic treatment with therapeutic dosage of L-Dopa, but a chronic exposure to L-Dopa in PD patients and MPTP lesioned monkeys causes severe LID [108].

Loss of dopaminergic neurons leads to dysfunctions in pre- and post- synaptic dopaminergic transmission which are dramatically involved in the pathogenesis of LID. At a presynaptic level, the neurodegeneration of DA neurons leads to severe fluctuations in brain DA levels because of the impaired storage of endogenous DA. This means sudden rise in DA levels in the synaptic space, leading to peak-dose dyskinesia, and a dramatic drop in DA availability, which causes wearing off dyskinesia. In addition, in advanced stages, where the presynaptic dopaminergic system is severely compromised, the striatal serotonergic terminals can functionally assist or replace dopaminergic terminals in converting L-Dopa to DA, and storing DA into vesicles, since they express both aromatic amino acid decarboxylase and VMAT2. Contrary to dopaminergic terminals, however, serotonergic neurons cannot regulate dopamine release, due to the lack of the presynaptic feedback control mediated by D_2 receptors [110]. For this reason, this dysregulated release of dopamine from serotonergic terminals in combination with the intermittent oral intake of L-Dopa contribute to fluctuations in extracellular DA levels and pulsatile stimulation of D_1 receptors which has been demonstrated to underlie the appearance of LID [45, 110]. There are several studies which support this thesis [111], and the key role of the serotonin system has been confirmed by a very recent study in which the BDNF-stimulated increase of serotonergic innervation in the striatum resulted in worsening LID in parkinsonian rats [112].

The striatum in LID

The striatum is the main input nucleus of BG network and has the crucial function of integrating incoming inputs from the cortex and thalamus in order to finely regulate motor behavior.

As previously discussed, the striatum is mainly formed by two large subpopulations of GABAergic MSNs: dMSNs, which project to GPi/SNr and predominantly express dopaminergic D_1 receptors, and iMSNs, which project to GPe and predominantly express dopaminergic D_2 receptors [45, 113].

Stimulation of dMSNs facilitates motor activity through inhibition of the GPi/SNr and potentiation of the transmission between the thalamus and cortex. By contrast, stimulation of iMSNs inhibits the GPe leading to disinhibition of subthalamic glutamatergic transmission towards the GPi/SNpr. The result is a decrease of thalamo-cortical firing and inhibition of voluntary movement [43]. Dopamine positively modulates voluntary movement, increasing excitability of dMSNs via D_1 receptors and decreasing the excitability of iMSNs via D_2 receptors.

In dyskinetic conditions, striatal dMSNs are overactive, resulting in a reduction in GPi/SNpr activity, as widely demonstrated by in vivo microdialysis studies showing an increase of GABA release in SNpr [72, 114, 115] and a reduction of GABA levels in the thalamus [116, 117] after L-Dopa injection in dyskinetic animals.

It has been demonstrated that the overactivity of dMSNs is due to upregulation of D_1 receptor signaling. In the DA-depleted striatum of hemiparkinsonian rats or parkinsonian patients, G_{olf} is upregulated resulting in an enhancement of DA-stimulated cAMP production [45], cAMP-dependent protein kinase A (PKA) activation and increased phosphorylation of the dopamine- and cAMP-dependent phosphoprotein of 32 kDa (DARPP-32) [118, 119], which is selectively expressed in striatal MSNs, at Thr34 (pThr34-DARPP-32). Consistently, the striatum of dyskinetic rats contains abnormally high levels of pThr34-DARPP-32 [120]. These data were confirmed in MPTP lesioned non-human primates, where the hypersensitization of striatal D_1 receptors has also been reported [121]. pThr34-DARPP-32 is a potent inhibitor of protein phosphatase-1(PP-1), an important dephosphorylating protein, resulting in an amplification of D_1 receptor related responses [122]. Moreover, pThr34-DARPP-32 plays a crucial role in the modulation of ERK1/2 [123], promoting the phosphorylation of these two mitogen-activated kinases. Specifically, pThr34-DARPP-32 activates the mitogen-activated protein kinase/ERK

kinase (MEK) and at the same time inhibits the striatal-enriched phosphatase STEP, which dephosphorylates ERK [123].

The increased expression and hypersensitivity of D_1 receptors and signaling pathway at dMSNs after L-Dopa treatment, and the fact that D_2 receptor levels expressed by iMSNs are quite unaffected by L-Dopa treatment [121], indicate that dMSNs have a predominant role in sustaining LID manifestation [124]. To reinforce the evidence of a key role of the overactive dMSNs in LID, a recent study showed that a specific group of dMSNs in the dorsolateral striatum is very active during the expression of dyskinesia, and that optogenetic inhibition of these neurons led to a significant reduction of the severity of LID [125].

Although the crucial role of the dMSNs in LID is well established, the involvement of iMSNs remains to be clarified. During LID, dramatic synaptic remodeling in iMSNs has been observed [45, 126], which could be reversed by the chemogenic stimulation of these neurons [126]. Moreover, the activation of iMSNs can inhibit the prodyskinetic property of L-Dopa in 6-OHDA lesioned mice, likely by the modulation of pallido-suthalamic pathway or by the collateral inhibition of the dMSNs at the striatal level [127]. Taken together, all the data suggest that L-Dopa leads to dyskinesia through the aberrant activation of a specific group of dMSNs via D_1 receptor in combination with the D_2 driven hypoactivity of iMSNs. Today, our knowledge is deeper than in the past, but we still do not have the clear and full view of the mechanisms underlying LID. Research is still ongoing.

Management of LID

Nowadays, there is no drug that can prevent LID development when chronically combined with L-Dopa, but clinicians can use several strategies to manage the dyskinetic condition and ameliorate the life quality of PD patients [128, 129].

First, a good strategy is the adjustment of DA replacement therapy by reducing the dose of L-Dopa and increasing the frequency of daily administration and/or adding a DA receptor agonist. To attain stable levels of L-Dopa and reduce motor fluctuations, new L-Dopa formulations are available, such as modified release medications, such as prolonged release combinations of L-Dopa and carbidopa or entacapone.

- *Duodopa*®: Duodopa is a gel delivered to intestinal tract via a PEG-J tube which is connected to a portable infusion pump. The pump delivers the drug gel continuously in the proximal small intestine, providing a more stable plasma L-Dopa concentration and a continuous stimulation of the dopaminergic receptors in

the striatum [130]. The last report [131], in agreement with previous studies, showed that 6 months after Duodopa® therapy, the motor complications and dyskinesia were significantly improved in all PD patients, along with depression and anxiety.

- *Non-dopaminergic treatments*:
  - *Amantadine*. Amantadine is the only drug with clinical based evidence of anti-dyskinetic effect in PD patients with motor fluctuations. The therapeutic effect is likely due to its antagonism at the glutamatergic NMDA receptor. The first evidence of amantadine efficacy was reported in 1998 in a small group of PD patients [132], where this drug significantly decreased the severity of peak-dose dyskinesia. After this first study, several clinical trials confirmed the anti-dyskinetic property of amantadine [128].
  - *Antiepileptic drugs*. Although there were promising results in dyskinetic macaques, levetiracetam did not produce a beneficial effect of on levodopa-induced dyskinesia in patients [133].
  - *Safinamide*. Safinamide has a dual mechanism of action, i.e MAO-B blockade and Glu release inhibition [134-136]. First discovered as anticonvulsant, it has been recently approved as add-on therapy with L-Dopa in mid- to late-stage fluctuating idiopathic Parkinson disease [137]. Safinamide has been found effective in attenuating established dyskinesia in MPTP-treated macaques [138] but not 6-OHDA hemilesioned rats [139]. In humans, safinamide did not significantly reduce dyskinesia in the overall population of PD patients enrolled in Study018 [137], although post-hoc analysis revealed a beneficial antidyskinetic effect in a subgroup of patients showing higher dyskinetic scores at baseline [140].
  - *Antipsychotic drugs*. Clozapine has a proven anti-dyskinetic effect, but the mechanism of action is unknown. The proposed mechanism of action includes antagonistic binding to striatal dopamine D_2 and serotonin $5HT_{2A}$. By the way, another drug from the same chemical family, quetiapine, which shows antagonistic properties on $5HT_{2A}$ has a very mild antidyskinetic effect with severe side effects, such as drowsiness and sedation [102].
  - *Eltoprazine*. It is a partial agonist of serotonergic $5HT_{1A/B}$ receptors. Eltoprazine therapeutic effect is thought to be due to the stimulation of presynaptic serotonergic autoreceptors and reduction of ectopic DA release

from serotonergic terminals. After solid preclinical evidence, clinical studies have shown mild antidyskinetic efficacy [102].

- *Deep Bran Stimulation* (DBS). DBS is a surgical practice in which an electrode is implanted in the STN or GPi of selected PD patients with severe motor fluctuations. The GPi-DBS showed very strong results although the underlying mechanism is not clear. Some studies suggest that the therapeutic effect is due to the stimulation of the inhibitory activity of GPe terminals in GPi or the collaterals of GPi neurons in the posterior ventral pallidus. Others suggest that the stimulation of the GPi reverses the abnormal neuronal activity in the BG network in the dyskinetic condition. Also, STN-DBS proved beneficial for PD symptoms and also improved LID. During surgery, however, a lesion of STN could occasionally occur and dyskinesia could appear in the patient. Usually, this is a temporary event and surgeons use this as readout of the correct placement of the electrode. The implant-induced dyskinesia lasts for a short period after surgery but if it persists an additional GPi implantation could be done. Again, the mechanism is not clear, but it is believed that the beneficial effects of DBS on dyskinesia are due to the reduction of L-Dopa daily dosage [128].

N/OFQ/NOP receptor system and LID

Since the discovery of the NOP receptor [141] and N/OFQ as its endogenous ligand [142, 143], different studies disclosed a role of the N/OFQ-NOP receptor system in pathological conditions, such as PD and LID.

Paradoxically classified as a non-opioid member of the opioid receptor family [141], the NOP receptor is a GPCR coupled to Gi/o. The NOP receptor is structurally very similar to other members of the opioid receptor family. More than 70% amino acid residues are conserved through these receptors, although its pharmacology and biology are quite different [96]. Indeed, the NOP receptor does not bind classical opioid ligands, likewise N/OFQ does not bind to the classical opioid receptors [141]. For instance, N/OFQ is a heptadecapeptide, structurally very close to an opioid peptide, dynorphin A [142, 143], which is considered a selective, endogenous ligand of the kappa opioid (KOP) receptor. However, N/OFQ has a 1000-fold lower affinity for the KOP than for the NOP receptor [144]. Moreover, N/OFQ has no affinity for the MOP or DOP receptors. Therefore, the N/OFQ-NOP–receptor system is a pharmacologically independent system, distinct from the classical opioid systems. Following activation of the receptor, the Gα subunit

dissociates from the Gβγ, causing the deactivation of the adenylate cyclase (AC) and, consequently, a drop of intracellular levels of cAMP. In the meantime, the Gβγ dimer interacts with specific effectors, such as K^+ channels, leading to cell hyperpolarization. Moreover, the NOP receptor negatively regulates voltage-dependent calcium channels [96]. It has also been shown that the NOP receptor is also involved in several downstream events, such as the phosphorylation of MAPKs [145] or protein kinase C [146], the modulation of gene transcription/transduction [147], cytoskeleton rearrangement [148] and chemotaxis [149]. Specifically, we should mention that the activation of ERK is G protein dependent and is abolished when PKC is blocked [150]. Moreover, through the activation of ERK, the NOP receptor can induce the transcription of Elk-1 and Sap1a [151].

N/OFQ and the NOP receptor are expressed throughout the CNS and in many peripheral organs of rodents [152, 153], nonhuman primates [154, 155] and humans [156, 157].

NOP receptors are expressed in several brain regions involved in a large number of central functions including pain, learning and memory, mood, neuroendocrine control, food intake and motor control [96]. Specifically, NOP receptors are found in high amount in pain-related brain regions, such as the periaqueductal gray (PAG), thalamic nuclei, somatosensory cortex, rostral ventral medulla, lateral parabrachial nucleus, spinal cord, and dorsal root ganglia (DRGs)[153, 158]. NOP receptor activation in supraspinal regions leads to the blockade of the actions of opiate analgesics [159, 160], which explains the anti-opioid effects of N/OFQ when administered intracerebroventricularly. Moreover, NOP receptors are also highly expressed in regions involved in in the meso-cortico-limbic reward circuitry, such as ventral tegmental area (VTA), nucleus accumbens, prefrontal cortex, central amygdala and medial habenula-interpedunclear nucleus [158]. Consistent with their central anti-opioid effects, NOP agonists attenuate the rewarding effects of opiates and other drugs of abuse. The NOP receptor mediates primarily inhibitory functions, since in these brain regions, it reduces the release of the neurotransmitters (e.g. DA) that mediate rewarding effects [96].

N/OFQ and the NOP receptor are involved in regulation of motor function [97]. It has been shown that they are expressed in VTA and SNpc, specifically the NOP receptor is on dopaminergic neurons and N/OFQ in non-dopaminergic, likely GABAergic, interneurons [161]. N/OFQ injected in the cerebral ventricle or SNr causes dual regulation of motor function, with stimulation observed in a narrow range of low doses, and inhibition in a wider range of high doses [162, 163]. Thus, motor inhibition predominates, as also confirmed by motor inhibition induced by small molecule NOP receptor agonists, and by motor facilitation induced by NOP receptor antagonists [80, 164]. Although reduction of

DA release could explain the motor inhibiting effect of N/OFQ, an additional mechanism might be represented by the modulation of DA signals at MSNs. In fact, in 2008, it was shown that N/OFQ reduced D_1 receptor-induced cAMP production in the nucleus accumbens and dorsal striatum [165] and more recently that N/OFQ or the small molecule NOP receptor agonist AT-403 inhibited the D_1 receptor-stimulated number of ERK-positive neurons in striatum [98, 99]. Indeed, NOP and D_1 receptors appear to co-localize postsinaptically, on the dendritic spines of MSNs [165].

The first evidence of the involvement of N/OFQ-NOP receptor system in PD was published in 2002 [161]. Since then, a number of studies have confirmed a pathogenic up-regulation of N/OFQ transmission in the parkinsonian brain, disclosing that NOP receptor antagonists improve parkinsonian motor symptoms and provide neuroprotective benefits in rodent and non-human primate models of PD [164]. Relevant to the present study, N/OFQ and NOP receptor agonists proved to exert anti-dyskinetic effects in animal models of LID [98, 99]. Indeed, N/OFQ or NOP receptor agonists Ro 65-6570, AT-403 and AT-390, reduced the severity of abnormal involuntary movements (AIMs) in L-DOPA-primed rats or nonhuman primates [98, 99]. However, it is known that NOP receptor stimulation causes sedation [96]. While Ro 65-6570 did not show any sedative effect in treated animals, the more selective NOP receptor agonists, AT-403 and AT-390 induced strong sedation/hypolocomotion, that at least partly overlapped the anti-dyskinetic effect. However, for AT-403 a single dose (0.03 mg/Kg) was identified in which the anti-dyskinetic effect was dissociated from the sedative one. Unfortunately, this dose induced just a mild and transient antidyskinetic effect [99].

RGS4 and LID

The role of RGS4 in LID is quite unexplored but published literature suggests that RGS4 blockade might be useful to improve the dyskinetic condition. An elegant study in a rat model of LID [28] demonstrated that a positive allosteric modulator (PAM) of muscarinic M4 receptor reduced AIM severity. These Authors suggested that the hypofunction of the muscarinic M4 receptor in striatal cholinergic interneurons is involved in the increased acetylcholine release during LID. Since RGS4 is upregulated in cholinergic interneurons after dopamine depletion [25], it was hypothesized that RGS4 upregulation is responsible of the inhibition of the M4-driven negative feedback on acetylcholine release. Another group reported a reduction of AIMs development in a rat model of LID, following repeated RGS4 blockade with antisense oligonucleotides [29]. Based on this evidence, it is quite

clear that a potential antidyskinetic strategy targeted on RGS4 might focus on RGS4 inhibitors.

Aim of the study

As mentioned before, the antidyskinetic effect of AT-403 partly overlapped with its sedative effect. Nonetheless, we identified an AT-403 dose (0.03 mg/Kg) at which the anti-dyskinetic effect was dissociated from the sedative one. Unfortunately, this dose induced just a mild and transient antidyskinetic effect. Therefore, we asked whether it could be possible to improve the antidyskinetic property of AT-403 without at the same time affecting its sedative properties, in other words widen the therapeutic window, by modulating the signaling cascade downstream the NOP receptor. To this aim we decided to target RGS4.

Indeed based on previous literature we know that: i) RGS4 might be a negative modulator of NOP receptor signaling, since this GPCR is coupled to a Gi/o protein; ii) these two proteins share the same distribution in brain and in neuronal subpopulations, iii) considering the strong functional and morphological analogies between NOP and the classical opioid receptors, previous studies have reported the ability of RGS4 to negative modulate MOP [100] and DOP [94] receptors.

To verify our hypothesis, we investigated this interaction between RGS4 and NOP receptor in transfected HEK293T cells, then in a native system, represented by striatal slices of naïve mice. Then, the effect of a highly selective RGS4 inhibitor, CCG-203920, on the anti-dyskinetic effect of AT-403 in a rat model of LID was evaluated. We assessed the effect of AT-403 in the presence or the absence of CCG-203920 both on the expression of AIMs and the global motor performance in the rotarod test. Then, we investigated the impact of our treatments on two molecular markers of LID in rodents, i.e. the increase of pERK and pGluR1 levels in the dyskinetic striatum.

Materials and methods

In vitro experiments

Cell culture and transfection

Human embryonic kidney (HEK-293T) cells were maintained in a humidified incubator at 37°C with 5% CO2 and grown to 90-95% confluence in Dulbecco's modified Eagle's medium (DMEM) supplemented with 10% fetal bovine serum (FBS), 100 U/ml penicillin and 100 µg/ml streptomycin. Cells were transfected using Lipofectamine 2000 according to the manufacturer's recommended protocol. All transfections were performed under serum-free conditions in Opti-MEM. Transfections were allowed to proceed for 4-5 h before the media was changed back to DMEM with 10 % FBS. Experiments were run 24 h after transfection. For cAMP assays, cells were plated in 6-mm dishes. DNA was kept constant at 6 µg and 6 µl of Lipofectamine2000 per plate was used. Empty vector (pcDNA3.1+) was used to adjust the total amount of DNA. The absence of any changes in pcDNA3.1+ transfected cells and the variations in cAMP levels in D_1/NOP transfected cells after treatment with specific ligands were used as a functional readout of the transfection [166]. This is possible because HEK293T cells do not natively express D_1/NOP receptors. In Fig.1 is a schematic representation of the protocol.

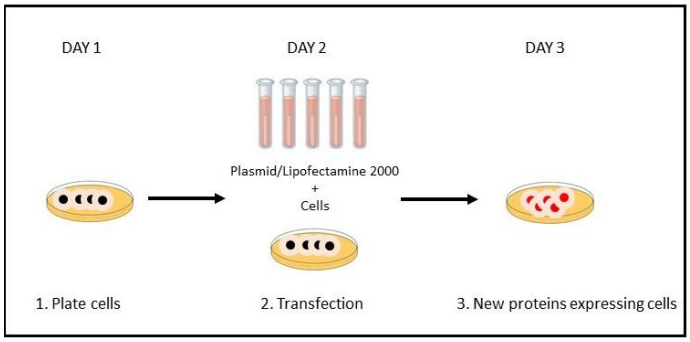

Fig. 1 Schematic representation of transfection protocol in HEK293T cells.

cAMP measurements in HEK293T cells

LANCE Ultra cAMP assays (Perkin Elmer; Waltham, MA) were performed in accordance with the manufacturer's instructions. Briefly, the day before the assay, HEK-293T cells were transfected as indicated above. On the day of experiment, cells were dissociated from dishes using Versene 1M. Then cells (2,000 cells/well in 5µl) were transferred to a white

384-well microplate (Perkin Elmer) and incubated with various concentrations of N/OFQ and SKF-38393 (D_1 receptor agonist; final 40 nM; 5 µl/well) for 30 min at room temperature. A cAMP standard curve was generated in triplicate according to the manual. Finally, europium (Eu)-cAMP tracer (5 µl) and ULight™-anti-cAMP (5 µl) were added to each well and incubated for 1 h at room temperature. The plate was read on a TR-FRET microplate reader (Synergy NEO; Biotek, Winooski, VT). In Fig.2, a simplified protocol for cAMP assay is shown.

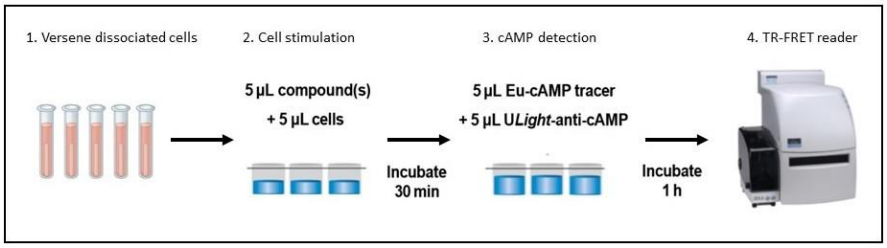

Fig. 2 Schematic representation of cAMP assay protocol.

ERK measurement in vitro

Adult male C57Bl6 mice were decapitated after cervical dislocation, and brain slices were freshly prepared according to the protocol previously described [98, 99]. The brains were rapidly removed and put on a cool glass plate filled with ice-cold sucrose-based dissecting solution (87 mM NaCl, 2.5 mM KCl, 7 mM MgCl2, 1 mM NaH2PO4, 75 mM sucrose, 25 mM NaHCO3, 10 mM D-glucose, 0.5 mM CaCl2, 2 mM kynurenic acid), carbogenated (95% O2, 5% CO2) and subsequently mounted on the vibratome stage (Vibratome, VT1000S-Leica Microsystems); 200-µm-thick slices were cut and transferred into a brain slice chamber (Brain slice chamber-BSC1 – Scientific System design Inc., Mississauga, ON, Canada) and allowed to recover for 1 h at 32°C, with a constant perfusion of carbogenated artificial CSF (ACSF: 124 mM NaCl, 5 mM KCl, 1.3 mM MgSO4, 1.2 mM NaH2PO4, 25 mM NaHCO3, 10 mM D-glucose, 2.4 mM CaCl2). The D1 receptor agonist SKF38393 (100 µM) was applied for 10 min in the presence of AT-403 (30 nM), CCG-203920 (500 nM) or vehicle. After fixation in 4% paraformaldehyde (PFA) for 15 min at room temperature, slices were rinsed three times in PBS and cryoprotected in 30% sucrose solution overnight at 4°C. On the following day, slices were further cut into 18-µm-thick slices using a cryostat (Leica CM1850) and mounted onto SuperFrost Plus slides (Thermo Scientific). Immunohistochemistry was performed following the protocol described in Papale et al. [167]: 1 h after blocking in 5% normal goat serum and 0.1% Triton X-100

solution, slices were incubated overnight at 4°C with anti-phospho-p44/42 MAP kinase (Thr202/Tyr204) (1:1000, Cell Signaling Technology cat. #4370 L). Sections were then incubated with biotinylated goat anti-rabbit IgG (1:200, Vector Laboratories, cat. #BA-1000) for 2 h at room temperature. Detection of the bound antibodies was carried out using a standard peroxidase-based method (ABC-kit, Vectastain, Vector Labs), followed by a 3,3'-diamino-benzidine (DAB) and H_2O_2 solution. Images were acquired from the striatum at 40× magnification using a brightfield microscope (Leica Macro/Micro Imaging System), and the number of pERK positive cells in the striatum was counted in each slice.

In vivo experiments

Animals

Male Sprague-Dawley rats (150 g, Charles River, Calco, Italy) were housed in the new animal facility of University of Ferrara, LARP, with free access to food and water, under regular lighting conditions (12 hr dark/light cycle). Animals were housed in groups of 2 for a cage with environmental enrichments. At the end of the experiments, rats were killed with an overdose of isoflurane. Experimental procedures involving the use of animals were approved by the Ethical Committee of the University of Ferrara and the Italian Ministry of Health (license 714/2016-PR). Adequate measures were taken to minimize animal pain and discomfort. Seven 3-month-old male C57Bl6 mice were used for ERK studies in slices in vitro. Mice were housed in a standard facility at Cardiff University, under regular conditions of light (12 h light/dark cycle), with food and water ad libitum. Experimenters were blinded to treatments.

Unilateral 6-OHDA lesion

Unilateral lesion of dopaminergic neurons was carried out under isoflurane anaesthesia as previously described [70]. The neurotoxin 6-OHDA (12.5 μg free base, dissolved in 0.9% saline solution containing 0.02% ascorbic acid) was stereotactically injected in the medial forebrain bundle according to the following coordinates from bregma: antero-posterior = -4.4 mm, mediolateral = ±1.2 mm, dorsoventral = -7.8 mm below dura [168]. In order to select rats that were successfully hemi-lesioned, 2 weeks after 6-OHDA injection, motor impairment was assessed though two motor tests (bar-, drag-test) [70].

L-DOPA treatment and abnormal involuntary movements rating

Rats that successfully performed bar and drag test were treated for 21 days with L-DOPA (6 mg/kg + benserazide 15 mg/kg, s.c., once daily) to induce AIMs, a correlate of LID, as previously described [79, 98, 99, 115]. This represents the best validated model of dyskinesia in rodents [128, 169, 170]. Rats were observed for 1 min, every 20 min, during the 3 h that followed L-DOPA injection or until dyskinetic movements ceased. Dyskinetic movements were classified based in their topographical distribution into three subtypes [169, 170]: (i) axial AIM, that is, twisted posture or turning of the neck and upper body toward the side contralateral to the lesion; (ii) forelimb AIM, that is, jerky and dystonic movements and/or purposeless grabbing of the forelimb contralateral to the lesion; and (iii) orolingual AIM, that is, orofacial muscle twitching, purposeless masticatory movement and contralateral tongue protrusion. Each AIM subtype was rated on a frequency scale from 0 to 4 (1, occasional; 2, frequent; 3, continuous but interrupted by an external distraction; 4, continuous and not interrupted by an external distraction). In addition, the amplitude of these AIMs was measured on a scale from 0 to 4 based on a previously validated scale [170]. Axial, Limb and Orolingual (ALO) AIMs total value were obtained as the sum of the product between amplitude and frequency of each observation [170]. Therefore, to be considered fully dyskinetic, an animal has to score ≥ 100. In the Fig.3, it is shown the experimental design.

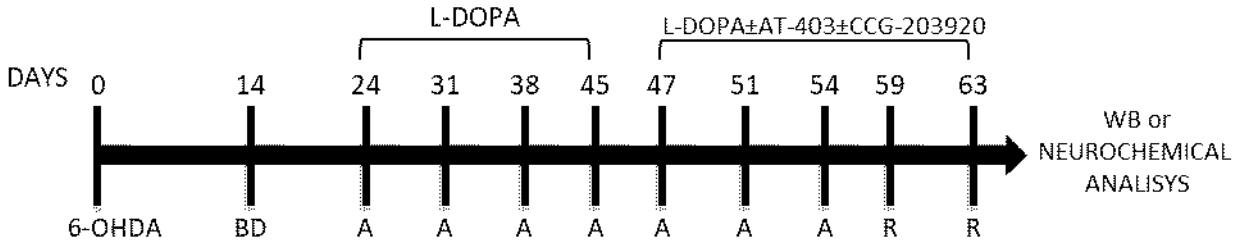

Fig. 3 *Experimental design.*

Western blot analysis

Dyskinetic rats were treated with saline or CCG-203920 (10 mg/Kg, i.p.), five minutes later with AT-403 (0.03 mg/Kg) or saline, and 10 min later with L-DOPA (6 mg/Kg + benserazide 12mg/Kg, s.c.). Thirty minutes after L-DOPA, rats were anesthetized with isoflurane, killed by decapitation and striata rapidly dissected and frozen in liquid nitrogen and stored at -80°C until analysis. Tissues were homogenized in lysis buffer (SDS buffer, protease inhibitor cocktail and phosphatase inhibitor cocktail) and centrifuged at 18000×g at 4°C for 15 min. Supernatants were collected, and protein levels were quantified using

the bicinchoninic acid protein assay kit (ThermoScientific). Thirty micrograms of protein per sample were separated on a 4-12% gradient polyacrylamide precast gels (Bolt® 4-12% Bis-TrisPlus Gels, Life Technologies) in a Bolt® Mini Gel Tank apparatus (Life Technologies). Proteins were then transferred onto a polyvinyldifluoride membrane, blocked for 60 min with 5% non-fat dry milk in 0.1% Tween20 Tris-buffered saline and incubated overnight at 4°C with anti-Thr202/Tyr204-phosphorylated ERK1/2 (pERK) rabbit monoclonal antibody (Merck Millipore, cat. #05-797, 1:1000), anti-ERK1/2 (totERK) rabbit polyclonal antibody (Merck Millipore cat. #06-182, 1:5000), anti-phospho-Ser845 GluR1 (pGluR1) rabbit polyclonal antibody (PhosphoSolution, #p1160-645 1:1000), anti-Glutamate receptor 1 (totGluR1) rabbit polyclonal antibody (Merck Millipore #AB1504, 1:1000), anti-Tyrosine hydroxylase (TH) rabbit monoclonal antibody (Merck Millipore, #AB152,1:1000), anti-αtubulin (αTub) rabbit monoclonal antibody (Merck Millipore, #04-1117, 1:25000).

Membranes were washed, then incubated 1 h at room temperature with horseradish peroxidase-linked secondary antibodies (Merck Millipore, cat. #12-348, 1:2000). Immunoreactivity was visualized by enhanced chemiluminescence detection kit (Perkin Elmer), and images were acquired using the ChemiDoc MP System quantified using the Image Lab Software (Bio-Rad). Membranes were then stripped and re-probed with rabbit monoclonal anti-tubulin antibody (Merck Millipore, cat. #04-1117,1:50000). Data were analyzed by densitometry, and the optical density of specific totERK, totGluR1, RGS4 or TH bands was normalized to the corresponding tubulin levels. The optical density of specific pERK and pGluR1 bands were normalized on totERK and totGluR1 levels, respectively [99].

Statistical analysis

Motor performance was expressed as time (in seconds) on rod (rotarod-test). The AIMs rating was expressed as the ALO score (frequency x amplitude). Statistical analysis was performed by parametric one-way ANOVA, two-way repeated measure ANOVA or Student t-test, as appropriate. ALO AIMs data were analyzed by non-parametric ANOVA followed by the Dunn's test, or by the Mann-Whitney test when only two groups were compared. P values <0.05 were considered statistically significant.

All data was analyzed using GraphPad Prism 8.0 (GraphPad; LaJolla, CA).

Materials

AT-403 (2-(1-(1-((1s,4s)-4-isopropylcyclohexyl)piperidin-4-yl)-2-oxoindolin-3-yl)-Nmethylacetamide) was synthesized by Dr NT Zaveri at Astraea Therapeutics (Mountain View, CA, USA). CCG-203920 was obtained from Prof Richard R Neubig (Michigan State University, East Lansing, MI, USA). L-DOPA and benserazide were purchased from Sigma-Aldrich (Milano, Italy). 6-OHDA hydrobromide and N/OFQ were purchased from Tocris Bioscience (Bristol, UK). AT-403 was dissolved in 2% CH3COOH 1M and 4% DMSO water, L-DOPA, benserazide and CCG-203920 were dissolved in saline, 6-OHDA was dissolved in 0.02% ascorbic acid saline. N/OFQ and SKF38393 were dissolved in water. LANCE Ultra cAMP assay was purchased from Perkin Elmer (Waltham, MA). All plasmids were purchased from cDNA Resource center (Bloomsburg, PA).

Results

In vitro experiments

RGS4 negatively modulates NOP receptor-driven inhibition of D_1-stimulated cAMP production in HEK293T cells

The crosstalk between NOP and RGS4 was investigated in a cellular model. To this aim, we used as a readout the inhibition of D_1-stimulated cAMP production driven by the $G\alpha_{i/o}$ coupled to the NOP receptor in HEK293T cells. We performed the assay with two different compounds, the NOP receptor endogenous ligand (N/OFQ), and the small molecule agonist, AT-403, which was used in the in vivo experiments.

In cells transfected with the NOP receptor only (Fig.4), N/OFQ inhibited in a concentration-dependent manner cAMP production stimulated by SKF-38393 (40 nM). In these conditions, N/OFQ showed a pIC_{50}=7.82 and a maximal inhibition of cAMP production of 60%. Co-transfection of RGS4 with the NOP receptor caused a rightward shift of the concentration-response curve of N/OFQ (Fig. 4) with a reduction of its potency (pIC_{50} 7.18). Maximal efficacy was slightly but not significantly reduced (-28%). In order to investigate whether NOP receptor signaling might be regulated by other RGS proteins, we compared the response of N/OFQ in the presence of RGS19, which is structurally very similar to RGS4 and reported to interact with NOP receptor signaling [101]. When NOP receptor and RGS19 were co-transfected, the N/OFQ curve was shifted on the right (Fig.10), with a reduction of N/OFQ potency (pIC_{50} 7.27). Also, in this case, maximal N/OFQ efficacy was reduced, but non-significantly (-38.97%).

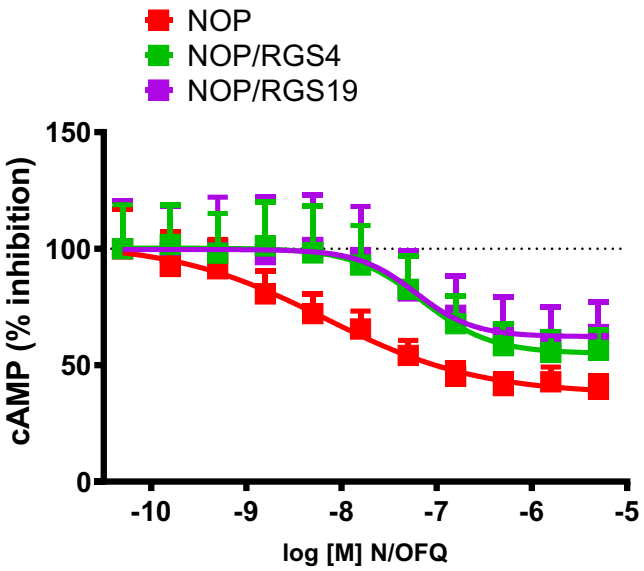

Fig. 4 Concentration–response curves of N/OFQ is shaped by RGS4 and RGS19. Data are mean ± SEM of n = 7-8 experiments per group.

We next investigated whether RGS4 and RGS19 were able to modulate also the effect of AT-403. As shown for N/OFQ, AT-403 (Fig.5) inhibited in a concentration-dependent manner the D_1-stimulated cAMP production, showing higher potency (pIC_{50}=9.92) and similar efficacy (maximal inhibition of 67%). RGS4 co-transfection caused a rightward shift of the AT-403 curve, with a reduction of the pIC_{50} (9.24) and maximal efficacy (-20%). Again, we also investigated the response of AT-403 in the presence of RGS19 and found that also RGS19 shifted to the right the curve of AT-403 (Fig.11), leading a reduction of AT-403 pIC_{50} (8.90) and maximal efficacy (-35%).

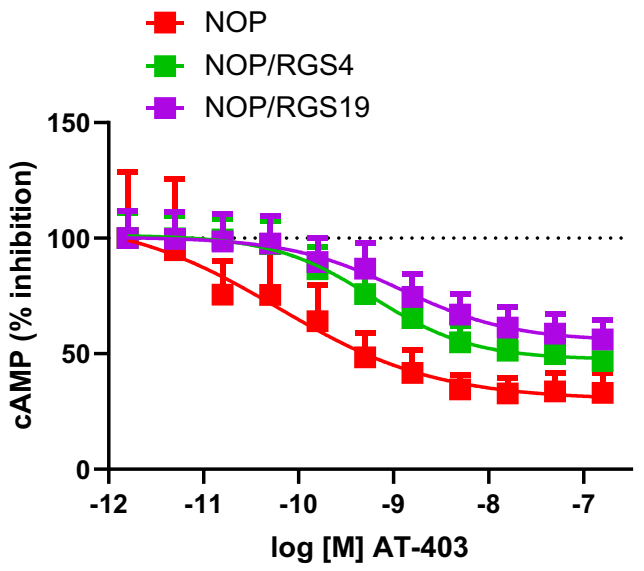

Fig. 5 Concentration–response curves of AT-403 is shaped by RGS4 and RGS19. Data are mean ± SEM of n = 7 experiments per group.

CCG-203920 potentiated the NOP receptor mediated response in striatal slices

To confirm the occurrence of a RGS4-NOP receptor interaction, in collaboration with Dr Riccardo Brambilla at the University of Cardiff (Cardiff, UK), we investigated the impact of the RGS4 inhibitor CCG-203920 on the NOP responses in a native system. Relying on the well-established NOP receptor inhibitory activity on D_1 signaling, we investigated whether RGS4 could affect the AT-403 mediated inhibition of the SKF38393-induced ERK-positive cell number in slices of mouse striatum. Therefore, in the first set of experiments (Fig.6), application of the D_1 receptor agonist SKF38393 (100 μM) to striatal slices of naïve mice caused an approximately four-fold increase in the number of pERK immunoreactive cells over basal. AT-403 (30 nM) alone had no effect on basal pERK level but reduced the D_1 receptor mediated response by 56%. CCG-203920, ineffective alone, markedly and significantly potentiated the AT-403 effect. In fact, when co-applied with CCG-203920, AT-403 fully inhibited the D_1 stimulation.

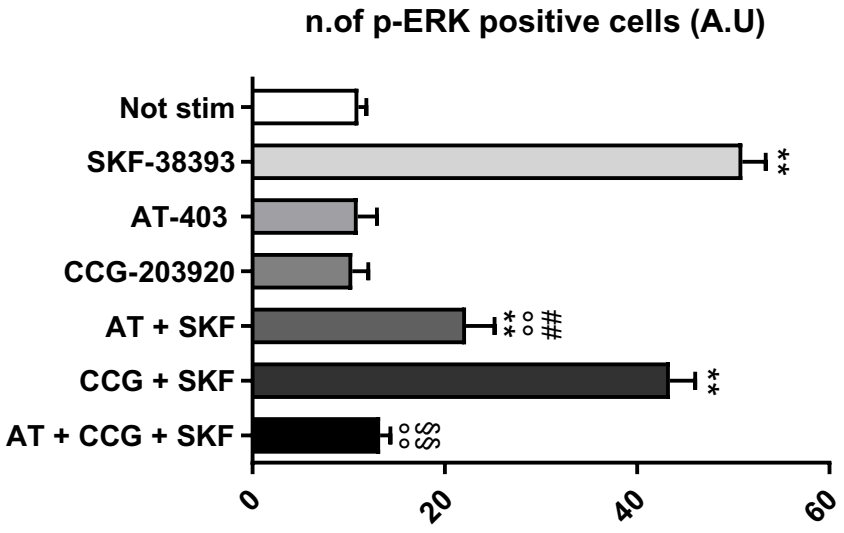

*Fig. 6 CCG-203920 potentiated the AT-403 driven inhibition of D_1 receptor-stimulated ERK signalling in striatum. Number of ERK-positive cells in striatal slices of naïve mice following simultaneous application of SKF38393 (100μM), AT-403 (30 nM) and CCG-203920 (500 nM). Data are mean ± SEM of n = 7 mice per group. **p < 0.05, significantly different from not stimulated vehicle; °°p < 0.01, significantly different from SKF38393 alone; ##p<0.01 different from AT-403 alone. § p<0.05, significantly different from AT + SKF. Two-way ANOVA followed by the Bonferroni post hoc test.*

In vivo experiments

CCG-203920 extended the antidyskinetic effect of AT-403

In a previous study, we described a dose-dependent anti-dyskinetic effect of AT-403 in a rat model of LID [99]. At the highest dose tested (0.1 mg/Kg) AT-403 exerted strong sedation that overlapped the antidyskinetic effect. Conversely, at the dose of 0.03 mg/Kg,

AT-403 exerted a mild and transient antidyskinetic effect in the absence of sedation. In order to improve the antidyskinetic effect of this AT-403 dose, we challenged AT-403 (0.03 mg/Kg s.c.) with L-Dopa (6 mg/Kg + benserazide 15 mg/Kg s.c.) in the presence or absence of CCG-203920. AT-403 alone delayed the onset of AIMs by 40 min, however it did not affect the overall duration and severity of the response. Interestingly, co-administration of CCG-203920 caused a further 20 min delay in AIM appearance, without significantly affecting the overall response to AT-403 (Fig.7), suggesting that RGS4 blockade potentiates the NOP agonist induced antidyskinetic effect.

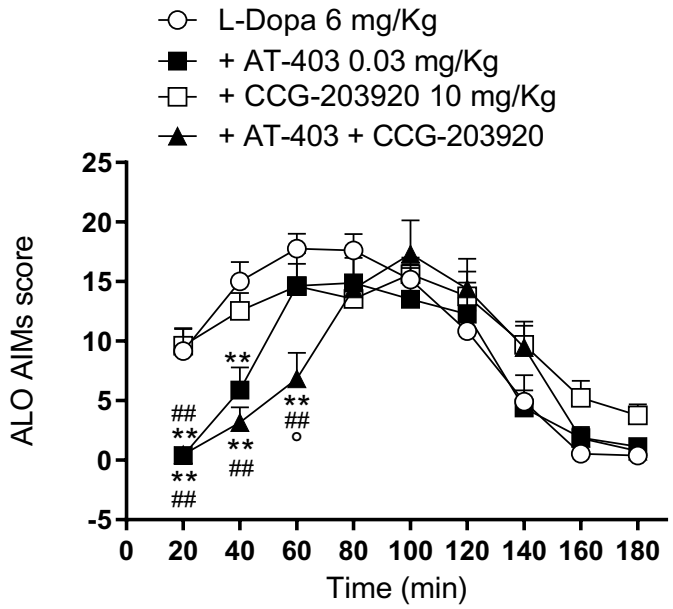

*Fig. 7 CCG-203920 extended the antidyskinetic effect of AT-403. ALO AIMs were scored in 6-OHDA hemilesioned dyskinetic rats following challenge with L-Dopa (6 mg/Kg plus benserazide 15 mg/Kg, s.c.) combined with vehicle, AT-403 (0.03 mg/Kg, s.c.) or CCG-203920 (10 mg/Kg, i.p). Values are mean ± SEM of 8-13 rats per group. *p<0.05, **p<0.01, different from L-Dopa; ## p<0.01, different from L-Dopa + CCG-203920; °p<0.05, different from L-Dopa + AT-403. Two-way repeated measure ANOVA followed by the Bonferroni post hoc test.*

CCG-203920 did not affect the improvement of rotarod performance "ON" L-Dopa induced by AT-403

The AIMs evaluation suggested that CCG-203920 increased the antidyskinetic effect of AT-403 but did not tell whether the sedative component was also enhanced. To investigate this aspect, we performed a rotarod test to measure overall motor ability ON and OFF L-Dopa. Briefly, L-Dopa administration causes AIMs in dyskinetic animals, leading to motor incoordination and a consequent reduction of the time spent on rod. A truly antidyskinetic compound alleviates dyskinesia and consequently improves rotarod performance.

Conversely, if the compound has primary hypolocomotive or sedative effects the reduction of AIMs will be associated with a lack of improvement of rotarod performance [99].
In Fig.8, the motor performance before (OFF) and one hour after (ON) the administration of L-Dopa is presented. As expected in the L-Dopa group the time spent on the rod after L-Dopa administration was dramatically reduced (-60%), due to the induction of AIMs. When animals were pretreated with AT-403, rotarod performance improved, albeit not fully recovering. CCG-203920 administration did not worsen the beneficial effect of AT-403, indicating that RGS4 blockade did not potentiate AT-403-induced sedation.

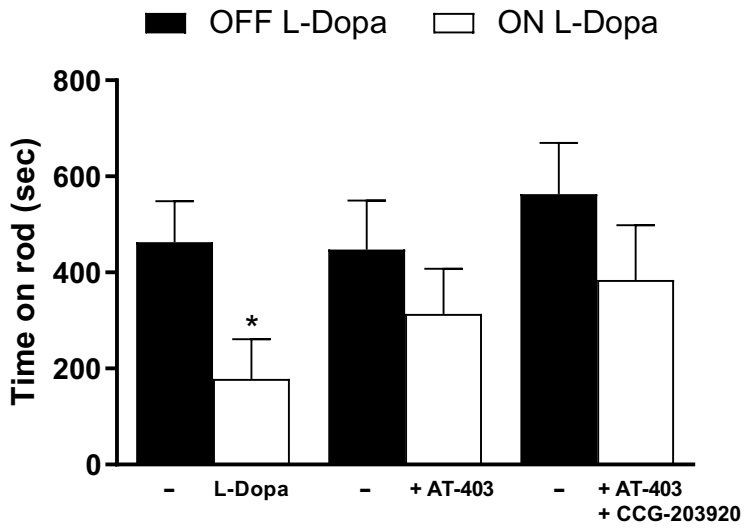

*Fig. 8 CCG-203920 did not reverse the improvement of rotarod performance induced by AT-403 ON L-Dopa. Rotarod performance was evaluated (as time on rod in seconds) before and 60 min after drug administration. 6-OHDA hemi-lesioned dyskinetic rats were treated with L-Dopa (6 mg/Kg plus benserazide 15 mg/Kg, s.c.) combined with vehicle, AT-403 (0.03 mg/Kg, s.c.) or CCG-203920 (10 mg/Kg, i.p.). Values are mean ± SEM of 8 rats per group. *p<0.05, different from OFF L-Dopa (Student t test, two tailed for unpaired data).*

CCG-203920 potentiated the AT-403 inhibition of ERK signaling in striatum

The dyskinetic condition has a dramatic impact on gene expression and posttranslational protein modifications in dMSNs. These changes strictly correlate with the occurrence of aberrant dopamine D_1 receptor transmission, which leads to alterations in phosphorylating activity of several downstream kinases, such as PKA, and DARPP-32. A direct consequence of the hyperactivity of DARPP-32 is the increased phosphorylation of ERK1/2, a well-accepted correlate of LID in rodents [171, 172]. In a previous study we showed that AT-403 (0.1 mg/Kg) was able to normalize the L-Dopa induced pERK levels in the lesioned striatum [99]. In the present study, we investigated whether the lower AT-403 dose (0.03 mg/Kg) alone or in combination with CCG-203920 could normalize the L-Dopa-induced increase of pERK in the striatum of dyskinetic rats (Fig. 9A). As expected, L-Dopa administration induced a significant increase of pERK levels in the lesioned

striatum relative to the unlesioned striatum of dyskinetic rats (+47%). This increase was unaffected by pre-treatment with AT-403 (+79%) or CCG-203920 (+117%) alone. However, when combined with CCG-203920, AT-403 was able to suppress the L-Dopa increased of pERK levels in the lesioned striatum.

In Fig. 9B, we showed that our treatments did not affect total protein levels, suggesting that the changes observed were due to the activation of the pathway and not to change in protein expression.

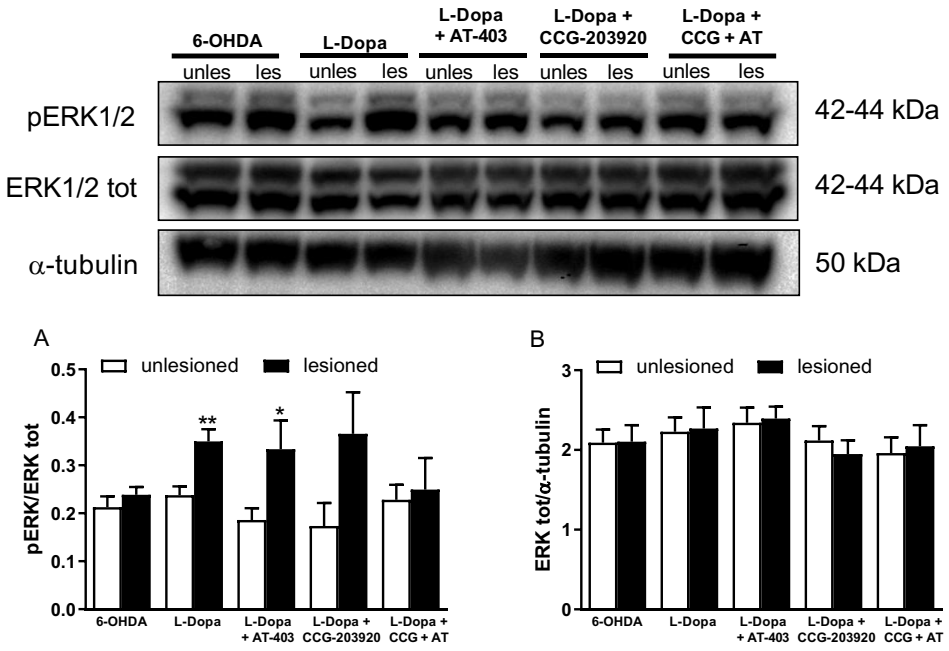

*Fig. 9 AT-403 in combination with CCG-203920 inhibited D1 receptor stimulated ERK signaling in striatum. Western blot representative images (upper panel) and quantification (lower panel) of pERK (A) and total ERK (B) in the striatum of 6OHDA hemi-lesioned, L-Dopa-naïve or dyskinetic rats. Dyskinetic rats were treated with AT-403 (0.03 mg/Kg, s.c.) or vehicle and, 10 min later, challenged with L-Dopa (6 mg/Kg, i.p.). CCG-203920 (10 mg/Kg, i.p.) or vehicle were administered 5 min before AT-403. Values are mean ± SEM of 6-7 rats per group. *p<0.05, **p<0.01, different from non-lesioned. Unpaired t-test followed by the Newman– Keuls post-hoc test.*

AT-403 inhibited D_1 receptor-stimulated pGluR1 phosphorylation in striatum

The increase of pGluR1 levels is another correlate of LID in rodents [171]. GluR1 is a subunit of the AMPA glutamate receptor, which is physiologically phosphorylated by PKA activated by dopamine via D_1 receptors. We therefore investigated whether, similar to ERK1/2, CCG-203920 also potentiated the ability of AT-403 (0.03 mg/Kg) to modulate pGluR1 levels. As expected, L-Dopa elevated pGluR1 levels in the lesioned stratum (+52%). However, different from ERK1/2, AT-403 alone was able to normalize pGluR1 levels (Fig. 8A), in line with the well-known inhibitory influence of NOP receptors over

canonical D_1 signalling. CCG-203920 did not alter the AT-403-driven normalization of pGluR1 levels. Again, neither treatment affected total protein amounts (Fig. 8B).

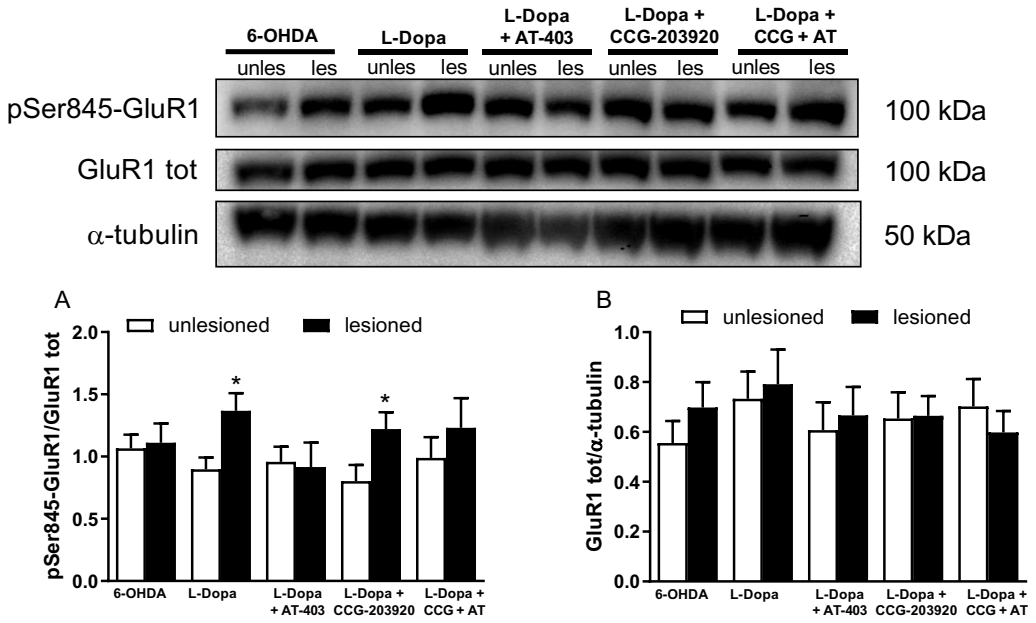

*Fig. 10 AT-403 inhibited D1 receptor-stimulated pGluR1 phosphorylation in striatum. Western blot representative images (upper panel) and quantification (lower panel) of pGluR1 (A) and total GluR1 (B) in the striatum of 6-OHDA hemilesioned, L-Dopa-naïve or dyskinetic rats. Dyskinetic rats were treated with AT-403 (0.03 mg/Kg, s.c.) or vehicle and, 10 min later, challenged with L-Dopa (6 mg/Kg, i.p.). CCG-203920 (10 mg/Kg, i.p.) or vehicle were administered 5 min before AT-403. Values are mean ± SEM of 6-7 rats per group. *p<0.05, **p<0.01, different from unlesioned. Statistical analysis was performed by Unpaired t-test followed by the Newman–Keuls post-hoc test.*

Striatal RGS4 levels were reduced following DA-depletion and rescued by L-Dopa

In vivo data suggest that RGS4 inhibitors might have antidyskinetic potential. In order to investigate whether RGS4 inhibitors correct a plastic adaptation of RGS4 occurring as a consequence of DA depletion and/or L-Dopa administration [26], RGS4 levels were measured by Western analysis in the striatum of naïve, 6-OHDA hemilesioned and 6-OHDA hemilesioned, L-Dopa-primed (i.e. dyskinetic) rats. Specifically, in dyskinetic rats we measured RGS4 levels both ON and OFF L-Dopa, to investigate whether the acute stimulation of D_1 receptors could influence the RGS4 expression in the dyskinetic striatum. A strong decrease in RGS4 protein levels was found in both the lesioned (-58%) and unlesioned (-46%) striatum of 6-OHDA animals, when compared with respective naïve counterparts (Fig. 11A). In addition, there was a significant reduction of RGS4 levels in the lesioned relative to the unlesioned striatum (Fig. 11B). Chronic L-Dopa normalized RGS4 levels and the lesioned-to-unlesioned ratio (OFF group). However, acute L-Dopa (ON group) reversed the lesioned-to-unlesioned ratio, causing a 44% increase of RGS4

levels in the lesioned striatum. This suggests that RGS4 is upregulated in the lesioned striatum of dyskinetic animals, following aberrant stimulation of D_1 receptor signaling by L-Dopa.

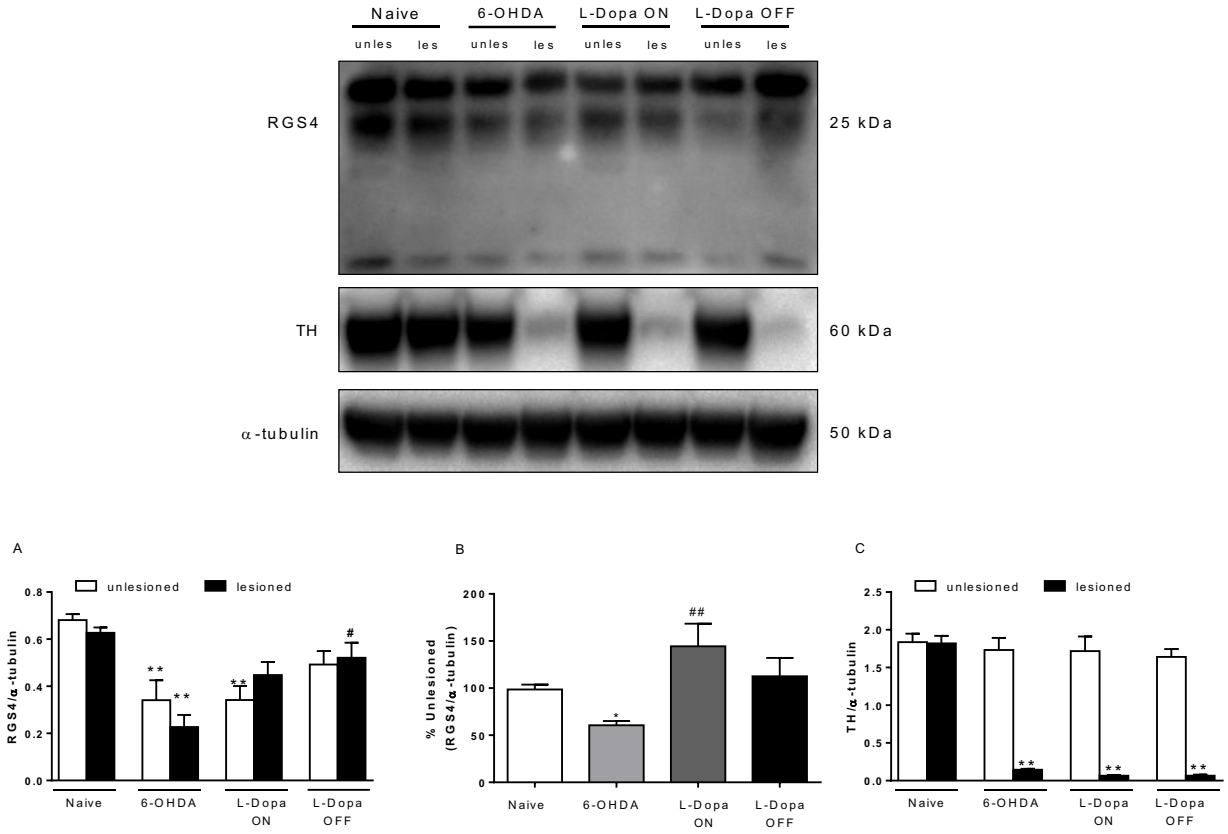

*Fig. 11 RGS4 levels dropped after DA depletion and rose after L-Dopa treatment causing LID. Western blot representative images (upper panel) and quantification (lower panel) of RGS4 and TH, expressed as absolute values (A and C, respectively) or as percentage of RGS4 in the lesioned vs non-lesioned striatum (B) in the striatum of naïve, 6OHDA hemi-lesioned, or dyskinetic rats. Values are mean ± SEM of 11 (Naïve), 9 (6-OHDA),7 (L-Dopa ON),6 (L-Dopa OFF) rats per group. A-B *p<0.05, **p<0.01, different from Naive; #p<0.05, ## p<0.01, different from 6-OHDA one-way ANOVA. C **<0.01 different from contralateral. (A, B) One-way ANOVA followed by the Newman-Keuls for parametric analysis (A) or one-way ANOVA (Kruskal-Wallis) followed by the Dunn test for non-parametric analysis (B). (C) Student t-test, two-tailed for unpaired data.*

Discussion

The present study provides the first evidence of a functional interaction between RGS4 and NOP receptor *in vivo* and *in vitro*. Moreover, we demonstrated that pharmacological inhibition of RGS4 potentiates the NOP receptor-driven antidyskinetic effect in a model of LID, without affecting NOP-receptor induced sedation, suggesting that RGS4 might differentially modulate NOP receptor mediated responses.

RGS4 is a negative modulator of opioid receptors signaling in a very fine and specific manner [93, 94, 173]. Previous studies demonstrated that RGS4 negatively regulated reward and physical dependence induced by the MOP receptor agonist morphine but did not affect morphine-induced analgesia or tolerance [93]. This was very surprising since the same study reported that RGS4 positively affected the analgesic effect of methadone and fentanyl [93]. More recently, it was shown that RGS4 modulated DOP receptor-mediated behavioral outcomes in mice [94, 173]. At first, Zachariou and collaboratos [173] demonstrated that RGS4 is involved in SNC80 mediated antidepressant like behaviors, showing a better performance in the forced swimming test of RGS4 knockout mice compared to wild type mice. Then, Jutkiewicz and collaborators [94] published a very inspirational study which reported the ability of RGS4 to differentially mediate SNC80-stimulated DOP receptor outcomes. Specifically, they showed that the total or partial genetic deletion of RGS4 as well as acute pharmacological inhibition of RGS4 with CCG-203769, increased SNC80-induced antinociception and antihyperalgesia, but did not affect the pro-convulsant action of the DOP agonist. Thus, RGS4 appeared to be able to potentiate selective DOP-receptor mediated responses. Likewise, we reasoned that, if RGS4 differentially regulated opioid related behaviors, we could target this GPCR modulator to improve the safety and clinical profile of NOP receptor agonists.

The interaction between RGS4 and the NOP receptor was first demonstrated in a cell model, i.e. HEK293T cells. We transfected RGS4, NOP receptor and D_1 receptor, and used as readout of the NOP receptor activity the inhibition of D_1 stimulated cAMP production, a G protein mediated intracellular function [166]. When HEK293T were transfected only with NOP, N/OFQ inhibited the D_1-stimulated cAMP production showing similar efficacy but lower potency than AT-403 (pIC_{50} 7.82 vs 9.92, respectively). This differs from previous studies showing that N/OFQ and AT-403 had similar potencies in the [^{35}S]GTPγS assay in membranes (EC_{50} 3.6 vs 6.3 nM)[99] and in the intracellular Ca^{2+} mobilization assay in CHO_{NOP} cells (pEC_{50}=9.92; [174]). These differences might reflect the different preparations and cell lines, as well as the intracellular pathways used as readout of the

NOP receptor activation. Nonetheless, consistent with the abovementioned studies, N/OFQ and AT-403 induced the same maximal inhibition in the D_1-stimulated cAMP production confirming that AT-403 is a full agonist of NOP receptor [174].

The finding that co-transfection of RGS4 shifted to the right the N/OFQ curve with a significant decrease of potency suggests that RGS4 negatively couples to $G_{i/o}$ to inhibit NOP receptor signaling, providing the first evidence of a RGS4-NOP receptor interaction. This effect is shared by another RGS protein, RGS19, functionally very similar to RGS4, which was reported to negatively modulate NOP receptor signaling *in vitro* [101]. Thus, both RGS4 and RGS19 modulate NOP signaling in an artificial system. Whether this also occurs in a native system remains to be determined. Nonetheless, this finding discloses the intriguing possibility that RGS4 and RGS19 might modulate different NOP receptor mediated responses *in vivo.* Therefore, addressing this point might be very useful in order to achieve therapeutic versus unwanted effects of NOP receptor agonists.

To further confirm the occurrence of a RGS4-NOP interaction in a native system, we investigated whether RGS4 inhibition potentiates the NOP response in striatal slices. We previously demonstrated that N/OFQ and AT-403 inhibited the increase in ERK-positive striatal neurons (likely MSNs) induced by D_1 receptor agonist SKF38393 [98, 99]. In this model, we now show that CCG-203920 potentiates the effect of a concentration of AT-403 causing 73.9% inhibition of D_1 receptor-stimulated ERK-positive neurons.

Since the elevation of pERK levels in the DA-depleted striatum is considered a molecular correlate of LID, we finally investigated whether CCG-203920 could potentiate the NOP receptor agonist-induced attenuation of LID and its neurochemical correlates *in vivo*.

Indeed, we found that CCG-203920 potentiated the antidyskinetic response to AT-403 without concurrently potentiating its sedative/hypolocomotive effects. The rotarod test was instrumental to make this statement. In fact, the rotarod test performed ON levodopa allowed us to correlate AIMs severity with the global motor performance of dyskinetic rats. A truly antidyskinetic drug attenuates AIMs improving the motor performance [98, 99]. In line with this, CCG-203920 prolonged the attenuation of AIMs induced by AT-403 without worsening the positive effect of AT-403 on rotarod performance. This suggests that the delay in AIMs appearance induced by RGS4 blockade is due to potentiation of the anti-dyskinetic property of AT-403 and not a consequence of the amplification of its sedative component.

To confirm the view that the effect of CCG-203920 is truly mediated by interference with the molecular pathways underlying LID, we monitored its impact on the biochemical correlates of LID. The aberrant D_1 signaling characterizing LID results in an enhancement

of Gα and Gβγ downstream pathways, such as cAMP/PKA and MAPKs cascades [171]. Specifically, the increased activity of PKA via the canonical and non-canonical pathways leads to phosphorylation of several downstream effectors in striatal dMSNs, among which the GluR1 subunit of glutamate AMPA receptor and ERK1/2 [171, 172]. We previously reported that a 3-fold higher dose of AT-403 (0.1 mg/Kg) than that used in the present study (0.03 mg/Kg) normalized pERK levels and blunted LID [99]. Interestingly, we now show that the low 0.03 mg/Kg AT-403 dose, ineffective alone, normalized pERK levels, when combined to CCG-203920. This confirms that RGS4 blockade potentiates the ability of the compound to modulate MAPKs pathway changes underlying LID. On the contrary, CCG-203930 did not affect the AT-403 inhibition of pGluR1 levels. However, we should note that AT-403 alone fully inhibited the rise of pGluR1 associated with dyskinesia, which might have prevented to see further inhibition ("floor effect") by CCG-203920.

Overall, these data indicate that RGS4 blockade improves the NOP agonist mediated antidyskinetic effect without amplifying its sedative effects. This would indicate that RGS4 blockade would be helpful to widen the therapeutic window of AT-403 and improve its clinical profile.

Interestingly, previous studies showed the potential involvement of RGS4 in the pathogenesis of LID and specifically it was reported that blockade of this protein might be therapeutic for dyskinesia [28, 29]. Specifically, it has been shown that the chronic treatment with antisense oligonucleotides targeting RGS4 reduced AIM development during L-Dopa priming in a rat model of LID [29]. Moreover, RGS4 upregulation in striatal ChIs in dyskinetic conditions [25] was proposed to be responsible for M4 receptor hypofunction, showing that selective inhibition of RGS4 in striatum potentiated M4 activity [28].

Pharmacological blockade of RGS4 is expected to affect GPCRs other than the NOP receptor, inducing off-target effects in brain or neuronal populations not involved in LID. Although the overall selectivity issue of RGS4 inhibitors cannot be addressed at the moment, investigating the status of the RGS4 system (expression, protein levels, …) might help foresee whether a RGS4 inhibitor would selectively target and correct a pathological condition of RGS4 overexpression induced by dyskinesia. We therefore investigated RGS4 levels in striatum in order to assess whether RGS4 is affected by the state of DA transmission. Our data showed a downregulation of RGS4 after DA depletion in the lesioned striatum, as previously described [26, 29]. Surprisingly, such a reduction was also observed in the unlesioned striatum, suggesting a high sensitivity of RGS4 to changes in dopaminergic system. Nonetheless, lower RGS4 levels in the lesioned relative to the

unlesioned striatum were found, suggesting that DA depletion induces a greater reduction of RGS4. Indeed, chronic L-Dopa normalized RGS4 levels, as well as the lesioned-to-unlesioned ratio (OFF L-Dopa conditions). Interestingly, however, dyskinesia induction 30 min after acute L-Dopa (ON L-Dopa conditions) caused a reversal of the lesioned-to-unlesioned ratio, indicating upregulation of RGS4. This supports the therapeutic potential of RGS4 inhibitors to treat LID. These data nicely reconcile with a previous ex-vivo study in 6-OHDA hemilesioned dyskinetic rats where RGS4 expression was evaluated by in situ hybridization [29]. In this study, it was shown that RGS4 expression was reduced in the lesioned striatum after DA depletion, then increased following chronic L-Dopa treatment. However, the increase was more marked 1 hour after L-Dopa administration (i.e. ON L-Dopa) than after 24 hours (i.e. OFF L-Dopa). In that study, RGS4 blockade by continuous delivery via osmotic mini pumps of antisense oligonucleotide against RGS4 was found to be effective in preventing LID development. We failed to demonstrate a beneficial effect of CCG-203920 alone on established LID, which might be due to the different phase of dyskinesia development examined (induction vs expression) and/or the different degree of RGS4 blockade attained with the therapeutic strategies. In fact, in our study RGS4 activity was acutely blocked with a pharmacological inhibitor whereas in the other study [29] RGS4 expression was blocked with continuous delivery of antisense nucleotide via osmotic mini pumps. Nonetheless, although the level of RGS4 inhibition reaching in vivo conditions remained to be determined, we demonstrated that a 10 mg/Kg dose of RGS4 inhibitor was sufficient to potentiate the NOP receptor-mediated anti-dyskinetic effect induced by AT-403.

CHAPTER IV

Conclusions and future perspectives

This study investigated the involvement of RGS4 in movement disorders involving the BG network. In the first study, we showed that RGS4 inhibitors counteract neuroleptic-induced akinesia in mice, possibly acting along the indirect pathway. RGS4 inhibitors might thus represent a novel pharmacological approach to attenuate the extrapyramidal side effects of antipsychotics and improve their clinical profile. Nonetheless, key questions need to be answered. For instance, which RGS4-regulated GPCR is involved in the antiakinetic effect of CCG compounds. If the hypothesis of the involvement of the serotonergic system proves correct, this study will bear strong translational potential, because it has been proposed that new, "atypical" antipsychotics are less cataleptogenic due to a combined action at D_2 and 5HT1A receptors. Besides the mechanistic unsolved question, another crucial point to be investigated is the *in vivo* selectivity of CCG compounds. The phenotypic characterization of RGS4 knockout mice, and their response to neuroleptic will help confirm the role of RGS4 in neuroleptic-induced akinesia and demonstrate that the antiakinetic effects of CCGs observed in mice are not due to an *off-target* action on other RGS proteins, such as RGS8 or RGS19.

The second study revealed for the first time an interaction between RGS4 and the NOP receptor. As previously shown for the MOP and DOP receptors, RGS4 inhibits NOP receptor mediated responses. This points to RGS4 inhibitors as a tool for potentiating the pharmacological effects of NOP receptor agonists. Intriguingly, as shown for the other opioid receptors modulated by RGS4, the modulation exerted by RGS4 might selectively affect some but not all NOP receptor mediated responses. In fact, we proved that RGS4 blockade potentiated the antidyskinetic effect of a selective NOP receptor agonist without concurrently enhancing its sedative action. Again, assessing NOP responses in RGS4 knockout mice will help understand which responses are modulated by RGS4.

Considering the number of therapeutic applications of NOP receptor agonists [175], the evidence of RGS4-NOP receptor interaction opens a wide range of opportunities not only in the field of motor disorders. For instance, NOP receptor agonists have analgesic and anxiolytic actions that might be potentiated by RGS4 inhibitors.

An important take-home message of this research is that we can powerfully modulate GPCRs mediated intracellular pathways and behavioral outcomes targeting modulators of GPCRs signaling, such as RGS4. Small molecules RGS4 inhibitors, and potentially also RGS4 positive modulator, might represent a new tool to improve the selectivity, therapeutic action, and/or safety of GPCR-based drugs.

Abbreviations

6-OHDA = 6-hydroxydopamine

ACh = acetylcholine

AIMs = abnormal involuntary movements

BG = basal ganglia

ChIs = cholinergic interneurons

DA = dopamine

DIP= drug induced parkinsonism

DOP= δ-oppioid receptor

EGRF= epidermal growth factor receptor

ERK 1/2 = extracellular signal–regulated kinase

GABA = γ-aminobutyric acid

GAP= GTPase activating protein

Glu = glutamate

GP = globus pallidus

L-DOPA = 3,4-dihydroxy-L-phenylalanine

LID = Levodopa-induced dyskinesia

MFB = medial forebrain bundle

mGluRs= metabotropic glutamate receptors

MOP= μ-oppioid receptor

MSNs = medium spiny neurons

N/OFQ= nociception/orphanin FQ

NIP= neuroleptic induced parkinsonism

NOP= N/OFQ peptide receptor

PD = Parkinson's disease

PKA = protein kinase A

RGS= Regulators of G-protein signaling

SNpc = substantia nigra pars compacta

SNpr = substantia nigra pars reticulate

STN = subthalamus

TD= tardive dyskinesia

Bibliography

1. Sriram, K. and P.A. Insel, *G Protein-Coupled Receptors as Targets for Approved Drugs: How Many Targets and How Many Drugs?* Mol Pharmacol, 2018. **93**(4): p. 251-258.
2. Oldham, W.M. and H.E. Hamm, *Heterotrimeric G protein activation by G-protein-coupled receptors.* Nat Rev Mol Cell Biol, 2008. **9**(1): p. 60-71.
3. Eichel, K. and M. von Zastrow, *Subcellular Organization of GPCR Signaling.* Trends Pharmacol Sci, 2018. **39**(2): p. 200-208.
4. Siderovski, D.P., et al., *A new family of regulators of G-protein-coupled receptors?* Curr Biol, 1996. **6**(2): p. 211-2.
5. Siderovski, D.P., S.P. Heximer, and D.R. Forsdyke, *A human gene encoding a putative basic helix-loop-helix phosphoprotein whose mRNA increases rapidly in cycloheximide-treated blood mononuclear cells.* DNA Cell Biol, 1994. **13**(2): p. 125-47.
6. De Vries, L., et al., *GAIP is membrane-anchored by palmitoylation and interacts with the activated (GTP-bound) form of G alpha i subunits.* Proc Natl Acad Sci U S A, 1996. **93**(26): p. 15203-8.
7. Dohlman, H.G., et al., *Inhibition of G-protein signaling by dominant gain-of-function mutations in Sst2p, a pheromone desensitization factor in Saccharomyces cerevisiae.* Mol Cell Biol, 1995. **15**(7): p. 3635-43.
8. Wu, H.K., et al., *Differential expression of a basic helix-loop-helix phosphoprotein gene, G0S8, in acute leukemia and localization to human chromosome 1q31.* Leukemia, 1995. **9**(8): p. 1291-8.
9. Sjogren, B., *The evolution of regulators of G protein signalling proteins as drug targets - 20 years in the making: IUPHAR Review 21.* Br J Pharmacol, 2017. **174**(6): p. 427-437.
10. Siderovski, D.P. and F.S. Willard, *The GAPs, GEFs, and GDIs of heterotrimeric G-protein alpha subunits.* Int J Biol Sci, 2005. **1**(2): p. 51-66.
11. Roy, A.A., et al., *RGS2 interacts with Gs and adenylyl cyclase in living cells.* Cell Signal, 2006. **18**(3): p. 336-48.
12. Gold, S.J., et al., *Regulators of G-protein signaling (RGS) proteins: region-specific expression of nine subtypes in rat brain.* J Neurosci, 1997. **17**(20): p. 8024-37.
13. Erdely, H.A., et al., *Regional expression of RGS4 mRNA in human brain.* Eur J Neurosci, 2004. **19**(11): p. 3125-8.
14. Schwendt, M., S.A. Sigmon, and J.F. McGinty, *RGS4 overexpression in the rat dorsal striatum modulates mGluR5- and amphetamine-mediated behavior and signaling.* Psychopharmacology (Berl), 2012. **221**(4): p. 621-35.
15. Ghavami, A., et al., *Differential effects of regulator of G protein signaling (RGS) proteins on serotonin 5-HT1A, 5-HT2A, and dopamine D2 receptor-mediated signaling and adenylyl cyclase activity.* Cell Signal, 2004. **16**(6): p. 711-21.
16. Anderson, G.R., E. Posokhova, and K.A. Martemyanov, *The R7 RGS protein family: multi-subunit regulators of neuronal G protein signaling.* Cell Biochem Biophys, 2009. **54**(1-3): p. 33-46.
17. Traver, S., et al., *The RGS (regulator of G-protein signalling) and GoLoco domains of RGS14 co-operate to regulate Gi-mediated signalling.* Biochem J, 2004. **379**(Pt 3): p. 627-32.
18. Salim, S., et al., *Identification of RGS2 and type V adenylyl cyclase interaction sites.* J Biol Chem, 2003. **278**(18): p. 15842-9.
19. Xie, Z., et al., *RGS13 acts as a nuclear repressor of CREB.* Mol Cell, 2008. **31**(5): p. 660-70.
20. Schwarz, E., *A gene-based review of RGS4 as a putative risk gene for psychiatric illness.* Am J Med Genet B Neuropsychiatr Genet, 2018. **177**(2): p. 267-273.
21. Avrampou, K., et al., *RGS4 Maintains Chronic Pain Symptoms in Rodent Models.* J Neurosci, 2019. **39**(42): p. 8291-8304.

22. Bosier, B., et al., *Inhibition of the regulator of G protein signalling RGS4 in the spinal cord decreases neuropathic hyperalgesia and restores cannabinoid CB1 receptor signalling.* Br J Pharmacol, 2015. **172**(22): p. 5333-46.
23. Yoon, S.Y., et al., *Intrathecal RGS4 inhibitor, CCG50014, reduces nociceptive responses and enhances opioid-mediated analgesic effects in the mouse formalin test.* Anesth Analg, 2015. **120**(3): p. 671-7.
24. Taccola, G., et al., *A new model of nerve injury in the rat reveals a role of Regulator of G protein Signaling 4 in tactile hypersensitivity.* Exp Neurol, 2016. **286**: p. 1-11.
25. Ding, J., et al., *RGS4-dependent attenuation of M4 autoreceptor function in striatal cholinergic interneurons following dopamine depletion.* Nat Neurosci, 2006. **9**(6): p. 832-42.
26. Geurts, M., J.M. Maloteaux, and E. Hermans, *Altered expression of regulators of G-protein signaling (RGS) mRNAs in the striatum of rats undergoing dopamine depletion.* Biochem Pharmacol, 2003. **66**(7): p. 1163-70.
27. Blazer, L.L., et al., *Selectivity and anti-Parkinson's potential of thiadiazolidinone RGS4 inhibitors.* ACS Chem Neurosci, 2015. **6**(6): p. 911-9.
28. Shen, W., et al., *M4 Muscarinic Receptor Signaling Ameliorates Striatal Plasticity Deficits in Models of L-DOPA-Induced Dyskinesia.* Neuron, 2015. **88**(4): p. 762-73.
29. Ko, W.K., et al., *RGS4 is involved in the generation of abnormal involuntary movements in the unilateral 6-OHDA-lesioned rat model of Parkinson's disease.* Neurobiol Dis, 2014. **70**: p. 138-48.
30. Xie, Y., et al., *Breast cancer migration and invasion depend on proteasome degradation of regulator of G-protein signaling 4.* Cancer Res, 2009. **69**(14): p. 5743-51.
31. Cheng, C., et al., *Regulator of G-protein signaling 4: A novel tumor suppressor with prognostic significance in non-small cell lung cancer.* Biochem Biophys Res Commun, 2016. **469**(3): p. 384-91.
32. Michaelides, M., et al., *Striatal Rgs4 regulates feeding and susceptibility to diet-induced obesity.* Mol Psychiatry, 2018.
33. Madigan, L.A., et al., *RGS4 Overexpression in Lung Attenuates Airway Hyperresponsiveness in Mice.* Am J Respir Cell Mol Biol, 2018. **58**(1): p. 89-98.
34. Tysnes, O.B. and A. Storstein, *Epidemiology of Parkinson's disease.* J Neural Transm (Vienna), 2017. **124**(8): p. 901-905.
35. Parkinson, J., *An essay on the shaking palsy. 1817.* J Neuropsychiatry Clin Neurosci, 2002. **14**(2): p. 223-36; discussion 222.
36. Halliday, G.M., et al., *Neuropathology underlying clinical variability in patients with synucleinopathies.* Acta Neuropathol, 2011. **122**(2): p. 187-204.
37. Dickson, D.W., et al., *Neuropathological assessment of Parkinson's disease: refining the diagnostic criteria.* Lancet Neurol, 2009. **8**(12): p. 1150-7.
38. Poewe, W., et al., *Parkinson disease.* Nat Rev Dis Primers, 2017. **3**: p. 17013.
39. Iacono, D., et al., *Parkinson disease and incidental Lewy body disease: Just a question of time?* Neurology, 2015. **85**(19): p. 1670-9.
40. Braak, H., et al., *Staging of brain pathology related to sporadic Parkinson's disease.* Neurobiol Aging, 2003. **24**(2): p. 197-211.
41. Rocha, E.M., B. De Miranda, and L.H. Sanders, *Alpha-synuclein: Pathology, mitochondrial dysfunction and neuroinflammation in Parkinson's disease.* Neurobiol Dis, 2018. **109**(Pt B): p. 249-257.
42. Halliday, G.M. and H. McCann, *The progression of pathology in Parkinson's disease.* Ann N Y Acad Sci, 2010. **1184**: p. 188-95.
43. Albin, R.L., A.B. Young, and J.B. Penney, *The functional anatomy of basal ganglia disorders.* Trends Neurosci, 1989. **12**(10): p. 366-75.
44. Young, C.B. and J. Sonne, *Neuroanatomy, Basal Ganglia*, in *StatPearls*. 2019: Treasure Island (FL).

45. Cenci, M.A., H. Jorntell, and P. Petersson, *On the neuronal circuitry mediating L-DOPA-induced dyskinesia.* J Neural Transm (Vienna), 2018. **125**(8): p. 1157-1169.
46. Nicola, S.M., J. Surmeier, and R.C. Malenka, *Dopaminergic modulation of neuronal excitability in the striatum and nucleus accumbens.* Annu Rev Neurosci, 2000. **23**: p. 185-215.
47. Zhai, S., et al., *Striatal synapses, circuits, and Parkinson's disease.* Curr Opin Neurobiol, 2018. **48**: p. 9-16.
48. Aubert, I., et al., *Phenotypical characterization of the neurons expressing the D1 and D2 dopamine receptors in the monkey striatum.* J Comp Neurol, 2000. **418**(1): p. 22-32.
49. Le Moine, C. and B. Bloch, *D1 and D2 dopamine receptor gene expression in the rat striatum: sensitive cRNA probes demonstrate prominent segregation of D1 and D2 mRNAs in distinct neuronal populations of the dorsal and ventral striatum.* J Comp Neurol, 1995. **355**(3): p. 418-26.
50. Tanimura, A., et al., *Striatal cholinergic interneurons and Parkinson's disease.* Eur J Neurosci, 2018. **47**(10): p. 1148-1158.
51. Tepper, J.M., et al., *Heterogeneity and diversity of striatal GABAergic interneurons.* Front Neuroanat, 2010. **4**: p. 150.
52. Oorschot, D.E., *Total number of neurons in the neostriatal, pallidal, subthalamic, and substantia nigral nuclei of the rat basal ganglia: a stereological study using the cavalieri and optical disector methods.* J Comp Neurol, 1996. **366**(4): p. 580-99.
53. Lanciego, J.L., N. Luquin, and J.A. Obeso, *Functional neuroanatomy of the basal ganglia.* Cold Spring Harb Perspect Med, 2012. **2**(12): p. a009621.
54. Susatia, F. and H.H. Fernandez, *Drug-induced parkinsonism.* Curr Treat Options Neurol, 2009. **11**(3): p. 162-9.
55. Shin, H.W. and S.J. Chung, *Drug-induced parkinsonism.* J Clin Neurol, 2012. **8**(1): p. 15-21.
56. Steck, H., *[Extrapyramidal and diencephalic syndrome in the course of largactil and serpasil treatments].* Ann Med Psychol (Paris), 1954. **112**(2 5): p. 737-44.
57. Wilson, J.A. and W.J. MacLennan, *Review: drug-induced parkinsonism in elderly patients.* Age Ageing, 1989. **18**(3): p. 208-10.
58. Divac, N., et al., *Second-generation antipsychotics and extrapyramidal adverse effects.* Biomed Res Int, 2014. **2014**: p. 656370.
59. Tarsy, D., R.J. Baldessarini, and F.I. Tarazi, *Effects of newer antipsychotics on extrapyramidal function.* CNS Drugs, 2002. **16**(1): p. 23-45.
60. Lerner, T.N. and A.C. Kreitzer, *RGS4 is required for dopaminergic control of striatal LTD and susceptibility to parkinsonian motor deficits.* Neuron, 2012. **73**(2): p. 347-59.
61. Turner, E.M., et al., *Small Molecule Inhibitors of Regulators of G Protein Signaling (RGS) Proteins.* ACS Medicinal Chemistry Letters, 2012. **3**(2): p. 146-150.
62. Blazer, L.L., et al., *A nanomolar-potency small molecule inhibitor of regulator of G-protein signaling proteins.* Biochemistry, 2011. **50**(15): p. 3181-92.
63. Turner, E.M., et al., *Small Molecule Inhibitors of Regulator of G Protein Signalling (RGS) Proteins.* ACS Med Chem Lett, 2012. **3**(2): p. 146-150.
64. Conn, P.J. and J.P. Pin, *Pharmacology and functions of metabotropic glutamate receptors.* Annu Rev Pharmacol Toxicol, 1997. **37**: p. 205-37.
65. Saugstad, J.A., et al., *RGS4 inhibits signaling by group I metabotropic glutamate receptors.* J Neurosci, 1998. **18**(3): p. 905-13.
66. Cabello, N., et al., *Metabotropic glutamate type 5, dopamine D2 and adenosine A2a receptors form higher-order oligomers in living cells.* J Neurochem, 2009. **109**(5): p. 1497-507.
67. Ciruela, F., et al., *Adenosine receptor containing oligomers: their role in the control of dopamine and glutamate neurotransmission in the brain.* Biochim Biophys Acta, 2011. **1808**(5): p. 1245-55.
68. Shen, W., et al., *Dichotomous dopaminergic control of striatal synaptic plasticity.* Science, 2008. **321**(5890): p. 848-51.

69. Viaro, R., M. Marti, and M. Morari, *Dual motor response to l-dopa and nociceptin/orphanin FQ receptor antagonists in 1-methyl-4-phenyl-1,2,5,6-tetrahydropyridine (MPTP) treated mice: Paradoxical inhibition is relieved by D(2)/D(3) receptor blockade.* Exp Neurol, 2010. **223**(2): p. 473-84.
70. Marti, M., et al., *Blockade of nociceptin/orphanin FQ transmission attenuates symptoms and neurodegeneration associated with Parkinson's disease.* J Neurosci, 2005. **25**(42): p. 9591-601.
71. Longo, F., et al., *Age-dependent dopamine transporter dysfunction and Serine129 phospho-alpha-synuclein overload in G2019S LRRK2 mice.* Acta Neuropathol Commun, 2017. **5**(1): p. 22.
72. Brugnoli, A., et al., *Genetic deletion of Rhes or pharmacological blockade of mTORC1 prevent striato-nigral neurons activation in levodopa-induced dyskinesia.* Neurobiol Dis, 2016. **85**: p. 155-163.
73. Viaro, R., et al., *Pharmacological and genetic evidence for pre- and postsynaptic D2 receptor involvement in motor responses to nociceptin/orphanin FQ receptor ligands.* Neuropharmacology, 2013. **72**: p. 126-38.
74. Viaro, R., et al., *Nociceptin/orphanin FQ receptor blockade attenuates MPTP-induced parkinsonism.* Neurobiol Dis, 2008. **30**(3): p. 430-8.
75. Mabrouk, O.S., M. Marti, and M. Morari, *Endogenous nociceptin/orphanin FQ (N/OFQ) contributes to haloperidol-induced changes of nigral amino acid transmission and parkinsonism: a combined microdialysis and behavioral study in naive and nociceptin/orphanin FQ receptor knockout mice.* Neuroscience, 2010. **166**(1): p. 40-8.
76. Paxinos, G.a.W., C., *The mouse Brain in Stereotaxic Coordinates, 2nd ed.* Academic Press, 2001.
77. Brodkin, J., et al., *Reduced stress-induced hyperthermia in mGluR5 knockout mice.* Eur J Neurosci, 2002. **16**(11): p. 2241-4.
78. Cosford, N.D., et al., *3-[(2-Methyl-1,3-thiazol-4-yl)ethynyl]-pyridine: a potent and highly selective metabotropic glutamate subtype 5 receptor antagonist with anxiolytic activity.* J Med Chem, 2003. **46**(2): p. 204-6.
79. Mela, F., et al., *In vivo evidence for a differential contribution of striatal and nigral D1 and D2 receptors to L-DOPA induced dyskinesia and the accompanying surge of nigral amino acid levels.* Neurobiol Dis, 2012. **45**(1): p. 573-82.
80. Marti, M., et al., *The nociceptin/orphanin FQ receptor antagonist J-113397 and L-DOPA additively attenuate experimental parkinsonism through overinhibition of the nigrothalamic pathway.* J Neurosci, 2007. **27**(6): p. 1297-307.
81. Bido, S., M. Marti, and M. Morari, *Amantadine attenuates levodopa-induced dyskinesia in mice and rats preventing the accompanying rise in nigral GABA levels.* J Neurochem, 2011. **118**(6): p. 1043-55.
82. Pozzi, L., et al., *Opposite regulation by typical and atypical anti-psychotics of ERK1/2, CREB and Elk-1 phosphorylation in mouse dorsal striatum.* J Neurochem, 2003. **86**(2): p. 451-9.
83. Molteni, R., et al., *Antipsychotic drug actions on gene modulation and signaling mechanisms.* Pharmacol Ther, 2009. **124**(1): p. 74-85.
84. Hakansson, K., et al., *Regulation of phosphorylation of the GluR1 AMPA receptor by dopamine D2 receptors.* J Neurochem, 2006. **96**(2): p. 482-8.
85. Hornykiewicz, O., *Basic research on dopamine in Parkinson's disease and the discovery of the nigrostriatal dopamine pathway: the view of an eyewitness.* Neurodegener Dis, 2008. **5**(3-4): p. 114-7.
86. Rangel-Barajas, C., I. Coronel, and B. Floran, *Dopamine Receptors and Neurodegeneration.* Aging Dis, 2015. **6**(5): p. 349-68.
87. Fuxe, K., et al., *Dopamine heteroreceptor complexes as therapeutic targets in Parkinson's disease.* Expert Opin Ther Targets, 2015. **19**(3): p. 377-98.

88. Young, C.D., et al., *Clozapine pretreatment modifies haloperidol-elicited forebrain Fos induction: a regionally-specific double dissociation.* Psychopharmacology (Berl), 1999. **144**(3): p. 255-63.
89. Lindenbach, D., et al., *Effects of 5-HT1A receptor stimulation on striatal and cortical M1 pERK induction by L-DOPA and a D1 receptor agonist in a rat model of Parkinson's disease.* Brain Res, 2013. **1537**: p. 327-39.
90. Angelique M. Lione, M.E., Stanley L. Lin, and Daniel S. Cowen, *Activation of Extracellular Signal-Regulated Kinase (ERK) and Akt by Human Serotonin 5-HT1B Receptors in Transfected BE(2)-C Neuroblastoma Cells Is Inhibited by RGS4.* Journal of Neurochemistry. **75**: p. 934 –938.
91. Pereira, A., G. Fink, and S. Sundram, *Clozapine-induced ERK1 and ERK2 signaling in prefrontal cortex is mediated by the EGF receptor.* J Mol Neurosci, 2009. **39**(1-2): p. 185-98.
92. Pereira, A., et al., *Quetiapine and aripiprazole signal differently to ERK, p90RSK and c-Fos in mouse frontal cortex and striatum: role of the EGF receptor.* BMC Neurosci, 2014. **15**: p. 30.
93. Han, M.H., et al., *Brain region specific actions of regulator of G protein signaling 4 oppose morphine reward and dependence but promote analgesia.* Biol Psychiatry, 2010. **67**(8): p. 761-9.
94. Dripps, I.J., et al., *The role of regulator of G protein signaling 4 in delta-opioid receptor-mediated behaviors.* Psychopharmacology (Berl), 2017. **234**(1): p. 29-39.
95. Chu Sin Chung, P. and B.L. Kieffer, *Delta opioid receptors in brain function and diseases.* Pharmacol Ther, 2013. **140**(1): p. 112-20.
96. Toll, L., et al., *Nociceptin/Orphanin FQ Receptor Structure, Signaling, Ligands, Functions, and Interactions with Opioid Systems.* Pharmacol Rev, 2016. **68**(2): p. 419-57.
97. Mercatelli, D., et al., *Managing Parkinson's disease: Moving ON with NOP.* Br J Pharmacol, 2019.
98. Marti, M., et al., *Nociceptin/orphanin FQ receptor agonists attenuate L-DOPA-induced dyskinesias.* J Neurosci, 2012. **32**(46): p. 16106-19.
99. Arcuri, L., et al., *Anti-Parkinsonian and anti-dyskinetic profiles of two novel potent and selective nociceptin/orphanin FQ receptor agonists.* Br J Pharmacol, 2018. **175**(5): p. 782-796.
100. Wang, Q., L.Y. Liu-Chen, and J.R. Traynor, *Differential modulation of mu- and delta-opioid receptor agonists by endogenous RGS4 protein in SH-SY5Y cells.* J Biol Chem, 2009. **284**(27): p. 18357-67.
101. Xie, G.X., et al., *N-terminally truncated variant of the mouse GAIP/RGS19 lacks selectivity of full-length GAIP/RGS19 protein in regulating ORL1 receptor signaling.* J Mol Biol, 2005. **353**(5): p. 1081-92.
102. Pandey, S. and P. Srivanitchapoom, *Levodopa-induced Dyskinesia: Clinical Features, Pathophysiology, and Medical Management.* Ann Indian Acad Neurol, 2017. **20**(3): p. 190-198.
103. Fabbrini, G., et al., *Levodopa-induced dyskinesias.* Mov Disord, 2007. **22**(10): p. 1379-89; quiz 1523.
104. Ku, S. and G.A. Glass, *Age of Parkinson's disease onset as a predictor for the development of dyskinesia.* Mov Disord, 2010. **25**(9): p. 1177-82.
105. Kostic, V., et al., *Early development of levodopa-induced dyskinesias and response fluctuations in young-onset Parkinson's disease.* Neurology, 1991. **41**(2 (Pt 1)): p. 202-5.
106. Iravani, M.M. and P. Jenner, *Mechanisms underlying the onset and expression of levodopa-induced dyskinesia and their pharmacological manipulation.* J Neural Transm (Vienna), 2011. **118**(12): p. 1661-90.
107. Putterman, D.B., et al., *Evaluation of levodopa dose and magnitude of dopamine depletion as risk factors for levodopa-induced dyskinesia in a rat model of Parkinson's disease.* J Pharmacol Exp Ther, 2007. **323**(1): p. 277-84.

108. Boyce, S., et al., *Nigrostriatal damage is required for induction of dyskinesias by L-DOPA in squirrel monkeys.* Clin Neuropharmacol, 1990. **13**(5): p. 448-58.
109. Schneider, J.S., *Levodopa-induced dyskinesias in parkinsonian monkeys: relationship to extent of nigrostriatal damage.* Pharmacol Biochem Behav, 1989. **34**(1): p. 193-6.
110. Carta, M. and E. Bezard, *Contribution of pre-synaptic mechanisms to L-DOPA-induced dyskinesia.* Neuroscience, 2011. **198**: p. 245-51.
111. Carta, M. and A. Bjorklund, *The serotonergic system in L-DOPA-induced dyskinesia: pre-clinical evidence and clinical perspective.* J Neural Transm (Vienna), 2018. **125**(8): p. 1195-1202.
112. Tronci, E., et al., *BDNF over-expression induces striatal serotonin fiber sprouting and increases the susceptibility to l-DOPA-induced dyskinesia in 6-OHDA-lesioned rats.* Exp Neurol, 2017. **297**: p. 73-81.
113. Gerfen, C.R. and D.J. Surmeier, *Modulation of striatal projection systems by dopamine.* Annu Rev Neurosci, 2011. **34**: p. 441-66.
114. Mela, F., et al., *Antagonism of metabotropic glutamate receptor type 5 attenuates l-DOPA-induced dyskinesia and its molecular and neurochemical correlates in a rat model of Parkinson's disease.* J Neurochem, 2007. **101**(2): p. 483-97.
115. Paolone, G., et al., *Eltoprazine prevents levodopa-induced dyskinesias by reducing striatal glutamate and direct pathway activity.* Mov Disord, 2015. **30**(13): p. 1728-38.
116. Borroto-Escuela, D.O., et al., *On the existence of a possible A2A-D2-beta-Arrestin2 complex: A2A agonist modulation of D2 agonist-induced beta-arrestin2 recruitment.* J Mol Biol, 2011. **406**(5): p. 687-99.
117. Porras, G., et al., *L-dopa-induced dyskinesia: beyond an excessive dopamine tone in the striatum.* Sci Rep, 2014. **4**: p. 3730.
118. Nishi, A., G.L. Snyder, and P. Greengard, *Bidirectional regulation of DARPP-32 phosphorylation by dopamine.* J Neurosci, 1997. **17**(21): p. 8147-55.
119. Svenningsson, P., et al., *Regulation of the phosphorylation of the dopamine- and cAMP-regulated phosphoprotein of 32 kDa in vivo by dopamine D1, dopamine D2, and adenosine A2A receptors.* Proc Natl Acad Sci U S A, 2000. **97**(4): p. 1856-60.
120. Picconi, B., et al., *Loss of bidirectional striatal synaptic plasticity in L-DOPA-induced dyskinesia.* Nat Neurosci, 2003. **6**(5): p. 501-6.
121. Aubert, I., et al., *Increased D1 dopamine receptor signaling in levodopa-induced dyskinesia.* Ann Neurol, 2005. **57**(1): p. 17-26.
122. Fienberg, A.A., et al., *DARPP-32: regulator of the efficacy of dopaminergic neurotransmission.* Science, 1998. **281**(5378): p. 838-42.
123. Valjent, E., et al., *Regulation of a protein phosphatase cascade allows convergent dopamine and glutamate signals to activate ERK in the striatum.* Proc Natl Acad Sci U S A, 2005. **102**(2): p. 491-6.
124. Feyder, M., A. Bonito-Oliva, and G. Fisone, *L-DOPA-Induced Dyskinesia and Abnormal Signaling in Striatal Medium Spiny Neurons: Focus on Dopamine D1 Receptor-Mediated Transmission.* Front Behav Neurosci, 2011. **5**: p. 71.
125. Girasole, A.E., et al., *A Subpopulation of Striatal Neurons Mediates Levodopa-Induced Dyskinesia.* Neuron, 2018. **97**(4): p. 787-795 e6.
126. Alcacer, C., et al., *Chemogenetic stimulation of striatal projection neurons modulates responses to Parkinson's disease therapy.* J Clin Invest, 2017. **127**(2): p. 720-734.
127. Dobbs, L.K., et al., *Dopamine Regulation of Lateral Inhibition between Striatal Neurons Gates the Stimulant Actions of Cocaine.* Neuron, 2016. **90**(5): p. 1100-13.
128. Bastide, M.F., et al., *Pathophysiology of L-dopa-induced motor and non-motor complications in Parkinson's disease.* Prog Neurobiol, 2015. **132**: p. 96-168.
129. Picconi, B., et al., *Motor complications in Parkinson's disease: Striatal molecular and electrophysiological mechanisms of dyskinesias.* Mov Disord, 2018. **33**(6): p. 867-876.
130. Politis, M., et al., *Sustained striatal dopamine levels following intestinal levodopa infusions in Parkinson's disease patients.* Mov Disord, 2017. **32**(2): p. 235-240.

131. Ciurleo, R., et al., *Assessment of Duodopa((R)) effects on quality of life of patients with advanced Parkinson's disease and their caregivers.* J Neurol, 2018. **265**(9): p. 2005-2014.
132. Verhagen Metman L, D.D.P., van den Munckhof P, Fang J, Mouradian MM, Chase TN., *Amantadine as treatment for dyskinesias and motor fluctuations in Parkinson's disease.* Neurology, 1998. **50**: p. 1323-6.
133. Wong, K.K., et al., *A randomized, double-blind, placebo-controlled trial of levetiracetam for dyskinesia in Parkinson's disease.* Mov Disord, 2011. **26**(8): p. 1552-5.
134. Salvati, P., et al., *Biochemical and electrophysiological studies on the mechanism of action of PNU-151774E, a novel antiepileptic compound.* J Pharmacol Exp Ther, 1999. **288**(3): p. 1151-9.
135. Caccia, C., et al., *Safinamide: from molecular targets to a new anti-Parkinson drug.* Neurology, 2006. **67**(7 Suppl 2): p. S18-23.
136. Morari, M., et al., *Safinamide Differentially Modulates In Vivo Glutamate and GABA Release in the Rat Hippocampus and Basal Ganglia.* J Pharmacol Exp Ther, 2018. **364**(2): p. 198-206.
137. Borgohain, R., et al., *Two-year, randomized, controlled study of safinamide as add-on to levodopa in mid to late Parkinson's disease.* Mov Disord, 2014. **29**(10): p. 1273-80.
138. Gregoire, L., et al., *Safinamide reduces dyskinesias and prolongs L-DOPA antiparkinsonian effect in parkinsonian monkeys.* Parkinsonism Relat Disord, 2013. **19**(5): p. 508-14.
139. Gardoni, F., et al., *Safinamide Modulates Striatal Glutamatergic Signaling in a Rat Model of Levodopa-Induced Dyskinesia.* J Pharmacol Exp Ther, 2018. **367**(3): p. 442-451.
140. Cattaneo, C., et al., *Long-Term Effects of Safinamide on Dyskinesia in Mid- to Late-Stage Parkinson's Disease: A Post-Hoc Analysis.* J Parkinsons Dis, 2015. **5**(3): p. 475-81.
141. Mollereau, C., et al., *ORL1, a novel member of the opioid receptor family. Cloning, functional expression and localization.* FEBS Lett, 1994. **341**(1): p. 33-8.
142. Meunier, J.C., et al., *Isolation and structure of the endogenous agonist of opioid receptor-like ORL1 receptor.* Nature, 1995. **377**(6549): p. 532-5.
143. Reinscheid, R.K., et al., *Orphanin FQ: a neuropeptide that activates an opioidlike G protein-coupled receptor.* Science, 1995. **270**(5237): p. 792-4.
144. Mollereau, C., et al., *Distinct mechanisms for activation of the opioid receptor-like 1 and kappa-opioid receptors by nociceptin and dynorphin A.* Mol Pharmacol, 1999. **55**(2): p. 324-31.
145. Fukuda, K., et al., *Activation of mitogen-activated protein kinase by the nociceptin receptor expressed in Chinese hamster ovary cells.* FEBS Lett, 1997. **412**(2): p. 290-4.
146. Lou, L.G., L. Ma, and G. Pei, *Nociceptin/orphanin FQ activates protein kinase C, and this effect is mediated through phospholipase C/Ca2+ pathway.* Biochem Biophys Res Commun, 1997. **240**(2): p. 304-8.
147. Wnendt, S., et al., *Agonistic effect of buprenorphine in a nociceptin/OFQ receptor-triggered reporter gene assay.* Mol Pharmacol, 1999. **56**(2): p. 334-8.
148. Lowry, W.E., et al., *Csk, a critical link of g protein signals to actin cytoskeletal reorganization.* Dev Cell, 2002. **2**(6): p. 733-44.
149. Trombella, S., et al., *Nociceptin/orphanin FQ stimulates human monocyte chemotaxis via NOP receptor activation.* Peptides, 2005. **26**(8): p. 1497-502.
150. Hawes, B.E., et al., *Nociceptin (ORL-1) and mu-opioid receptors mediate mitogen-activated protein kinase activation in CHO cells through a Gi-coupled signaling pathway: evidence for distinct mechanisms of agonist-mediated desensitization.* J Neurochem, 1998. **71**(3): p. 1024-33.
151. Bevan, N., et al., *Nociception activates Elk-1 and Sap1a following expression of the ORL1 receptor in Chinese hamster ovary cells.* Neuroreport, 1998. **9**(12): p. 2703-8.
152. Florin, S., et al., *Autoradiographic localization of [3H]nociceptin binding sites from telencephalic to mesencephalic regions of the mouse brain.* Neurosci Lett, 1997. **230**(1): p. 33-6.

153. Florin, S., J. Meunier, and J. Costentin, *Autoradiographic localization of [3H]nociceptin binding sites in the rat brain.* Brain Res, 2000. **880**(1-2): p. 11-6.
154. Bridge, K.E., et al., *Autoradiographic localization of (125)i[Tyr(14)] nociceptin/orphanin FQ binding sites in macaque primate CNS.* Neuroscience, 2003. **118**(2): p. 513-23.
155. Kimura, Y., et al., *Brain and whole-body imaging in rhesus monkeys of 11C-NOP-1A, a promising PET radioligand for nociceptin/orphanin FQ peptide receptors.* J Nucl Med, 2011. **52**(10): p. 1638-45.
156. Berthele, A., et al., *[3H]-nociceptin ligand-binding and nociceptin opioid receptor mrna expression in the human brain.* Neuroscience, 2003. **121**(3): p. 629-40.
157. Lohith, T.G., et al., *Brain and whole-body imaging of nociceptin/orphanin FQ peptide receptor in humans using the PET ligand 11C-NOP-1A.* J Nucl Med, 2012. **53**(3): p. 385-92.
158. Neal, C.R., Jr., et al., *Opioid receptor-like (ORL1) receptor distribution in the rat central nervous system: comparison of ORL1 receptor mRNA expression with (125)I-[(14)Tyr]-orphanin FQ binding.* J Comp Neurol, 1999. **412**(4): p. 563-605.
159. Morgan, M.M., et al., *Antinociception mediated by the periaqueductal gray is attenuated by orphanin FQ.* Neuroreport, 1997. **8**(16): p. 3431-4.
160. Pan, Z., N. Hirakawa, and H.L. Fields, *A cellular mechanism for the bidirectional pain-modulating actions of orphanin FQ/nociceptin.* Neuron, 2000. **26**(2): p. 515-22.
161. Norton, C.S., et al., *Nociceptin/orphanin FQ and opioid receptor-like receptor mRNA expression in dopamine systems.* J Comp Neurol, 2002. **444**(4): p. 358-68.
162. Marti, M., C. Trapella, and M. Morari, *The novel nociceptin/orphanin FQ receptor antagonist Trap-101 alleviates experimental parkinsonism through inhibition of the nigro-thalamic pathway: positive interaction with L-DOPA.* J Neurochem, 2008. **107**(6): p. 1683-96.
163. Marti, M., et al., *Blockade of nociceptin/orphanin FQ receptor signaling in rat substantia nigra pars reticulata stimulates nigrostriatal dopaminergic transmission and motor behavior.* J Neurosci, 2004. **24**(30): p. 6659-66.
164. Arcuri, L., et al., *Genetic and pharmacological evidence that endogenous nociceptin/orphanin FQ contributes to dopamine cell loss in Parkinson's disease.* Neurobiol Dis, 2016. **89**: p. 55-64.
165. Olianas, M.C., et al., *Activation of nociceptin/orphanin FQ-NOP receptor system inhibits tyrosine hydroxylase phosphorylation, dopamine synthesis, and dopamine D(1) receptor signaling in rat nucleus accumbens and dorsal striatum.* J Neurochem, 2008. **107**(2): p. 544-56.
166. Feng, H., et al., *Movement disorder in GNAO1 encephalopathy associated with gain-of-function mutations.* Neurology, 2017. **89**(8): p. 762-770.
167. Papale, A., et al., *Impairment of cocaine-mediated behaviours in mice by clinically relevant Ras-ERK inhibitors.* Elife, 2016. **5**.
168. Paxinos, G.a.W., C,, *The Rat Brain in Stereotaxic Coordinates* Academic Press, 1982.
169. Cenci, M.A., C.S. Lee, and A. Bjorklund, *L-DOPA-induced dyskinesia in the rat is associated with striatal overexpression of prodynorphin- and glutamic acid decarboxylase mRNA.* Eur J Neurosci, 1998. **10**(8): p. 2694-706.
170. Cenci, M.A. and M. Lundblad, *Ratings of L-DOPA-induced dyskinesia in the unilateral 6-OHDA lesion model of Parkinson's disease in rats and mice.* Curr Protoc Neurosci, 2007. **Chapter 9**: p. Unit 9 25.
171. Santini, E., et al., *Critical involvement of cAMP/DARPP-32 and extracellular signal-regulated protein kinase signaling in L-DOPA-induced dyskinesia.* J Neurosci, 2007. **27**(26): p. 6995-7005.
172. Pavon, N., et al., *ERK phosphorylation and FosB expression are associated with L-DOPA-induced dyskinesia in hemiparkinsonian mice.* Biol Psychiatry, 2006. **59**(1): p. 64-74.
173. Stratinaki, M., et al., *Regulator of G protein signaling 4 [corrected] is a crucial modulator of antidepressant drug action in depression and neuropathic pain models.* Proc Natl Acad Sci U S A, 2013. **110**(20): p. 8254-9.

174. Ferrari, F., et al., *In vitro pharmacological characterization of a novel unbiased NOP receptor-selective nonpeptide agonist AT-403.* Pharmacol Res Perspect, 2017. **5**(4).
175. Ko, M.-C. and G. Caló, *The Nociceptin/Orphanin FQ Peptide Receptor*. Vol. 254. 2019: Springer.